

From Department of Microbiology, Tumor and Cell Biology  
Karolinska Institutet, Stockholm, Sweden

# **HYBRID ANTIBACTERIAL MICRONEEDLE PATCHES AGAINST SKIN INFECTIONS**

Jill Ziesmer



**Karolinska  
Institutet**

Stockholm 2023

All previously published papers were reproduced with permission from the publisher.

Published by Karolinska Institutet.

Printed by Universitetservice US-AB, 2023

© Jill Ziesmer, 2023

ISBN 978-91-8016-907-3

Cover illustration: artistic rendition by Jill Ziesmer of hybrid microneedles

# Hybrid antibacterial microneedle patches against skin infections

## THESIS FOR DOCTORAL DEGREE (Ph.D.)

By

**Jill Ziesmer**

The thesis will be defended in public at Eva & Georg Klein lecture hall, Solnavägen 9, 171 65 Solna, Friday the 10th of February 2023 starting at 9:00 am.

*Principal Supervisor:*

Assoc. Prof. Dr. Georgios A. Sotiriou  
Karolinska Institutet  
Department of Microbiology, Tumor and Cell  
Biology

*Co-supervisor(s):*

Assoc. Prof. Dr. Keira Melican  
Karolinska Institutet  
Department of Neuroscience

Prof. Dr. Liv Eidsmo  
University of Copenhagen  
Department of Immunology and Microbiology

*Opponent:*

Prof. Dr. Martin Andersson  
Chalmers University of Technology  
Department of Chemistry and Chemical  
Engineering  
Division of Applied Chemistry

*Examination Board:*

Prof. Dr. Anna Norrby-Teglund  
Karolinska Institutet  
Department of Medicine

Prof. Dr. Muhammet Toprak  
KTH Royal Institute of Technology  
Department of Applied Physics

Prof. Dr. Hanne Mørck Nielsen  
University of Copenhagen  
Department of Pharmacy



*"The penicillin could not get the illness to stop, amoxicillin's just not real enough"*

- Till I Collapse, Eminem



## ***POPULAR SCIENCE SUMMARY OF THE THESIS***

The skin is an important part of our body that influences our well-being, health and happiness. It also provides the crucial function to protect us from the outside world and germs, for example bacteria. However, at some point most of us have experienced an infection of the skin, maybe noticeable in a rash, after a scratch or after surgery. In such infections, bacteria that are typically not supposed to grow in the skin now grow there or harmless bacteria now start to produce substances that harm us. The result is that the skin itches, it might form pus, or the wound may just not heal. While this is uncomfortable for the patient, it also risks spreading in the body causing life-threatening conditions or being transferred to other people. Therefore, it is very important that doctors have medications available that quickly and effectively treat these skin infections.

A common way to treat skin infections is by prescribing antibiotics which stop bacteria from growing. Antibiotics can be given via creams, tablets, or even injections. Unfortunately, such administrations might not always be very effective – remember the function of our skin is to protect us and this may also prevent drugs from entering the skin. The result is that sometimes the concentration of the antibiotic in the skin at the site of infection, where we want it to be, is low. The low antibiotic concentration reduces the success of the therapy, and the patient continues to suffer from the skin infection. Another problem with treating skin infections is the occurrence of bacteria that are resistant to antibiotics. This means that the antibiotic is not effective in stopping the bacterial growth any longer because the bacteria developed a protection against it.

A solution to both problems (low concentration of antibiotic in the skin and resistance of bacteria to the antibiotic) is to develop new medical treatments that provide local concentrations of antibiotic combined with additional treatment. In this thesis such a new medical treatment, called microneedle (MN) patches, is developed. MNs are small needles, hardly visible with the bare eye, that can be applied to the skin like a plaster. The small needles create tiny holes in the outer layer of the skin without pain which allows drugs to enter the skin easily. In addition to this, the MN patches allow to combine the antibiotic with other treatments, a promising one being the application of heat which damages the bacterial cell. The heat can be created by using a red-light lamp widely used in cosmetics and gold (Au) or silver (Ag) nanoparticles. These tiny plasmonic particles have the unique property of being photothermal, meaning that they can absorb the light from the lamp and release it in form of mild heat.

In summary, in this thesis we developed MN plasters which bring high concentrations of antibiotics and mild heat into the skin infection. This allows to improve the treatment of skin infections, even if they are caused by bacteria that are resistant. In **Paper I** of this thesis we introduce the antibiotic-loaded MN plasters, and in **Paper II** and **Paper III** we developed MN with nanoparticles that can heat up. In **Paper IV** we finally combine the work by development of a single, hybrid MN that contains both antibiotic and heat.

## ***Abstract***

Skin and soft tissue infections (SSTIs) are a major healthcare burden that has increased in incidence since the beginning of the 21<sup>st</sup> century resulting in an annual spending of approximately 15 b\$ in 2012 in the United States (US).<sup>1</sup> Treatment of SSTIs is complex and typically involves the administration of antibiotics. However, the antibiotic therapy of SSTIs has multiple obstacles interfering with an efficient treatment outcome such as (i) limited local antibiotic penetration into the skin and (ii) rising antibiotic resistant SSTIs. The limitation of local drug penetration is associated with the route of administration. On the one hand, antibiotics can be given topically; however, the protective function of the skin limits the types of drugs that can efficiently be given via this route. On the other hand, systemic administration of the antibiotic parenterally or intravenously (IV) shows low local skin absorption while suffering from side effects associated with the systemic exposure of the body to the antibiotic. Furthermore, the rise in antibiotic resistance urgently calls for the development of novel antibacterial treatment options to optimize the antibacterial effect of current antibiotics and reduce further resistance development. A potential to improve the antibacterial effect of antibiotics is through multimodal therapies and as such the incorporation of heat from photothermal therapy (PTT) has been reported as a promising avenue to improve antibiotic efficiency.

In the scope of this thesis, microneedle (MN) arrays were developed to address the problems faced in the treatment of bacterial SSTIs. In the first part of this thesis, dissolvable MN arrays loaded with the antibiotic vancomycin (VAN) were developed and tested in *ex vivo* porcine infection models of methicillin-resistant *Staphylococcus aureus* (MRSA), a strain commonly found in SSTIs. The MN arrays allowed the delivery of high concentrations of VAN locally in the skin where it remained active to inhibit the growth of MRSA after only two applications for 10 minutes. The second part of this thesis describes the development of photothermal MN arrays with plasmonic Au/SiO<sub>2</sub> and Ag/SiO<sub>2</sub> nanoaggregates. Four different fabrication methods following traditional mold-and-casting methods using Au/SiO<sub>2</sub> revealed that the rational selection of the fabrication method allows for a control over the MN morphology, photothermal effect, and a reduction of nanoparticle (NP) deposition into the skin. Additionally, Ag/SiO<sub>2</sub> nanoaggregates were employed in nanocomposites of ultraviolet (UV)-curable resin to be used for the 3D printing of photothermal MN arrays. Such 3D-printed photothermal MN arrays allowed for the *in vitro* killing of the SSTI-associated bacterial species *S. aureus* and *Pseudomonas aeruginosa* by heat. However, final temperature of the planktonic samples reached >60 °C limiting the clinical potential of such photothermal MNs as monotherapies since such high temperatures may cause damage to healthy cells. Therefore, hybrid MN arrays were developed that incorporate both VAN and photothermal nanoaggregates to reduce the needed antibiotic and temperature dose through synergistic interactions. Such hybrid MNs were fabricated employing an outer, dissolvable, drug-loaded layer and an inner, non-dissolvable, photothermal core aiming to combine the advantages of (i) high local VAN delivery and (ii) intradermal PTT. We showed the successful synergistic growth inhibition of MRSA *in vitro* of such hybrid MN arrays. Overall, the work in this thesis introduces a potential novel treatment option for bacterial SSTIs.



## ***LIST OF SCIENTIFIC PAPERS***

- I. **Jill Ziesmer**, Poojabahen Tajpara, Nele-Johanna Hempel, Marcus Ehrström, Keira Melican, Liv Eidsmo, and Georgios A. Sotiriou  
**Vancomycin-Loaded Microneedle Arrays against Methicillin-Resistant *Staphylococcus Aureus* Skin Infections**  
*Advanced Materials Technologies*, 2021; 6; 2001307
- II. **Jill Ziesmer**, Isabel Sondén, Thomas Thersleff, and Georgios A. Sotiriou  
**Highly Efficient Near-IR Photothermal Microneedles with Flame-Made Plasmonic Nanoaggregates for Reduced Intradermal Nanoparticle Deposition**  
*Advanced Materials Interfaces*, 2022; 2201540
- III. **Jill Ziesmer**, Isabel Sondén, Padryk Merkl, and Georgios A. Sotiriou  
**Customizable Fabrication of Photothermal Microneedles with Plasmonic Nanoaggregates Using Low-cost Stereolithography 3D-printing**  
*Manuscript*
- IV. **Jill Ziesmer** and Georgios A. Sotiriou  
**Hybrid Microneedle Arrays for Antibiotic and near-IR Photothermal Synergistic Antimicrobial Effect Against Methicillin-Resistant *Staphylococcus aureus***  
*Manuscript*



### ***SCIENTIFIC PAPERS NOT INCLUDED IN THE THESIS***

- Zoi Kanaki, Chrysoula Chandrinou, Ioanna-Maria Orfanou, Christina Kryou, **Jill Ziesmer**, Georgios A. Sotiriou, Apostolos Klinakis, Constantin Tamvakopoulos, and Ioanna Zergioti  
**Laser-Induced Forward Transfer Printing on Microneedles for Transdermal Delivery of Gemcitabine**  
*International Journal of Bioprinting*, 2022; 8; 554
- Alessondra T. Speidel, Phillip R. A. Chivers, Christopher S. Wood, Derrick A. Roberts, Inês P. Correia, April S. Caravaca, Yu Kiu Victor Chan, Catherine S. Hansel, Johannes Heimgärtner, Eliane Müller, **Jill Ziesmer**, Georgios A. Sotiriou, Peder S. Olofsson, Molly M. Stevens  
**Tailored Biocompatible Polyurethane-Poly(ethylene glycol) Hydrogels as a Versatile Nonfouling Biomaterial**  
*Advanced Healthcare Materials*, 2022; 11; 2201378

### ***PATENTS FROM THE WORK OF THE THESIS***

- **Jill Ziesmer**, Padryk Merkl, Isabel Sondén, and Georgios A. Sotiriou  
**Microneedle Array Comprising a Water Insoluble Polymer and Photothermal Nanoparticles**  
20<sup>th</sup> of June 2022, Application no.: 2250731-3



# CONTENTS

1	INTRODUCTION.....	6
2	LITERATURE REVIEW .....	9
2.1	The skin.....	9
2.1.1	The physiology of the skin.....	10
2.1.2	The skin microbiome.....	14
2.1.3	Bacterial skin and soft tissue infections .....	16
2.1.4	Current treatment strategies for bacterial skin infections .....	21
2.1.5	Thermotherapy in dermatology.....	25
2.2	Nanomedicine for microbial infections.....	27
2.2.1	Inorganic NPs as antibacterial agents .....	28
2.2.2	Plasmonic NPs .....	31
2.2.3	NPs synthesis via FSP.....	33
2.3	MN arrays .....	35
2.3.1	Polymeric MNs for drug delivery .....	37
2.3.2	Antibacterial MNs .....	40
2.3.3	Photothermal MNs .....	41
3	RESEARCH AIMS.....	45
4	METHODOLOGICAL CONSIDERATIONS .....	47
4.1	Regarding MN fabrication and characterization.....	47
4.2	Regarding NPs synthesis and characterization .....	50
4.3	Regarding bacterial work.....	51
4.4	<i>Ex vivo</i> skin models .....	52
4.5	Ethical considerations .....	52
5	RESULTS & DISCUSSION .....	55
	Paper I: Vancomycin-Loaded Microneedle Arrays against Methicillin-Resistant <i>Staphylococcus Aureus</i> Skin Infections .....	55
	Paper II: Highly Efficient Near-IR Photothermal Microneedles with Flame- Made Plasmonic Nanoaggregates for Reduced Intra-dermal Nanoparticle Deposition.....	57
	Paper III: Customizable Fabrication of Photothermal Microneedles with Plasmonic Nanoaggregates Using Low-cost Stereolithography 3D- printing.....	59
	Paper IV: Hybrid Microneedle Arrays for Antibiotic and near-IR Photothermal Synergistic Antimicrobial Effect Against Methicillin-Resistant <i>Staphylococcus aureus</i> .....	61
6	CONCLUSIONS.....	63
7	FUTURE PERSPECTIVE.....	65
8	ACKNOWLEDGEMENTS.....	67
9	REFERENCES.....	73

## **LIST OF ABBREVIATIONS**

AMP	antimicrobial peptide
CFU	colony forming unit
DNA	deoxyribonucleic acid
DSC	differential scanning calorimetry
EDX	energy-dispersive X-ray spectroscopy
EELS	electron energy loss spectroscopy
FDA	Food and Drug Administration
FSP	flame spray pyrolysis
HMDSO	hexamethyldisiloxane
HPLC	high-pressure liquid chromatography
ICP-MS	inductively coupled plasma mass spectroscopy
IDSA	Infectious Disease Society of America
IV	intravenous
IR	infrared
LCD	liquid crystal display
LSP(R)	localized surface plasmons resonance
MIC	minimum inhibitory concentration
MN	microneedle
MRSA	methicillin-resistant <i>Staphylococcus aureus</i>
NR	nanorod
NSTI	necrotizing soft tissue infections
NP	nanoparticle
OD	optical density
PCL	polycaprolactone
PDMS	polydimethylsiloxane
PMMA	polymethylmethacrylate
PTT	photothermal therapy
PVA	polyvinyl alcohol
PVP	polyvinylpyrrolidone
ROS	reactive oxygen species
SEM	scanning electron microscope
SLA	stereolithography
SPIONS	superparamagnetic iron oxide NPs
SSI	surgical site infections
SSTI	skin and soft tissue infection
TEM	transmission electron microscope
US	United States
UV	ultraviolet
VAN	vancomycin
WHO	World Health Organization



# 1 INTRODUCTION

The skin covers an organism's entire body, efficiently interacting with the environment and providing a protective shield against external harm. The complex physiology of the skin and its outer layer, the epidermis, is a crucial factor in orchestrating the interactions with and protection against the environment. In a healthy state, the skin harbors a rich microbiome in fine harmony with the host and mutualistic/commensal microorganisms allowing for the control of harmful pathogenic colonization and protection against skin infections.<sup>2</sup> However, at times this microbial homeostasis can be disrupted and/or external injury is inflicted on the skin resulting in the emergence of skin and soft tissue infections (SSTIs). In fact, SSTIs have been rising in the first decade of the 21<sup>st</sup> century and pose a major health care burden corresponding to an annual spending in the United States (US) of approximately 15 b\$ in 2012.<sup>1</sup> The increasing emergence of SSTIs is not only a health threat to the affected patients but also to the community since skin pathogens can directly and indirectly be transmitted between humans.<sup>3</sup> Therefore, efficient treatment of SSTIs is a crucial aspect in maintaining high quality of health in our society. SSTIs can be categorized in various ways depending for example on the anatomical infection site, the microbial etiology, the symptom severity, or the presence of an underlying disease. Accordingly, the recommended treatment of SSTIs may vary significantly depending on how the infection presents.<sup>4</sup> Generally, antibiotic administration via topical or systemic routes is commonly recommended for many types of SSTIs. However, antibiotic penetration into the skin may be limited depending on the molecular properties of the antibiotic and the protective function of the skin. Furthermore, the ongoing rise of antibiotic-resistance is contributing to difficulties in successfully treating SSTIs.<sup>5</sup> To overcome the problems of (i) limitations in antibiotics delivery and (ii) maintaining the efficiency of antibiotics for the treatment of SSTIs, novel antibiotic delivery platforms need to be developed. One possibility to enhance the efficiency of antibiotics is the simultaneous administration of multiple therapy modalities that cause harm to the infectious bacteria via various pathways. In the scope of bacterial infections, the application of mildly elevated temperature can potentially improve the therapy via weakening of the bacteria through physical damage.<sup>6,7</sup>

One approach to improve the efficiency of antibacterial therapies is the use of nanoparticles (NPs).<sup>8</sup> Nanomaterials are materials in the nanoscale ( $10^{-9}$  m) that, due to their small size, exhibit different behaviors than their bulk counterpart. In the field of nanomedicine, these distinct behaviors are exploited for therapeutic or diagnostic inventions. The distinct behaviors of NPs and their high surface-to-volume ratio allows for antibacterial effects via processes such as (i) high metal-ion release, (ii) the production of reactive oxygen species (ROS), or (iii) heat dissipation.<sup>9,10</sup> The possibility of NPs to produce heat is based on the

---



interaction of plasmonic NPs with light. Plasmons are the collective oscillation of the free electron gas. In plasmonic NPs the frequency of the plasmons can effectively couple with the wavelength of the incident light resulting in energy absorption which can be released via heat dissipation.<sup>11–13</sup> Using light to increase the temperature for therapeutic purposes is called photothermal therapy (PTT). In PTT for biomedical application typically light in the near-infrared (IR) region is preferred due to the low unspecific absorption of near-IR wavelengths by tissue leading to lower radiative losses.<sup>14</sup> Two plasmonic nanomaterials with high light-to-heat conversion efficiencies are Ag and Au which upon tuning their size and shape can absorb near-IR light.<sup>13</sup> While Ag NPs may be beneficial in terms of material costs, Au NPs benefit from high biological and chemical inertness. An important aspect in translating nanomedicine to the clinics is the cost-efficient and scalable production of NPs. A NP synthesis technique commonly employed in industry is the aerosol synthesis such as flame spray pyrolysis (FSP).<sup>15,16</sup> FSP allows for the synthesis of Ag and Au NPs with control over their plasmonic properties by formation of the nanoaggregates with specific interparticle distance using SiO<sub>2</sub>.<sup>17–21</sup> Furthermore, FSP allows for the fabrication of large quantities of NP powder and the direct *in situ* deposition of NP films on substrates.<sup>22</sup> These powders or coatings can then be used for biomedical purpose such as PTT against bacterial infections. PTT damages bacteria resulting in enhanced therapy outcomes due to increasing antibiotic susceptibility and direct bacterial killing.<sup>23,24</sup> Therefore, PTT has been widely employed for the improvement of the treatment of SSTIs. However, a crucial aspect in translating NP-based PTT is the effective delivery of PTT locally to the infected skin.

Another approach for improving antibiotic efficiency is their adequate therapy administration to the infection site. In the field of dermatotherapies, microneedles (MNs) have gained traction in the past two decades for improved drug delivery to the skin.<sup>25,26</sup> MNs are small needles at the microscale commonly arranged in arrays on patches or plasters that can deliver their cargo intradermally while inflicting minor pain to the patient.<sup>27</sup> Due to these characteristics, MN arrays were extensively developed for intradermal vaccination.<sup>28</sup> However, the application of MNs was quickly expanded to other medical fields including their use in antibiotic<sup>29</sup> and NP delivery.<sup>30</sup> For drug delivery, polymeric MNs are of interest since they allow the incorporation of drugs or particles into the MN matrix with subsequent release of their cargo upon dissolution of the polymer after insertion into the moist skin environment.<sup>31</sup> As such, polymeric MN arrays were successfully employed to deliver various types of antibiotics both locally and systemically for the treatment of infections.<sup>29</sup> The work of **Paper I** extends the scientific literature on antibiotic-loaded MNs by exploring MNs loaded with the glycopeptide vancomycin (VAN), an antibiotic that can typically only be administered intravenously (IV), for the potential local treatment of methicillin-resistant *Staphylococcus aureus* (MRSA) skin infections. So far, various previous reports developed photothermal MNs; however, they were mostly applied for the treatment of skin cancers<sup>30</sup> and the application of photothermal MNs for antibacterial effects is scarce. Additionally, most photothermal MNs are dissolvable in nature, resulting in intradermal release of nanomaterials.<sup>32</sup> **Paper II** and **Paper III** of this thesis aim to extend the field by introducing

---

various novel methods to fabricate non-dissolvable, photothermal MNs loaded with FSP-made, plasmonic NPs of Au and Ag, respectively. Importantly, **Paper II** explores the removal of the nanomaterials after skin insertion and **Paper III** introduces a low-cost fabrication method for photothermal MNs effectively reducing bacterial growth of the SSTI-associated bacteria *S. aureus* and *P. aeruginosa*. Finally, both functionalities of local antibiotic release and PTT are combined in one treatment strategy, namely hybrid MN arrays as presented in **Paper IV**. The work of **Paper IV** evaluates the rational choice of polymers to control the hybrid MN morphology resulting in MNs with an outer dissolvable VAN-loaded shell and an inner non-dissolvable photothermal core showing synergistic antibacterial effect against MRSA.

## 2 LITERATURE REVIEW

In the literature review of this thesis, the physiology and microbiome of the skin in health and its aberration in bacterial infections is explained to build the foundation in evaluating the limitations of current antibiotic treatments for SSTIs. Subsequently, the reader will be presented with an overview of the approaches employed in this work, namely nanomedicine and MNs, for developing an innovative treatment strategy for SSTIs combining heat and local antibiotic delivery.

### 2.1 The skin

The skin is one of the largest organs of the human body with an average 2 m<sup>2</sup> in surface area,<sup>33</sup> which accounts for ~ 15 % of total body weight.<sup>34</sup> It effectively covers the body's external surface and thus provides physical protection for deeper tissues from the environment. Its composition of various cell types, skin appendages, commensal and mutualistic bacteria, and a rich extracellular matrix, orchestrates the skin barrier function. This intricate network and the skin homeostasis control the protection against chemical, physical, and biological damages from light, heat, injury, and infection. Furthermore, the skin regulates the body temperature, stores water and fat, permits the sensory reaction to temperature, touch, and pain, serves as the first immunological defense reaction, and provides both endocrine and exocrine functions. Therefore, the skin is a principal factor to maintain well-being and health in human and the disruption of the skin, or its proper function, can result in damages ranging from minor cosmetic discomfort up to chronic and life-threatening diseases. Therefore, it is of utmost importance to maintain appropriate dermatological health. To this end, various consumer health products, drug delivery devices, and pharmaceutical formulations have been developed to support the skin function, aid in the protection against injury, and treat dermatological diseases. In order to understand how such dermatological medical devices function and to rationally develop new treatment options, one needs to first understand the physiology of the skin in health and its deviations in disease.

### **2.1.1 The physiology of the skin**

The skin can be divided into three main layers with (i) the epidermis as the outer layer which is connected to (ii) the underlying dermis via the basement membrane. The epidermis and dermis together are also referred to as the cutis. Underneath the cutis lays the third skin layer (iii) the hypodermis which is also called subcutaneous tissue or fatty layer. The primary function of each layer differs depending on its physiology and the residing cell types. In the scope of this thesis, the epidermis is of specific interest since it constitutes the primary biological barrier for topical drug delivery while also regulating the bacterial colonization and reaction to infection. How the cells of the epidermis form this biological barrier through regeneration and terminal differentiation and what role they play in orchestrating the interaction with the environmental bacteria will be explained in more detail and illustrated in Figure 1. Afterwards, a brief overview of another biological barrier of the skin, the epidermal basement membrane, will briefly be explained followed by a general overview of the viable parts of the skin, the dermis and hypodermis.

#### ***The outer biological barrier: the stratum corneum***

The epidermis is a stratified epithelium that forms the outmost skin layer which itself consists of four to five layers depending on the body region.<sup>35</sup> The amount and thickness of the different epidermal layers varies significantly depending on the body site resulting in an epidermal thickness that can range from ~30 (e.g. in the face) to ~300  $\mu\text{m}$  (e.g. on the dorsum of the hand) thickness.<sup>36-38</sup> The outermost layer of the epidermis in direct contact with the environment and the air is the *stratum corneum*. In this layer, the epidermal cells, called keratinocytes, have terminated their differentiation and underwent complete cornification resulting in anucleate corneocytes that periodically shed off of the superficial layer *stratum disjunctum* in the form of scales.<sup>39,40</sup> The corneocytes are filled with a highly interconnected network of keratin filaments and filaggrin matrix and are embedded in a lipid-rich hydrophobic envelope in a brick-and-mortar fashion.<sup>41,42</sup> The *stratum corneum* constitutes the major barrier against the external environment: on the one hand, the corneocytes provide mechanical strength and protection against physical damage, maintain hydration, and prevent UV radiation to reach mitotically active cells of deeper epidermal layers.<sup>43</sup> On the other hand, its hydrophobic extracellular matrix regulates the permeation and penetration of molecules and exogenous material,<sup>44</sup> contains antimicrobial peptides (AMPs),<sup>45</sup> and initiates the corneocyte desquamation.<sup>43,46</sup> Furthermore, the lipid extracellular layer results in the acidic environment of the skin which serves as an antimicrobial defense and enables enzyme and cytokine activity and activation.<sup>47</sup> Finally, being the most superficial layer of the skin, the *stratum corneum* is in contact with diverse microbiota and is crucial in the maintenance of the skin microbial balance.<sup>48,49</sup>

#### ***Terminal differentiation of keratinocytes: how the skin builds the body's protection***

Keratinocytes in the epidermis originate from the basal cells in the bottom epidermal layer and undergo terminal differentiation and suprabasal migration forming the outer epidermal

---

layers. On the soles and palms, the skin comprises an epidermal layer directly underneath the *stratum corneum*, called the *stratum lucidum*, which contains dead keratinocytes embedded in a protein matrix rich in an intermediate form of keratin called eleidin.<sup>50</sup> The *stratum lucidum* provides a protection against physical damage to the skin. For the skin located not on the soles and palms, the epidermal skin layer directly underneath the *stratum corneum* is called the *stratum granulosum*. Here, the keratinocytes migrated from the underlying *stratum spinosum* undergoing differentiation into granular cells.<sup>51</sup> The keratinocytes start to lose their nuclei and secrete lamellar bodies into the extracellular space forming a hydrophobic lipid envelope which is crucial in the formation of the permeability and antimicrobial barrier function of the skin.<sup>52</sup> Furthermore, the granular cells contain large keratohyalin granules with a high amount of the histidine-rich protein profilaggrin comprising multiple active filaggrin monomers that bind and condense the keratin cytoskeleton thus participating in the cornification step of the programmed cell death of the keratinocytes.<sup>53-55</sup>

Underneath the *stratum granulosum*, the keratinocytes in the epidermis differentiate into squamous cells making up the *stratum spinosum* at a rate approximately on par with the epidermal shedding with around 30% of basal cells transitioning each week.<sup>56,57</sup> This differentiating may occur as such that the basal cells weakening their attachment to the basement membrane or divide in a perpendicular fashion to the basement membrane giving rise to a daughter cell in the *stratum spinosum*.<sup>58</sup> The basal-to-spinous layer transition is mainly characterized by the structural change in expression of distinct keratin intermediate filaments with K5 and K14 or K1 and K10 expressed in the basal or suprabasal layer, respectively.<sup>58,59</sup> This cell transitioning is regulated at a transcriptional level and is a main indicator for the effective switching of active proliferation in the epidermal stem cells towards the terminal differentiation in the keratinocytes.<sup>59</sup>

### ***Langerhans cells contribute to the regulation of the skin's bacterial colonization***

Besides keratinocytes, the *stratum spinosum* also contains tissue-resident antigen-presenting cells, the dendritic cells and Langerhans cells, which perform a key role in cutaneous immunology.<sup>60-62</sup> Dendritic cells are essential for the surveillance of the cutaneous environment through their periodic extension and retraction of their dendrites into the intercellular spaces of keratinocytes which allows them to sample surrounding material.<sup>63</sup> As such, they capture luminal antigens and upon sensing pathogenic stimuli, dendritic cells change their morphology, gene expression profile, phenotype and function in a process called maturation allowing them to migrate from the epidermis to the draining lymph nodes.<sup>64</sup> In the lymph nodes the antigen presentation of dendritic cells then promotes immunity and tolerance by priming and recruitment of T-cells. Furthermore, the scavenger function of Langerhans cells in the epidermis maintains the cutaneous homeostasis by clearing debris of apoptotic keratinocytes during steady state and after infections.<sup>64</sup> The superficial location of Langerhans cells in the skin makes them a key player in the effective regulation of the tolerance to commensal bacteria modulated by their limited uptake and presentation of bacterial antigens and their induction of regulatory T-cells.<sup>65,66</sup>

---

### ***The role of stem cells in the regeneration of the epidermis***

The bottom layer of the epidermis is the *stratum basale* which is attached to the underlying basement membrane via hemidesmosomes and thus physically separated from the dermis.<sup>67,68</sup> The basal cell layer consists of columnar stacked slow-cycling epidermal stem cells (~ 1 – 10% of basal cells)<sup>69</sup> connected to the basement membrane which through periodic division gives rise to transiently amplifying cells.<sup>57,70,71</sup> Those basal cells divide two to three times a week before they mature and undergo terminal differentiation executing an outwards migration which produces the outer epidermal layers.<sup>72</sup> It must be noted, that this classical hypothesis of an asymmetric, hierarchically organized epidermal proliferation unit has been expanded with alternative models suggesting regional specificity and stochastic switching between division and differentiation at the stem cell level;<sup>73–75</sup> however, a detailed introduction and discussion of the epidermal stem cell models is beyond the scope of this thesis. Basal cells are the only epithelial cells in the skin that are mitotically active and proliferate and therefore play a crucial role in wound healing and skin regeneration.<sup>76,77</sup> In fact, due to the germinating processes of the basal cells the *stratum basale* is also called *stratum germinativum*. Besides basal cells, the *stratum basale* contains melanocytes which generate the skin's coloration, are the major vitamin D producers, and contribute to the protection of the body against ultraviolet (UV) radiation damage through light absorption from melanin. In addition, Merkel cells responsible for the tactile function are located in the basal cell layer.

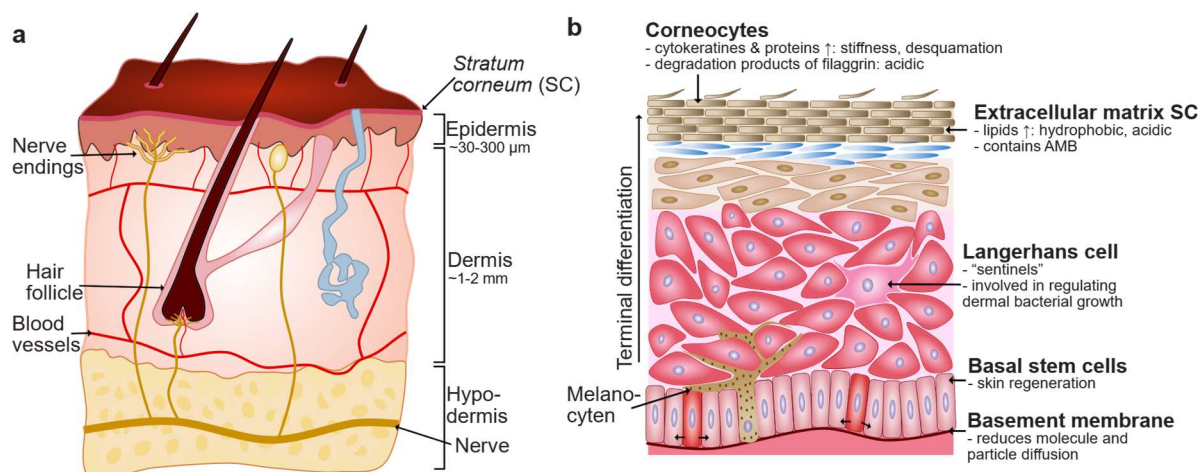


Figure 1: Illustration of the skin and epidermis. a) Overview of the physiology and thickness of the various skin layers, namely the epidermis, dermis, and hypodermis. The avascular epidermis obtains nutrients from the vasculature originating at the bottom of the dermis and/or in the hypodermis extending throughout the whole dermis. Nerves likewise originate in the bottom of the dermis and/or hypodermis and extending vertically to the upper skin layers. Free nerve endings and lamellar corpuscle function as mechanoreceptor to various physical stimuli such as temperature and touch. b) Illustration of the various cell layers in the epidermis and highlighted structural aspects of the epidermis and their role in the barrier function.

### ***The basement membrane***

Underneath the epidermis lies the dermis which is physically separated from the epidermis via the basement membrane. The basement membrane consists of glycoproteins and proteoglycans and comprises of two layers: (i) the *lamina lucida*, in which the basal cells of the epidermis are connected via anchoring filaments of hemidesmosomes and (ii) the *lamina densa* to which the dermis attaches via anchoring fibrils of collagen.<sup>78</sup> The basement membrane is crucial in the mechanical stabilization of the skin and defects in the membrane's components can result in shedding of the skin.<sup>79</sup> Furthermore, the basement membrane attenuates the diffusion of molecules and particles between the epidermis and dermis.<sup>80</sup>

### ***The dermis and the subcutaneous tissue***

The dermis is a connective tissue comprised of collagen, elastic fibers and an extracellular matrix containing glycosaminoglycans. Adjacent to the epidermis and basement membrane lays the papillary region which is a loosely arranged matrix of collagen fibers and areolar tissue which extends with finger-like projections into the epidermis.<sup>81</sup> These projections often contain dense networks of blood capillaries and tactile corpuscles; and the finger-like extensions allow for an increased surface area between the epidermis and dermis. Underneath the papillary layer sits the thicker region called reticular layer which is a dense connective tissue consisting of irregularly interweaved collagenous, elastic, and reticular fibers. Furthermore, the dermis contains many extracellular components, i.e. the skin appendages such as the hair follicle, sweat glands, apocrine and sebaceous glands, and the Pacinian corpuscles. In addition, nerve endings and blood capillaries interconnect throughout the whole dermis. Due to the various functional structures, the dermis fulfils the essential function of supplying the avascular epidermis with nutrients, provides structural and mechanical support, and aid in the thermoregulation and sensation. The most common cell type in the dermis are fibroblasts which produce collagen, elastin, and reticular fibers, and the extracellular matrix.<sup>81</sup> However, the dermis harbors various immune cells such as dermal dendritic cells, macrophages, mast cells, and T-cells. The dendritic cells in the dermis have been associated with the immune activation after bacterial invasion, in contrast to the Langerhans cells residing in the epidermis which are supposed to have reduced capabilities for bacterial antigen uptake and presentation.<sup>60,61</sup> Interestingly, the total area of a normal healthy skin costume has been assessed to contain  $2 \times 10^{10}$  skin-resident T-cells which is twice the amount of the number of T cells in the total blood volume in an adult.<sup>82</sup> While there are various types of T-cells that reside in healthy skin and under pathological conditions,  $T_H17$  cells have been associated with effective first-line defense against fungal and bacterial infections,<sup>83,84</sup> with an impaired interleukin-17 mediated immune response potentially contributing to persistent and recurrent infections.<sup>85</sup>

The final and deepest layer of the skin is the subcutaneous tissue which mainly consists of adipocytes, but also contains fibroblasts for the production of collagen fibers, and macrophages. The hypodermis contains nerves, the lymphatic and vascular vessels,<sup>86</sup> and in some cases large hair follicles and sweat glands originate in the hypodermis. The main

---

function of the hypodermis is the regulation of energy storage, thermoregulation and protection of the skeletal systems, organs and muscles.<sup>87</sup>

### **2.1.2 The skin microbiome**

After understanding the physiology of the skin, the reader will now be given an overview of the skin microbiome which is a crucial factor in the regulation of bacterial skin infections (Figure 2). As the exterior surface of the body the skin is not only a major barrier and protection against the environment but also a diverse ecosystem home to millions of bacteria, fungi, viruses, and mites which may extend into subepidermal layers.<sup>88</sup> Those microorganisms, and more specifically the abundant bacteria located on the skin, engage in a complex crosstalk between each other, the host, and foreign and potentially pathogenic organisms. As such, skin associated bacteria engage in host-microorganism relationships, regulate the growth of commensal and pathogenic bacteria, and contribute to the maintenance of a beneficial skin microenvironment. The habitat of the skin is controlled by various endogenous (i.e. host factors, physiology of different body sites)<sup>89</sup> and exogenous factors (i.e. antibiotic use, application of cosmetic products)<sup>90,91</sup> resulting in inter- and intrapersonal variation of the skin associated microbiota.<sup>92</sup> In general, the skin is considered an acidic, aerobic, desiccated, cool, high-lipid, high-salt, and nutrient-low environment; however, the skin appendages, such as hair follicles and sweat glands, constitute a more lipid-rich and anaerobic environment which may constitute a distinct microbial niche.<sup>92</sup> Furthermore, the skin is often categorized into three broad ecological niches based on difference in physiology and topography of various body sites: (i) oily and sebaceous (i.e. face), (ii) moist (i.e. armpits), or (iii) dry (i.e. volar forearm).<sup>2</sup>

#### ***Defining the habitat of the skin***

The various ecological niches significantly influence the presence of specific bacteria; however, in general the skin is mostly colonized by bacteria of various species of *Propionibacterium*, *Corynebacterium*, *Streptococci*, and *Staphylococci*. The lipophilic *Propionibacterium* spp. dominate oily and sebaceous ecological niches, while *Corynebacterium* and *Staphylococcus* spp. prefer niches of high humidity thus abundantly colonizing moist skin areas.<sup>93</sup> Those species predominantly inhabit the skin under commensal or mutualistic conditions in a relatively stable state, with microbial communities in adults being maintained for up to two years.<sup>94</sup> An important role of these host-mutualistic interactions is the education of the cutaneous immune system by the skin microbiota. Keratinocytes communicate with the skin microorganisms via pattern recognition receptors and upon binding of pathogen-associated molecular patterns they trigger the innate immune response resulting in the secretion of AMPs and cytokines.<sup>95</sup> While some AMPs are constantly expressed by the epidermal epithelial cells to prevent pathogenic colonization, they can also be induced and produced by specific microbiota which is considered an important multidirectional signaling mechanism effectively balancing the ecology of the skin microbiota.



***Commensal growth of bacteria on the skin using the example of *S. aureus****

An interesting example of the balancing act of the skin microbiota by effective host-mutualistic and microbe-microbe interactions is the commensal growth of *S. aureus* on the skin. It is estimated that around 30% of adults are asymptotically colonized by *S. aureus*;<sup>96,97</sup> however, it can also cause a variety of skin infections. The colonization of *S. aureus* can be inhibited and controlled by the production of antibiotics such as lugdunin and types of lantibiotics from the commensal bacteria *Staphylococcus lugdunensis* and *Staphylococcus hominis*.<sup>98</sup> Furthermore, *Staphylococcus epidermidis* can prevent biofilm formation of *S. aureus* via secretion of serine protease glutamyl endopeptidase. This secretion can also trigger the production of AMPs via keratinocyte-associated activation of the immune response further limiting the growth of *S. aureus*.<sup>2</sup> Besides a competitive exclusion of *S. aureus*, it was also found that the skin microbiota may regulate *S. aureus* via the shifting of its virulence. For example, co-culturing of *S. aureus* with *Corynebacterium striatum* increased gene transcription associated with a commensal state and attenuated the virulence profile of *S. aureus*.<sup>99</sup>

***What drives the shift of *S. aureus* from commensal to pathogenic?***

Although the host response in combination with the crosstalk of the skin microbiota typically regulates the healthy condition of the skin, pathogens such as *S. aureus* can frequently cause infections. Various stimuli such as environmental conditions of niches and host-signaling may drive the virulence of *S. aureus* enabling the infection of the skin. It is well known that *S. aureus* has a broad variety of virulence factors such as neutrophil-killing toxins, expression of protective surface molecules, or proteases for the degradation of host AMPs.<sup>100,101</sup> The virulence of *S. aureus* may also be different at the strain-level: for example, the MRSA strain USA300 has been shown to be hypervirulent via the overproduction of toxins and its fitness in the acidic environment of the skin, which combined may explain its dominant role in causing skin infections.<sup>102</sup> The virulence of staphylococcal strains is known to be influenced by the quorum sensing system which results in the responsive control of the accessory gene regulation.<sup>103</sup> As such, it was reported that even a single mutation of the accessory gene regulator quorum sensing system can alter MRSA phenotypes resulting in higher virulence associated with acute SSTIs.<sup>104</sup> To summarize, the skin microbiota allows for a complex crosstalk between the host and the microbiota which upon dysbiosis or imbalance may lead to the infection of the skin by pathogenic bacteria.

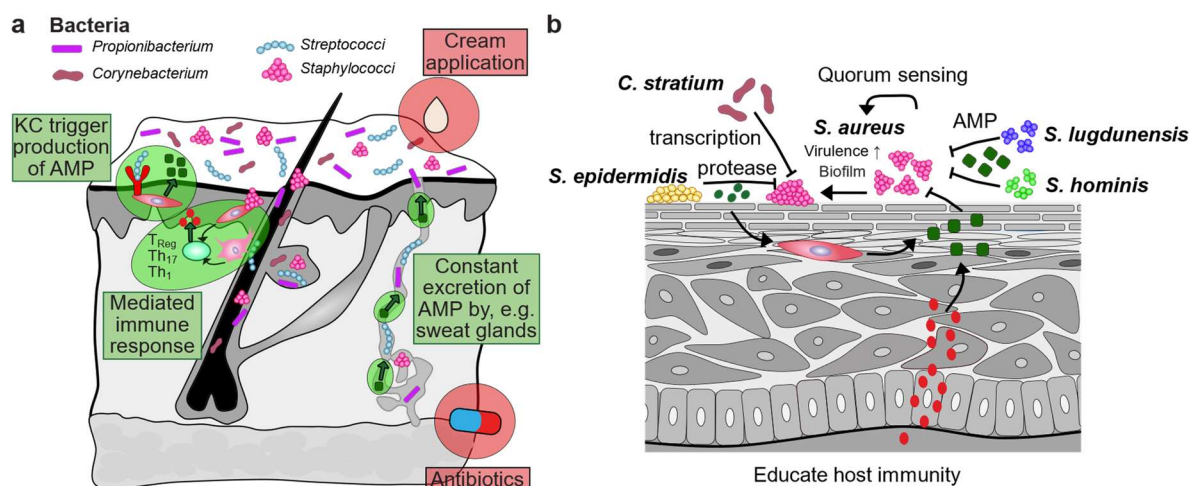


Figure 2: Schematic illustration of the skin microbiome. a) The healthy skin microbiome and selected intrinsic and extrinsic factors that can influence bacterial colonization. b) Control of the commensal growth of *S. aureus*. AMP attenuate the growth of *S. aureus* and can be produced by other bacteria, such as *S. lugdunensis* and *S. hominis*. The host response includes the production of AMP by keratinocytes which may be stimulate via cytokine secretion or direct stimulation of bacteria. *S. epidermidis* can reduce the biofilm formation of *S. aureus* by secretion of a protease and *C. stratum* influences the gene transcription of *S. aureus*. The peptide quorum sensing system of *S. aureus* influences its virulence. KC = keratinocytes.

### 2.1.3 Bacterial skin and soft tissue infections

In the following chapter, the reader will be provided with an overview of the burden and types of SSTIs, and the common bacteria associated with these infections. This lays the foundation to highlight the importance and challenges faced for the development of new treatment options for SSTIs as developed in the work of this thesis.

Considering that the skin is the largest organ of the human body, it comes to no surprise that at times the barrier structure it constitutes is disrupted allowing for the external invasion of pathogens. Such unwanted and maleficent invasion of pathogens, i.e. bacteria, fungi, parasites and viruses, are ubiquitous and suffered by almost everyone at some point in their life. Importantly, SSTIs can be considered a high-volume condition and since the early 2000s multiple studies even reported an increase in SSTIs. For example, from 1997 until 2005 the number of SSTIs in the US almost doubled accounting for 14.2 million ambulatory visits in 2005 according to Hersh *et al.*<sup>105</sup> Likewise, data from the Medical Expenditure Panel Survey showed an estimated 2.4 million patients in the US experiencing SSTIs in 2000 which increased to 3.3 million in 2012 across all healthcare settings and this trend was significantly driven by the two-fold increase of SSTIs in elderly patients.<sup>1</sup> However, Miller *et al.* reported contradicting trends based on ambulatory and inpatient visits in the US in an multicenter, retrospective cohort of 50 million commercially insured patients aged 0 – 64 years finding stable incidence rates of SSTIs from 2005 until 2010. However, they still observed 2.3 million cases of SSTIs which was higher than urinary tract infections or pneumonia, highlighting the relative importance of infections affecting the skin.<sup>106</sup> One study based on clinical and administrative data of 86 US emergency departments of academic medical

centers even reported a decreasing incidence of SSTIs between 2009 until 2014.<sup>107</sup> Therefore, it is not entirely certain whether the drastic increase of SSTIs in the beginning of the 21<sup>st</sup> century is still an ongoing trend. However, SSTIs certainly are a burden for the healthcare system and are suggested to be the third most common reason for hospital visits.<sup>108</sup> Not only does the high incidence of SSTIs strain medical facilities and the healthcare system, it also constitutes an overall economic burden. For example, Tun *et al.* estimated a tripling of US direct expenditures corresponding to around 15 b\$ in 2012, which was predominantly caused by rising outpatient and office-based visits.<sup>1</sup> These studies highlight the burden of SSTIs and that developing new treatment options could benefit many patients and the health care system. In general, the extent and severity of such infections varies greatly and correspondingly the treatment and management of it.

### ***Categorizing SSTIs***

To analyze the treatment and management of SSTIs and define shortcomings, one first needs to understand the pathophysiology of SSTIs. SSTIs are microbial invasions of the skin affecting the epidermis, dermis, hypodermis or even the skeletal muscles. The colonization of pathogens results in a host-response characterized by erythema, oedema, warmth, tenderness, itching, blistering, discharge, and/or pain.<sup>109</sup> The classification of SSTIs is complex and there is not one universally accepted categorization yet. For example, SSTIs may be classified depending on the anatomical site of infection, their microbial etiology or by their severity of local and systemic symptoms.<sup>110</sup> However, the classification of SSTIs provided by the Infectious Disease Society of America (IDSA) in their updated guidelines from 2014 may be summarized as the following: (i) impetigo or ecthyma, (ii) nonpurulent SSTIs (including erysipelas, (recurrent) cellulitis, and necrotizing infections), (iii) purulent SSTIs (including furuncle, carbuncle, and (recurrent) abscesses), (iv) surgical site infections (SSIs), (v) animal and human bite wounds (including cat scratch disease), (vi) infections in the immunocompromised host (including bacillary angiomatosis, cancer patients with neutropenia, or patients with cellular immunodeficiency), (vii) myonecrosis, and (viii) pyomyositis.<sup>4</sup> In the scope of this thesis, no specific type of SSTIs is targeted; therefore, a general overview will be provided for different SSTIs to understand the differences in their clinical presentation as summarized in Figure 3.

### ***Superficial infections: impetigo & ecthyma***

Impetigo is a superficial, contagious infection of the skin most commonly caused by *S. aureus* or beta-hemolytic *streptococci* and can affect previously healthy skin (primary impetigo) or originate at sites of abrasion, trauma or underlying conditions (secondary impetigo).<sup>111</sup> On the one hand, it can present itself as a nonbullous manifestation where lesions form from papules that progress to vesicles and pustules which ultimately break and form a thick, golden-colored crust and blisters. On the other hand, the bullous manifestation presents itself with enlarged vesicles filled with clear, yellow and later turbid, dark fluid that upon breakage leave a thin brown crust.<sup>112</sup> This clinical manifestation of impetigo is due to an exfoliative

---

toxin of *S. aureus* causing the loss of cell adhesion in the epidermis.<sup>113</sup> Bullous impetigo preliminary affects younger children, and if present in adults with appropriate demographic risk factors could indicate an undiagnosed HIV infection.<sup>114</sup> Ecthyma is the ulcerative form of impetigo often resulting from ineffective treatment of impetigo which affects deeper skin layers such as the dermis and is commonly caused by the beta-hemolytic *streptococci* and sometimes also by *S. aureus*.<sup>111</sup>

### ***Non-purulent SSTIs***

While impetigo and ecthyma affect the outer keratin layer of the epidermis which results in the formation of a crust, bacteria can also infect the skin without the involvement of the keratin layer in the non-purulent infections called erysipelas and cellulitis.<sup>115</sup> Erysipelas and cellulitis are caused from the colonization of bacteria, most commonly beta-hemolytic *streptococci* and *S. aureus*, entering through breaches in the skin barrier and manifest as regions of erythema, oedema, and warmth. Erysipelas affects the outer skin such as the epidermis and upper dermis and presents with raised, well-demarcated borders of infected skin and bright red coloration. In cellulitis the bacterial colonization extends into deeper skin layers such as the dermis and the upper subcutaneous fat resulting in less defined edges of infected skin compared to erysipelas.<sup>116</sup> The most severe type of non-purulent skin infections are necrotizing forms of cellulitis, fasciitis, or myositis which affect the dermis and hypodermis, fascia or skeletal muscles, respectively.<sup>117</sup> Necrotizing soft tissue infections (NSTIs) are rare but lethal bacterial infections of deeper soft tissues caused by bacterial entry through a break in the epithelium from traumas, cuts or burns.<sup>118</sup> NSTIs are characterized by necrotizing cells and gangrene and therefore have been referred to in the lay press as flesh-eating disease. They might be caused by a variety of bacteria such as streptococcal, staphylococcal, enterococcal, or *Enterobacteriaceae* species, and two-thirds of NSTIs are polymicrobial.<sup>119</sup> Importantly, NSTIs result from clotting of small blood vessels which prevents sufficient penetration of white and red blood cells into the infected tissue thus allowing more aggressive bacterial growth and causing cell death. The vascular thrombosis is warranted by a combination of strong microbial virulence and an insufficient host defense response with risk factors being diabetes, overweight, IV drug abuse, and peripheral arterial disease among others.<sup>120</sup>

### ***Purulent SSTIs***

If the SSTI involves the production of pus, the infection is referred to as a purulent SSTI with common examples being folliculitis, furuncles, carbuncles and abscesses listed here for their increasing severity. *S. aureus* is the most common causative pathogen for purulent SSTIs and infects a damaged or inflamed hair follicle in folliculitis, furuncles, and carbuncles.<sup>121</sup> However, other bacteria such as *streptococci*, *S. epidermidis* or *P. aeruginosa* have been implicated in those infections with the latter one often spread via contaminated water (therefore referred to as the hot tub folliculitis). Bacterial folliculitis can affect the superficial and deeper parts of the hair follicle and presents itself in form of small pustules and erythema

---

around the follicular orifices.<sup>121</sup> Typically, the pustules of folliculitis heal without scarring within a couple of days, however, if the healing and/or treatment is unsuccessful, the bacteria may spread into the surrounding tissue resulting in the formation of a furuncle.<sup>122</sup> Furuncles are known as boils characterized by warm, painful, erythematous, pus-filled lumps around a single hair follicle with a yellow or white point which often heal with scarring after drainage or discharge.<sup>123</sup> If the lumps form around and involve the infection of multiple hair follicles, they are called carbuncles that present as large, deep, swollen, erythematous and painful masses of pus that drain through multiple tracts.<sup>124</sup> Similar to carbuncle, abscesses are large, swollen, painful, fluctuant nodules filled with pus, but unlike carbuncle they form without the involvement of infected hair follicles and extend into the dermis and subcutaneous fat and may present with surrounding cellulitis.<sup>125</sup>

### ***SSTIs after external injury: SSIs and bite wounds***

Infections occurring within 30 days after surgery are referred to as SSIs and often derive from bacteria of the normal skin flora such as *S. aureus*.<sup>126,127</sup> However, in surgeries involving body cavities and especially if large contaminations of the surrounding tissue occurred other bacteria such as *Enterococcus faecalis* may be involved in SSIs. It is expected that all surgical wounds are to some degree contaminated but progression into SSIs is prevented if the host defense reaction is efficient, pathogenic virulence is minor, and sterile procedure was performed.<sup>126</sup> SSIs can vary in severity from (i) superficial incisional infections involving the epidermis, dermis and upper hypodermis to (ii) deeper incisional infections of the fascia and muscle or to (iii) organ infections. While superficial SSIs present with symptoms similar to erysipelas and cellulitis with involvement of pus, deep SSIs often involve abscess formation, fever, tenderness of the wound or even opening of the edges of the surgical incision.<sup>126</sup> Similar to SSIs, animal and human bite wounds are infections after external trauma caused to the skin that may resolve alone with an effective host defense system.<sup>128</sup>

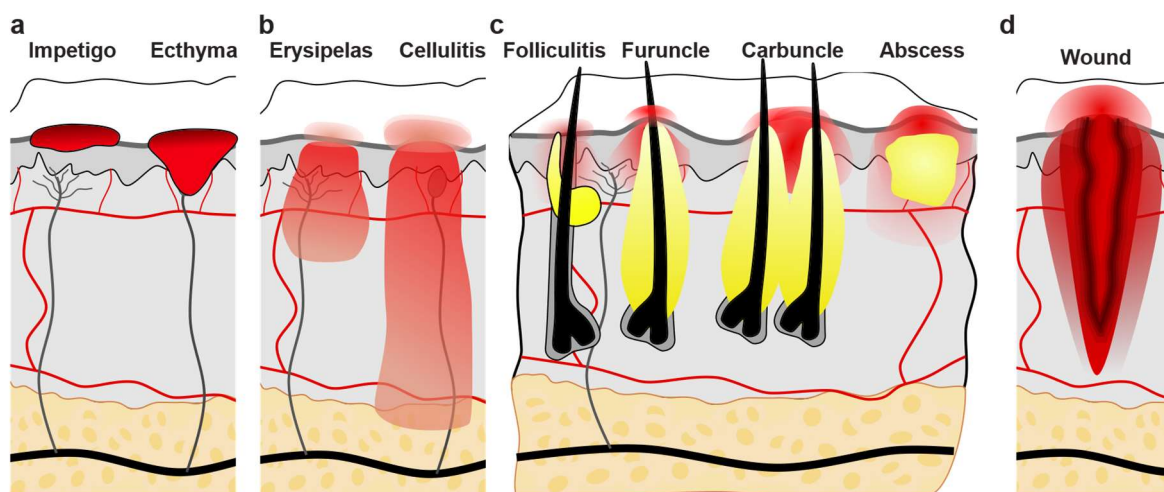


Figure 3: Illustration of the different common SSTIs, such as a) the superficial infections impetigo and ecthyma, b) the non-purulent infections erysipelas and cellulitis, c) purulent infections folliculitis, furuncle, carbuncle, and abscess, or d) SSTIs after an external wound such as bites, surgical incision or in diabetic ulcers.

However, the often polymicrobial infection of bite wounds does not only originate from the skin flora of the victim but is also reflective of the oral cavity of the biting animal or the microbiome of their ingested prey.<sup>129</sup>

### ***Diabetic foot ulcers are driven by insufficient host immune response***

Infections in the immunocompromised host carry their own difficulties depending on the immunodeficiency or -suppression at present. One common skin infection associated with a dysfunction of the immune system is the diabetic foot ulcer. In diabetic patients, a tissue injury to the foot is likely to heal hampered and slowly due to a combination of various factors such as an impaired vasculature, neuropathy, and insufficient host immune response. Such open wounds allow bacteria to colonize the tissue often in polymicrobial biofilm structures resulting in difficult-to-treat infections. A study by Smith *et al.* analyzed new and recurrent diabetic ulcers and found that 75 % of the ulcers were infected with multiple bacterial strains.<sup>130</sup> *S. aureus* and *Corynebacterium* are commonly found in diabetic ulcers and, while they may be commensal bacteria to the human skin, they may contribute to a pathogenic community in polymicrobial infections.<sup>131</sup> Due to the physiology of the diabetic foot ulcers which comprises necrotic tissue and low oxygen levels, facultative or obligate anaerobes are highly associated with the microbiology of such ulcers, too.<sup>130–132</sup> Furthermore, *P. aeruginosa*, *enterococci* strains, and *Enterobacteriaceae* are frequently found in diabetic ulcers.<sup>130</sup>

### ***The role of S. aureus and MRSA in SSTIs***

As outlined above the microbiome of the skin is highly variable and diverse, and likewise is the microbiology of SSTIs. Of global interest and also a major point of focus of the work in this thesis, is the bacteria *S. aureus*.

Multiple studies reported the microbiology of various SSTIs within the past decades and the rates of isolated pathogens from SSTIs of five selected studies published between 2007 to 2019 are summarized in Table 1. The type of etiological pathogens and their identification is highly dependent on the sampling procedure, microbiological laboratory testing and class of SSTIs,<sup>133</sup> and varied significantly in the studies selected in Table 1. Despite these variabilities, all the studies found that the majority of SSTIs are infected by gram-positive bacteria, specifically the bacteria *S. aureus*. In fact, a driving factor in the reported increase of SSTIs in the early 2000s may be associated with the rise in *S. aureus*-associated SSTIs: an analysis of the Nationwide Inpatient Sample and Census Bureau data revealed a 123 % increase in hospitalizations due to *S. aureus*-associated SSTIs from 2001 until 2009.<sup>134</sup> Of specific concern in this regard, is the rising frequency of MRSA-associated SSTIs since they may be particularly difficult to treat due to resistance-associated limitations in antibiotic availability and the hypervirulence of MRSA.<sup>135</sup> In the context of SSTIs, the incidence of MRSA lies between 11 to 37% (Table 1); however, other studies reported a more dominant role of MRSA in skin infections.<sup>136,137</sup>

Table 1: Bacterial species commonly isolated from SSTIs summarized for selected studies, the total percentage of isolates quantified for specimen may add up to above 100% for some studies depending on how polymicrobial infection were considered. <sup>a</sup>:“Other” specimen include samples taken from tissue, body fluid, or other body specimen such as abscesses, pustules, boils etc. Respiratory, cerebrospinal fluid and urine samples are not considered. <sup>b</sup>: all SSTIs diagnosed in in- and outpatient settings at infectious disease medical centers. Data taken and summarized from references <sup>138-142</sup>. CoNS: coagulase-negative *Staphylococci*.

	Moet <i>et al.</i> (2007) <sup>138</sup>	Ray <i>et al.</i> (2013) <sup>139</sup>	Tiwari <i>et al.</i> (2014) <sup>140</sup>	Garau <i>et al.</i> (2015) <sup>141</sup>	Esposito <i>et al.</i> (2019) <sup>142</sup>
<b>Type of SSTIs</b>	purulent SSTIs	SSTIs according to ICD9-CM	Discharging SSTIs	Complicated SSTIs	SSTIs <sup>b</sup>
<b>Population</b>	North America, 1998-2004	North Carolina US, 2009-2011	India, 2009-2011	European, IV antibiotic, 2010-2011	Italy, 2016-2017
<b>SSTIs tested, n</b>	5837	108,457	105	600	291
<b>Sampling</b>	Invasive sampling or swab	Blood (14%), other <sup>a</sup> (86%)	Pus and fluid	Blood (66%), swab (47%), aspiration (9%), biopsy (13%)	swab, biopsies, blood
<b>Isolated bacterial species (%)</b>					
<b>Gram-positive</b>	61	94	71	76	56
- <i>S. aureus</i>	45	81	66	41	38
- MRSA	36	37	/	11	22
- <i>E. faecalis</i>	<i>Enterococci</i>	/	/	6	7
- <i>E. faecium</i>	spp.: 9	/	/	2	2
- $\beta$ -haemolytic <i>Streptococci</i>	4	10	<i>Streptococci</i> spp: 5	17	1
- CoNS	3	/	/	12	5
<b>Gram-negative</b>	32	14	18	34	33
- <i>Pseudomonas</i>	11	/	3	/	17
- <i>E. coli</i>	7	/	4	/	7
- <i>Acinetobacter</i>	/	/	9	/	3

While it is unclear whether those differences in MRSA prevalence in SSTIs may be linked to variations in study design and sampling, it is a well-established fact that the MRSA prevalence varies globally with the US and Latin America specifically affected.<sup>143</sup> A common MRSA strain isolated from clinical specimen of SSTIs is the community-associated USA-300 which has also been used in work included in this thesis.<sup>144</sup>

Besides *S. aureus*,  $\beta$ -haemolytic *Streptococci* are common causative gram-positive pathogens of SSTIs with its prevalence ranging from 1 to 17% according to the studies presented in Table 1. The most common gram-negative bacteria to cause SSTIs is *P. aeruginosa* and some of these SSTIs such as burn wounds are associated with high morbidity and mortality.<sup>145</sup> Finally, it should be noted that many SSTIs are polymicrobial in nature with multiple pathogenic and commensal bacteria co-colonizing the infected tissue.<sup>146</sup>

#### 2.1.4 Current treatment strategies for bacterial skin infections

In addition to protecting the body from the invasion of pathogens, the *stratum corneum* also constitutes a penetration and permeation barrier against molecules and particles. The limited penetration of molecules challenges the successful drug delivery of topical and transdermal

drug formulation. Overcoming this biological barrier to improve dermatological drug delivery has been an extensive field of research and both formulation- and device-based approaches to improve transdermal drug delivery have been developed.<sup>147</sup> Alternatively, drug formulations can be administered through the oral or parenteral route which results in cutaneous absorption depending on the chemical and physical characteristics of the drug (Figure 4). In this chapter, the current treatments and their limitations for bacterial SSTIs are explained. This will form the basis in establishing the need that can be addressed with the novel treatment option, namely MNs, developed in the work of this thesis.

### ***Treating bacterial SSTIs***

The treatment of bacterial SSTIs is as complex as the microbiological etiology of skin infections and often involves the administration of antibiotics. A simplified treatment algorithm provided by the IDSA differentiates between purulent (such as furuncle, carbuncle, and abscesses) and nonpurulent infections (such as necrotizing infections, erysipelas and cellulitis).<sup>4</sup> For purulent SSTIs, the recommended therapy and management is incision and drainage first with additional empiric or defined antibiotic therapy depending on the severity of the infection. On the other hand, nonpurulent SSTIs ought to be treated with oral antibiotics in case of mild infections and with oral and/or IV antibiotics for moderate to severe infections. Culture and sensitivity analysis for severe disease progression is strongly recommended and in case of a suspected or confirmed MRSA infection, the IV administration of the antibiotic VAN is suggested.<sup>4</sup> The role of topical antibiotics for the treatment of SSTIs is limited to minor infections, such as nonbullous impetigo, that involve only few lesions.

### ***Mostly antibiotics with low molecular weight are administered topically***

Topical antibiotic delivery has several advantages such as limited systemic exposure and thus reduced systemic side effects, local delivery of high antibiotic concentrations to superficial skin layers, and ease of administration. However, topical and transdermal drug delivery is generally limited to molecules of specific physical and chemical properties. Due to the effective barrier function of the skin, only small molecules below molecular sizes of approximately 500 Da are considered to effectively penetrate the *stratum corneum*.<sup>148</sup> Besides the size restriction, drugs appropriate for topical drug delivery typically need to be lipophilic or amphiphilic in nature to effectively diffuse across both the lipid-rich cutaneous extracellular matrix and through hydrophilic cellular spaces.<sup>149</sup> To improve topical drug delivery, formulation-based approaches such as permeation enhancers<sup>150</sup> or nano-formulations<sup>151</sup> have been studied. Alternatively, the use of devices has been explored in the scientific literature to improve the delivery of antibiotics, i.e. iontophoresis, or MNs.<sup>147</sup> However, in the dermatological care and the clinics, topical antibiotics are commonly administered through creams, ointments, or gels. The most common topical antibiotics used for bacterial SSTIs are mupirocin, fusidic acid, retapamulin, erythromycin and neomycin.<sup>152</sup> However, their bioavailability, especially in deeper skin layers, is limited and there is a high risk of patients storing the topical formulations and inappropriately using them after self-

---



diagnosis.<sup>153</sup> Limited penetration depth and inappropriate use have resulted in rising antibiotic-resistance to topical antibiotics and therefore it is required to responsibly use topical antibiotics and/or develop improved transdermal delivery strategies.<sup>154</sup>

### **Oral and IV antibiotic delivery**

Many SSTIs need to be treated with an antimicrobial care often in form of oral or IV administration of antibiotics. While impetigo affecting only few lesions may be successfully managed by a topical antibiotic, for patients with multiple and/or large lesions or with progression to ecthyma oral antibiotics are recommended. For both purulent and non-purulent SSTIs systemic antibiotic therapy should be considered if the patient presents with signs of systemic infection. Initially and for mild infections, oral antibiotics, such as penicillin VK, cephalosporin, dicloxacillin, doxycycline, or clindamycin can show sufficient treatment effect.<sup>4</sup> However, if the SSTIs progresses during oral antibiotic therapy, if the patient is immunocompromised, or if there are clinical signs of deeper or necrotizing infections, the IV administration of antibiotics is recommended. IV antibiotics commonly administered for such severe SSTIs are oxacillin, cefazolin, daptomycin, clindamycin, and VAN.<sup>4</sup> In general, oral antibiotics have advantages over IV administered antibiotics such as the absence of injection-related infections, lower drug costs, no need for trained personnel and equipment for drug administration, earlier hospital discharge and higher patient comfort.<sup>155</sup> However, IV antibiotics have 100% bioavailability whereas oral antibiotics might suffer from first-pass metabolism and incomplete absorption.<sup>156</sup>

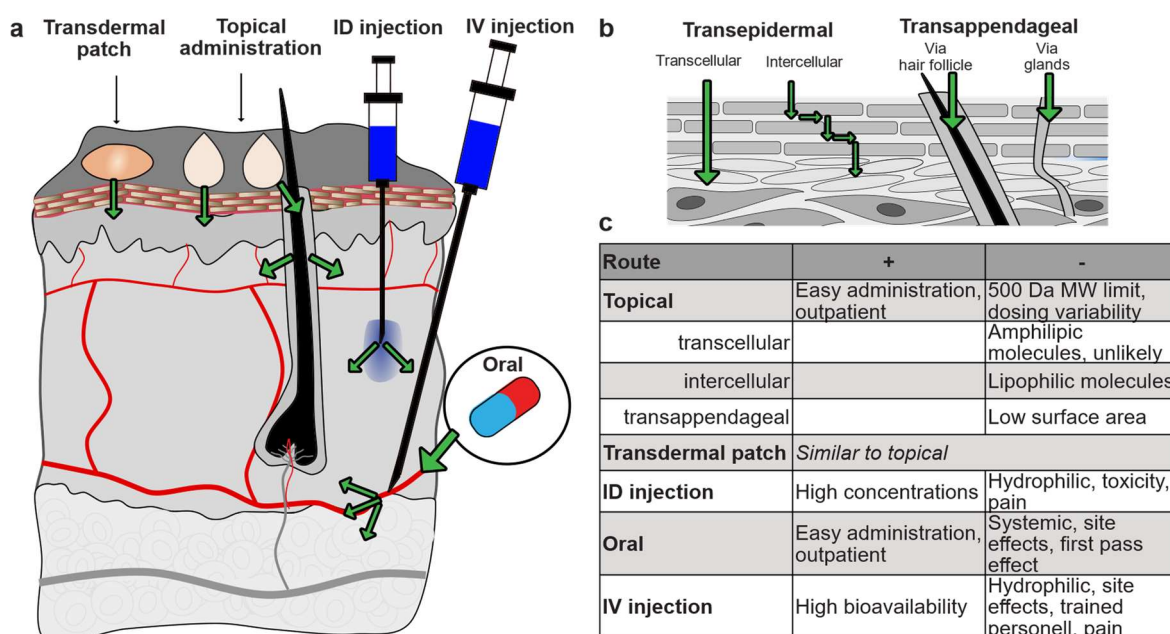


Figure 4: Schematic illustration and overview of skin drug delivery routes. a) Schematic visualizing the delivery routes to provide drug into the skin. b) Detailed overview of the drug penetration through the outer most permeation barrier, the *stratum corneum*. c) Table summarizing the main delivery routes and their advantage and disadvantages and/or challenges. ID = intradermal.

Furthermore, the absorption via the gastrointestinal tract involves the drug permeation across a biological barrier, thus antibiotics suitable for oral administration are restricted by their physicochemical properties (i.e. size, lipophilicity). Some studies evaluated the non-inferiority of oral antibiotics compared to their administration IV, showing that in some cases the parental route may be substituted by oral antibiotics.<sup>157–159</sup> However, this is highly dependent on the specific patient case and the choice of antibiotic because some antibiotics when given orally show significantly inferior bioavailability as those given IV.<sup>156</sup> Finally, due to the restrictions in the physicochemical properties some antibiotics cannot be successfully given orally.

### ***VAN is the gold standard for MRSA-associated infections***

One such antibiotic that cannot be given orally due to physicochemical properties is the glycopeptide VAN. VAN is a large peptide with a molecular weight of almost 1.5 kDa and it is hydrophilic in nature with a negative logarithmic octanol-water partition coefficient.<sup>160</sup> It acts by inhibiting the bacterial cell wall synthesis through binding of the terminal D-alanyl-D-alanine moieties of the peptides involved in crosslinking the N-acetylmuramic acid and N-acetylglucosamine polymer backbone of the cell wall.<sup>161</sup> Therefore, it is mainly active against gram-positive bacteria including *S. aureus* and has been the drug of choice for treatment of MRSA-associated infections.<sup>162</sup>

VAN cannot be given orally (unless gastrointestinal treatment is intended) since the absorption into the circulation is limited by its physicochemical properties (i.e. large size and high hydrophilicity). Therefore, it is mostly administered via IV injection; however, in regard to treatment of SSTIs, the effectiveness of VAN may be limited due to its poor skin penetration caused in part by the same unfavorable physicochemical properties that limits its gastrointestinal absorption.<sup>163</sup> As such, Skhirtladze *et al.* found that only around 30% of VAN administered into the plasma reaches the soft tissue in healthy patients, which is further reduced to approximately 10% in diabetics.<sup>164</sup> There have been some attempts in the scientific literature to develop topical or intradermal formulations of VAN for the treatment of MRSA<sup>165–168</sup> but to the best of the author's knowledge such inventions have not reached the stage of clinical testing.

### ***Treatment of resistant SSTIs***

The rise of antibiotic resistance threatens global health by reducing the successful outcome of antibacterial therapies. To address this issue, we urgently need to (i) increase the development of novel antibiotics,<sup>169</sup> and (ii) maintain and improve the antibacterial activity of current antibiotics. The urgency for the need of substantial efforts in the development of new antibiotics is specifically highlighted by the recent letter on the 16<sup>th</sup> of November 2022 on behalf of major pharmaceutical stakeholders such as Merck to the US government to enact the PASTEUR Act aiming to provide international regulation for financial incentives and stimulation of the antimicrobial pipeline.<sup>170</sup> Alternatively, combination therapy that improves the antibiotic efficiency via synergistic interactions may lower the clinical risk of resistance

---

development and thus the loss of antibacterial activity of current antibiotics.<sup>5</sup> While SSTIs are often not life-threatening conditions, antibiotic-resistant bacterial strains, e.g. MRSA, on the skin may easily spread via direct and indirect contact transmission.<sup>3</sup> Therefore, novel treatment options for resistant-SSTIs to maintain antibiotic efficiency are important. This importance is further highlighted by the categorization of the SSTI-associated pathogen *S. aureus* as a high global priority for the development of new antibacterial treatments by the World Health Organization.<sup>171</sup> The development of such innovative antibacterial treatments to improve the efficiency of antibiotics for the therapy of SSTIs was a main focus of the work presented in the thesis here.

### **2.1.5 Thermotherapy in dermatology**

The use of elevated temperatures and even heat for the enhancement of the therapy of various diseases is an ancient practice. The healing and medical effect of thermotherapy includes the alleviation of symptoms related to musculoskeletal and soft tissue injuries and diseases by increasing the blood circulation,<sup>172</sup> cellular activity,<sup>173</sup> and stimulating of the immune response.<sup>174</sup> Many of these advantages can already be elicited with benign hyperthermia using target temperatures between 39 to 42 °C.<sup>175</sup> Applying even higher temperatures above 42 °C may advance the therapy of diseases such as cancer or infections by ablating cancerous or pathogenic cells.<sup>176</sup> Yet, it is important to finely control the temperature window of the applied hyperthermia since tissue heat above 45-50 °C can cause protein denaturation and blood coagulation.<sup>6,7</sup> To apply such elevated temperatures has long been an accepted medical practice in the process of cauterization to close the blood circulation after amputation, remove tumors or prevent infections. Already Hippocrates wrote:

*“Those diseases which medicines do not cure, iron cures; those which iron cannot cure, fire cures; and those which fire cannot cure, are to be reckoned wholly incurable.”*

However, nowadays it is a well-established fact that the tissue damage after cauterization may increase the risk of infection due to decreased host immune responses and increase of necrotic debris from severe tissue damage which contribute to substantial bacterial growth.<sup>177</sup> Therefore, and with the invention of antibiotics, SSTIs are not commonly treated with cauterization to date. However, increasing levels of antibiotic resistance and a limitation in newly developed antibiotics has recently shifted the scientific interest back to the use of mildly elevated temperatures up to 60 °C for the therapy of various skin diseases such as SSTIs.<sup>178</sup>

#### ***Bacteria adapt to grow in temperature niche***

Bacteria have adapted to specific environmental conditions and the niches they inhabit can be species- and strain-specific.<sup>179</sup> One such condition is temperature, and bacteria can be categorized based on the temperature they preferentially grow at. Psychrophiles and thermophiles adapted to low (i.e. 0-20 °C) or high temperatures (i.e. 50-110 °C), respectively,

whereas bacteria that commonly colonize the human body are referred to as mesophiles. Mesophiles favor temperatures ranging from 33-41 °C and although they are able to acquire spontaneous mutations to resemble thermophilic variants,<sup>180</sup> those mutations are rare, require major genetic modifications, and rather constitute a long-term evolutionary transition.<sup>181,182</sup> Therefore, hyperthermia has been explored to treat bacterial infections and the therapy of SSTIs may benefit from additional thermotherapy.<sup>183</sup>

### ***Hyperthermia affects bacteria via direct damage and increased susceptibility to antibiotics***

The bacteria commonly associated with SSTIs, namely *S. aureus*,  $\beta$ - haemolytic *streptococci*, *P. aeruginosa* and *Escherichia coli*, are mesophiles growing in temperatures between 10 to 45 °C but preferably at physiological temperatures of approximately 37 °C.<sup>108</sup> Application of elevated temperature can interfere with the survival of these bacteria and induce cell death via damages to their cell wall and membrane,<sup>184</sup> to their deoxyribonucleic acid (DNA),<sup>185</sup> or via a reduction of their protein synthesis (Figure 5).<sup>186</sup> Furthermore, heat may increase the susceptibility of planktonic bacteria to antibiotics even in resistant strains.

For example, antibiotic-resistance may involve mutations in the cell wall<sup>187,188</sup> or membrane resulting in the reduced action and permeability of the antibiotic into the planktonic cells. Thus, increasing the cross-membrane permeability of antibiotics via heat can re-sensitize previously resistant bacteria.<sup>189</sup> In addition, bacteria often form biofilms which are rich environments of bacterial cells embedded in polysaccharides and proteins. It has been shown that elevating the temperature of *S. aureus* biofilms results in reduction of the mechanical integrity of the biofilm<sup>190</sup> and an increase in antibiotic penetration into the biofilm, thus increasing the susceptibility of bacteria to antibiotics.<sup>191,192</sup> Both the direct damage by heat and the synergistic effect of hyperthermia and antibiotics may constitute novel therapeutic interventions in the treatment of SSTIs. Importantly, it is less likely that bacteria acquire resistance against hyperthermia treatment opposed to antibiotics, since the physical heat damage harms multiple pathways within the pathogenic cell.<sup>23</sup> However, caution is warranted since the shock response to heat treatment may induce cross protection against antibiotics by inducing the bacteria to enter a dormant state.<sup>193,194</sup> A novel pathway to provide hyperthermia and antibiotics to the infections side is by using nanomedicine.

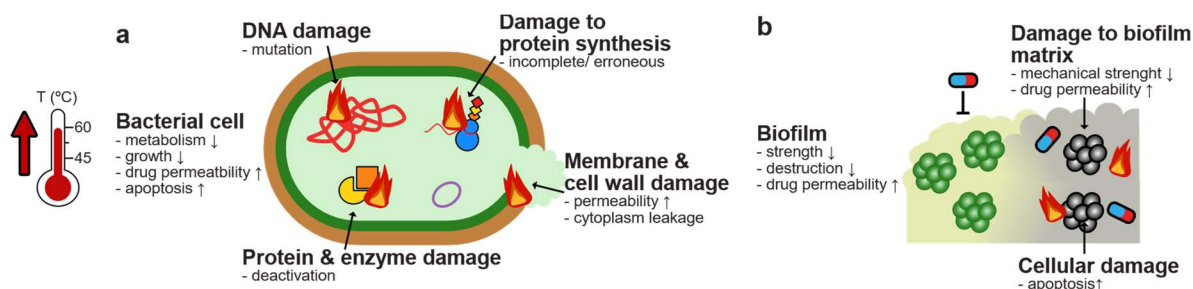


Figure 5: Schematic depiction of damage by slightly elevated heat of 45 – 60 °C on bacteria. Illustration of selected (a) cellular damages in the single bacterial cell, or (b) on the bacterial biofilm.

## 2.2 Nanomedicine for microbial infections

Nanomedicine involves the usage of nanomaterials for medical applications for the diagnosis, prevention, and treatment of diseases.<sup>195</sup> Nanomaterials are materials with at least one dimension in the nanoscale (~1-100 nm) which in size is comparable to 100,000<sup>th</sup> of a human hair.<sup>196</sup> The increased interest in the field of nanotechnology is due to the physicochemical characteristics of nanomaterials which are different from either the molecules and atoms alone or the bulk material. These unique physicochemical characteristics allow for novel applications, functionalities, and interactions with nanomaterials. Nanomaterials can be made from organic, inorganic, or biologically derived materials and their biomedical functionalities can range from using them as drug vehicles (i.e. for drug targeting) to exploiting their inherent characteristics (i.e. photothermal properties).

Infections are a global disease burden which were estimated to contribute to more than 20% of global deaths.<sup>197</sup> However, effective disease management is challenging owing to a lack of safe and effective drugs, increase of pathogen resistance, and poor patient adherence. To improve the treatment of infectious diseases, nanomaterials have been studied due to their potential to (i) sustain the systemic delivery and enhance the bioavailability of antimicrobials, (ii) enable local and/ or targeted drug delivery, and (iii) overcome difficult-to-treat or resistant infections.<sup>8</sup> In the following chapters, the reader will be provided with an overview of how nanomaterials can and have already been used in the treatment of infections.

### *Nanomaterials enhance the treatment of infections by improving drug delivery*

The prolonged release of systemically administered drugs may advance patient compliance due to less complicated and frequent dosing regimens. Such sustained drug delivery can be enabled via formulation in nanocarriers made from polymers or lipids.<sup>198,199</sup> Some formulations are already on the market or in clinical trials. For example, AmBisome<sup>®</sup> is a formulation of the antimicrobial amphotericin B in liposomes smaller than ~100 nm that is approved by the Food and Drug Administration (FDA) for the treatment of fungal infections.<sup>200</sup> More recently, the company Insmed Inc. developed an inhalable liposomal formulation of the antibiotic amikacin (ARIKAYCE<sup>®</sup>) which is marketed for the treatment of *M. avium*<sup>201,202</sup> and in clinical trials up to phase 3 for *P. aeruginosa* associated lung infections.<sup>203</sup>

### *Local antibiotic delivery by nanocarriers*

Besides a sustained release, nanocarriers may also allow for an improved local and/or targeted antibiotic delivery which may reduce side effects.<sup>204</sup> Polymyxin B is a highly potent antibiotic with limited application for systemic delivery due to severe side effects such as nephrotoxicity. Encapsulation of polymyxin B into liposomes results in the improvement of the drug efficiency and reduction of the minimum inhibitory concentration (MIC), which is caused by membrane fusion of the nanocarrier to the bacteria *P. aeruginosa* with subsequent high drug release locally to the bacterial cell.<sup>205,206</sup> Gelatine NPs have been developed for the encapsulation of VAN, which enables the controlled release of VAN only in presence of

gelatinase-positive bacterial strains achieving targeted killing of *S. aureus*, but not the mutualistic *S. epidermidis*.<sup>207</sup>

### ***NPs can help in overcoming resistance in bacteria by protecting antibiotics***

Both the sustained and local delivery of antibiotics aid in the treatment or prevention of antibiotic-intermediate or -resistant bacteria by increasing the duration and level of the drug above MICs in the tissues. However, nanomaterials also allow for overcoming resistant infections through various pathways. For example, a common resistance mechanism in bacteria involves the enzymatic degradation of antibiotics. Incorporating the antibiotic imipenem into NPs protected the drug from degradation by carbapenem-degrading enzymes typically expressed by the imipenem-resistant pathogen *P. aeruginosa*.<sup>208</sup>

## **2.2.1 Inorganic NPs as antibacterial agents**

NPs may have intrinsic antimicrobial properties which directly interfere with bacterial survival. In the scope of the here presented work, a specific focus will be placed on the intrinsic antimicrobial activities of inorganic NPs.<sup>10</sup> Inorganic NPs can exert antibacterial effect from various mechanisms which often include (i) the release of antimicrobial metal-ions, (ii) the production of ROS, or (iii) the dissipation of heat in hyperthermia treatment.

### ***Release of antibacterial ions from inorganic NPs***

The release of ions from inorganic NPs results in bactericidal activity through multiple actions such as binding of the ions to thiol (-SH) groups in amino acids such as cysteine.<sup>9</sup> Ions can also increase the permeability of the bacterial cell wall. For example, silver ions can destroy cross-linking bonds of the peptide chain in the bacterial cell wall, resulting in cell disintegration.<sup>209</sup> Perforation of the bacterial cell wall in turn allows for an increased diffusion of further ions or drugs into the pathogen while causing a harmful leakage of cytoplasm. Inside the cell, ions might block the formation of S-S bridges of cysteine residues in proteins. Blocking of thiol bridges interferes with correct enzymatic processes or successful protein folding, thus decreasing cell metabolism.<sup>209</sup> Furthermore, metal ions such as silver ions seem to have a high affinity to form complexes with nucleic acid which interferes with appropriate genetic transcription impeding cell division.<sup>209</sup>

Many inorganic NPs dissolve in physiological media allowing high ion release, where prominent ion-releasing NPs being are made of copper, zinc, gallium, or silver (Ag).<sup>10</sup> Ag is by far the most investigated and employed antibacterial NP with multiple antibacterial products already in market, patented, and/or in clinical trials.<sup>210</sup> For example, the products SilvaGard<sup>®</sup> and SilvaSorb<sup>®</sup> by the manufacturer AcryMed Inc. uses Ag NPs in coatings for medical devices or as topical wound dressings for infected wounds.<sup>211</sup> However, unlike copper or zinc, Ag is not an essential trace metal in the human body and so there have been some concerns about Ag-induced host toxicities.<sup>209</sup>

### ***Antibacterial effect of ROS can be a double-edged sword***

Various NPs have been developed to interact in the cellular ROS homeostasis with an attempt to improve therapies focusing on the increased production of ROS for treatment of infections.<sup>212</sup> Nanomaterials can induce elevated levels of ROS through different routes. Some materials, e.g. TiO<sub>2</sub>, absorb energy from exogeneous light resulting in electron-holes that interact with oxygen and water thus creating radicals.<sup>213</sup> In addition, some nanomaterials also called nanozymes, e.g. Fe<sub>3</sub>O<sub>4</sub> NPs, show peroxidase-like activity catalyzing the conversion of H<sub>2</sub>O<sub>2</sub> into hydroxyl radicals in Fenton-like reactions.<sup>214</sup> In a similar fashion, metal NPs such as Ag are oxidized by H<sub>2</sub>O<sub>2</sub> forming reactive hydroxyl radicals.<sup>215</sup> The high reactivity of ROS results in direct damages to DNA, proteins, and lipids which results in reduced bacterial metabolism and death.<sup>216</sup>

However, specifically in the scope of SSTIs the use of ROS for antibacterial therapies needs to be handled with caution. ROS are a double-edged sword in the fight against infections: on the one hand, ROS are generated endogenously by cells for signaling processes or in the fight against infections; on the other hand, elevated ROS levels are associated with numerous abnormalities (i.e. cancerous growth).<sup>217</sup> As such, ROS-generation might be beneficial for initial clearance of the bacteria from the skin.<sup>218</sup> For example, photocatalytic activity of TiO<sub>2</sub> NPs controlled by UV light allows for antibacterial effects against the SSTI-associated bacterial strains *S. aureus*, *P. aeruginosa*, *E. coli* and *E. faecium*.<sup>219</sup> However, prolonged exposure to elevated levels of ROS is associated with chronic, non-healing wounds and inflammation.<sup>220</sup>

### ***Antibacterial hyperthermia from magnetic NPs***

As explained above in 2.1.5, elevated temperatures show direct antibacterial effects and may enhance antibiotic therapy in infections. Inorganic NPs can be used for biomedical application because of their capability to generate heat by absorbing energy from electromagnetic radiation. The two most common energy sources for generating hyperthermia from inorganic NPs are (i) an alternating magnetic field, or (ii) light in PTT.<sup>221</sup> Superparamagnetic iron oxide NPs (SPIONS) are the most commonly researched metal-based nanomaterials for magnetic hyperthermia. SPIONS are small ferromagnetic particles containing single magnetic domains. Upon placing SPIONS in alternating magnetic fields they magnetize resulting in flipping of the magnetic moment upon switching the direction of the magnetic field. This resonant excitation results in the generation of heat due to different pathways described by theories such as the Néelian and Brownian relaxation. According to the Néelian theory energy is dissipated in form of heat when the magnetic dipole within a NP flips, whereas the theory of Brownian relaxation refers to the physical rotation of the NPs.<sup>222</sup> SPIONS for magnetic hyperthermia have predominantly been developed for cancer therapies with the product NanoTherm<sup>®</sup> from the company Magforce AG already used in clinics for the treatment of brain tumors.<sup>223</sup>

In the field of anti-bacterial therapy in SSTIs, to the best of the author's knowledge, the use of magnetic hyperthermia from inorganic NPs is relatively scarce.<sup>224</sup> One publication

reported antibacterial activity of iron oxide NPs under an alternating magnetic field against *S. aureus* but this required temperatures up to 100 °C which may interfere with the clinical success of such therapy.<sup>225</sup> Kim *et al.* employed lower temperatures of 45 °C from iron oxide NP hyperthermia which partially reduced *S. aureus* growth and improved wound healing in mice.<sup>226</sup> Furthermore, combinational therapy of magnetic NP hyperthermia with antibiotics may constitute a prospective SSTI therapy, i.e. VAN is more effective against *S. aureus* biofilm under magnetic NP hyperthermia.<sup>191</sup> However, the limited application of SPIONS for SSTIs to date may partially be explained with the fact that iron oxide NPs can cause severe allergic reactions, as highlighted by the FDA's Boxed Warning in 2015 for the use of the iron oxide NP-based product Feraheme®.<sup>227</sup>

### ***Antibacterial PTT from inorganic NPs***

PTT is a widely researched field for the generation of local heat in the ablation of bacterial infections.<sup>23,24</sup> In PTT, often inorganic NPs are used to absorb energy from photons of electromagnetic radiation and dissipate the energy in form of heat for localized hyperthermia. In the scope of this thesis, inorganic NPs-based PTT platforms for the treatment of SSTIs and in interaction with the antibiotic VAN will be highlighted.

The use of inorganic NPs for PTT therapy against bacterial infections in the skin and for improved wound healing is increasingly researched within the last decade. Already in 2016 Khan *et al.* evaluated the potential of Au nanorods (NRs) for the treatment of *P. aeruginosa* associated wounds in mice.<sup>228</sup> This was soon followed by Li *et al.* in 2017 who developed polymer films with graphene oxide coated Au nanospheres to eradicate *S. epidermidis* in a mice model.<sup>229</sup> Other groups also developed PTT-NPs platforms to treat *E.coli*<sup>230</sup> and MRSA<sup>231</sup> in cutaneous infections. The target temperatures in these studies reached 52 – 60 °C with required laser intensities up to 2 W cm<sup>-2</sup>.<sup>229</sup> Such high laser intensities may limit the potential of clinical translation of PTT because the permissible exposure limit in skin should be between 0.3 – 1.0 W cm<sup>-2</sup> at 780 – 1050 nm near-IR laser wavelength, according to the American Standard for Safe Use of Lasers.<sup>232</sup> To increase the therapeutic outcome of PTT while decreasing the necessary laser intensity, PTT is often delivered in synergy with other antibacterial mechanisms or drugs.

One way to improve NP-based PTT is by leveraging additional antibacterial properties of the NP system, such as ion release, or ROS generation. Various studies successfully treated SSTIs caused by *S. aureus*<sup>233–237</sup> or *E. coli*<sup>238,239</sup> with such multi-modal antibacterial NP-PTT systems employing inorganic nanomaterials such as copper, zinc, graphene oxide, carbon or Au. Most notably was the study by Li *et al.* who incorporated zinc into Prussian blue NPs for combined ion release and heat treatment, eradicating MRSA in SSTIs more efficiently than IV VAN or topical antibiotics such as fusidic acid at a low laser intensity of 0.3 W cm<sup>-2</sup>.<sup>240</sup> Besides inherent antimicrobial effects, PTT can also be used in combination with antibiotic therapy to improve the treatment efficacy which has been also explored in the work of this thesis. In the literature, *in vivo* mice SSTIs associated with *S. aureus* and *E. coli* were treated with PTT and the simultaneous delivery of the antibiotics such as ampicillin,<sup>241</sup>



daptomycin,<sup>242</sup> ciprofloxacin,<sup>243</sup> imipenem,<sup>244</sup> and moxifloxacin<sup>245</sup>; and some of the studies required laser intensities of only  $0.5 \text{ W cm}^{-2}$ . PTT has also successfully enhanced the treatment of VAN for *S. aureus* and MRSA-associated SSTIs in preclinical models.<sup>246–248</sup> Zhang *et al.* investigated the potential mechanism of the synergistic effect via measurement of released bacterial DNA and scanning electron microscopy (SEM) images of the cell wall morphology of *S. aureus*, indicating that the heat from PTT together with VAN may synergistically harm the bacterial envelope.<sup>246</sup> However, it is important to highlight that these PTT-based VAN delivery systems were injected subcutaneously into a bacterial abscess, which is not commonly performed in the clinics and may not be suitable for treatment of SSTIs that do not form abscesses (i.e. cellulitis).

### 2.2.2 Plasmonic NPs

In the above-described literature, materials commonly utilized for PTT are plasmonic NPs. In some metal NPs, free electrons on the surface of the nanomaterial can be excited by incident light resulting in the oscillation of the electron cloud. This oscillation of the electron cloud in particles with sizes similar or smaller than the wavelength of the incident light is also referred to as localized surface plasmons (LSP).<sup>11</sup> Upon matching the frequency of the light source with the electron cloud oscillation, the LSP might resonate (LSPR) generating highly amplified, local electric fields (Figure 6). The oscillation subsequently decays releasing energy via radiative decays (i.e. light scattering) or non-radiative decay (i.e. dissipation via heat).<sup>12</sup> Thus, plasmonic metal NPs can be used to generate local heat under light irradiation which is harnessed in PTT.

#### *Nanomaterials for plasmonic absorption in the near-IR spectrum*

The wavelength of the incident light that can be absorbed from the plasmonic NPs via LSPR is material- and structure-specific.<sup>13</sup> For application in the human body, it is preferred to use visible or near-IR light due to the reduced unspecific absorbance by the tissue. Specifically, near-IR light has been extensively used for biomedical application of plasmonic NPs because of its deep penetration into tissues.<sup>14</sup> The wavelength region of visible and near-IR spectrum is covered by NPs made from gold, silver, or copper, whereas aluminum, palladium, and platinum absorb in the UV region. In terms of light-to-heat conversion efficiency, Ag NPs are the preferred choice due to their strong and sharp LSPR and high absorption-to-scattering cross-sections.<sup>13</sup> However, compared to Au, Ag is less chemically stable and can cause *in vivo* toxicity, which is why Au nanomaterials are considered the most suitable biological-friendly plasmonic nanomaterial for biomedical applications.

#### *Structure of Au nanomaterials influences the light absorption*

Besides material-specificity, the light absorption of the LSPR can also be controlled by changes in the nanomaterial structure such as shape and size. Typically, Au nanospheres do not absorb light in the near-IR region. However, changing the aspect ratio of Au particles to a rod shape increases the wavelength of the LSPR absorption maximum with increasing

aspect ratios resulting in a red-shifted absorption (as described by the Gans theory).<sup>13</sup> Alternative Au-based nanomaterials commonly studied for near-IR plasmonic applications are Au-shells or Au-cages.<sup>249</sup> However, the light-to-heat conversion efficiency of Au nanomaterials such as NRs, shells and cages are highly dependent on the precise control of their structure which may require multiple and complex process steps; a potential disadvantage for industrial scale fabrication. For example, the company Nanospectra Biosciences Inc. provides the Au shells AuroShell<sup>®</sup> and reported successful treatment of prostate cancers in a clinical trial.<sup>250</sup> Assuming an average body weight of 70 – 90 kg, ~ 2 – 3 g of the AuroShell<sup>®</sup> were required for single treatment of each patient, highlighting the need for production of near-IR active Au NPs that are cost-effective with scalable production. While the shape strongly influences the optical resonance wavelength of the nanomaterial, the size of NPs can control their excitation cross-section. For photothermal application high relative contribution of the absorption with low scattering losses are preferred to increase non-radiative decay of the NPs which governs the heat dissipation. The absorption-to-scattering cross-section in Au nanospheres decreases with increasing NPs diameter, with primary particle diameters of approximately 20 nm considered to be most effective with scattering losses approaching zero.<sup>251</sup> While material choice, size and shape of the NPs influences the absorption peak of plasmonic NPs, the absorption can also be tuned by controlling a process called plasmonic coupling.

### ***Plasmonic coupling of Au nanospheres for near-IR absorption***

To overcome the disadvantages of a multi-step, complex fabrication process of near-IR active plasmonic Au nanomaterials, the absorption maximum of spherical Au NPs can be shifted by controlling their interparticle distance.<sup>252</sup> When two or more plasmonic NPs are at a proximity to each other with a distance lower than approximately one diameter's length, their individual LSPR hybridizes.

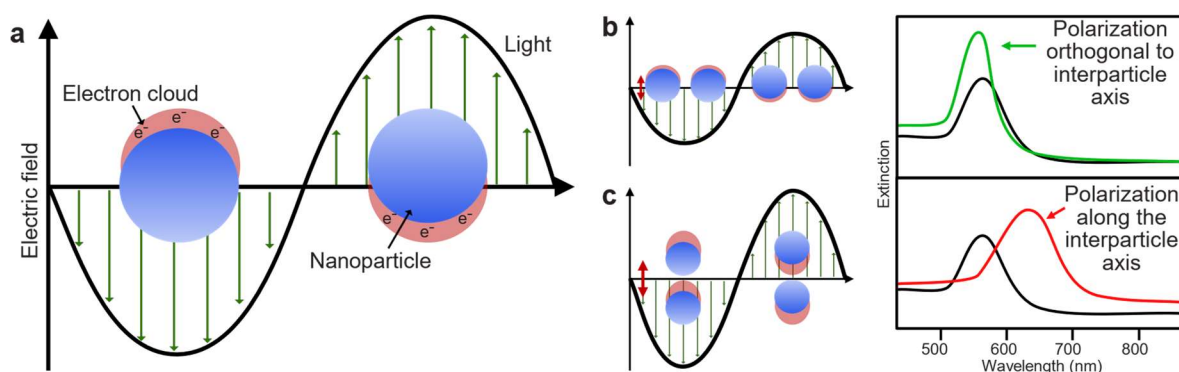


Figure 6: Schematic illustration of interaction of light with plasmonic NPs. a) General overview of generation of local electric field by coupling of the light frequency with the plasmon resonance due to displacement of the electron cloud resulting in light absorption. b,c) Influence of plasmonic coupling on the light absorption for polarization orthogonal to or along the interparticle axis resulting in a slight blue-shift, or distinct red-shift of the absorption peak, respectively.

This plasmon coupling tunes the LSPR of the coupled NP system and if the electric field polarization happens along the interparticle axis the light absorption redshifts with decreasing interparticle distance, enhancing the IR absorption.<sup>253</sup> Furthermore, constructive interference of the plasmons enhances the electric field of the NP system. However, at a sub-nanometer distance the classical plasmon interaction theory breaks down and different processes such as quantum mechanical effects (i.e. quantum tunnelling of electrons) can cause a blueshift in the light absorption, which is why it is important to finely tune the interparticle distance to an optimum.<sup>254</sup>

### **2.2.3 NPs synthesis via FSP**

The synthesis of NPs by flame aerosol technology is a widely employed process in industry for large scale particle production. In fact, the fabrication of flame-made NPs from companies like DuPont de Nemours Inc. constitute an estimated ~15 b\$/ year market with application as reinforcing agents in car tires (carbon blacks) or as whitening pigments in paints (TiO<sub>2</sub>).<sup>15</sup> More recently, flame aerosol synthesis has also been explored to produce more functionally complex NPs such as in the area of catalysis, sensors, and health care.<sup>16</sup> One limitation in the successful clinical translation of nanomedicines is the restriction in scale-up of many NPs synthesis techniques. The employment of flame synthesis might overcome this limitation since its proven industrial application, which was a main motivator for using flame-made NPs in the work of this thesis. In the following chapters, a brief overview of flame-made NPs for medical applications is provided to highlight the potential of using FSP for the fabrication of medical NPs.

#### ***Particle formation in FSP***

In general, flame aerosol technology can be categorized into three groups based on the precursor and combustion conditions: (i) vapor-fed aerosol flame synthesis, (ii) flame-assisted spray pyrolysis, or (iii) FSP.<sup>16</sup> The metal NPs used in this doctoral thesis were produced by FSP where a liquid organic solvent containing metal precursor is fed through a nozzle. With the aid of an oxygen outlet, the organometallic liquid precursor solution is aerosolized to form small, metal precursor-containing solvent droplets. By ignition of an oxygen-methane gas, a small pilot flame is used to combust the liquid solvent effectively creating a metal precursor vapor. The metal atoms in the vapor are supersaturated and by nucleation form product monomers which grow into clusters of NPs via surface reactions. These primary NPs coalesce and sinter to form nanoaggregates which upon leaving the high-temperature zone of the flame further arrange into large fractal-like agglomerates via Brownian coagulation.<sup>255,256</sup> Various process parameters can influence the properties of the NPs such as the high-temperature residence time, the vapor phase concentration, and the metal precursor composition.<sup>257</sup> Changing the burner configuration allows for the control over these parameters, e.g. increasing the precursor feed rate or decreasing the dispersion gas flow each increase the high-temperature residence time resulting in larger primary NP sizes.<sup>258</sup>

---

### ***Controlling plasmonic coupling in flame-made NPs***

The composition of the precursor influences the properties of the NP aggregates. For biomedical applications it is desirable to have plasmonic absorption in the near-IR region and Ag or Au NPs are promising candidates for PTT due to their high light-to-heat conversion efficiencies.<sup>17</sup> However, spherical Ag and Au NPs do not typically absorb light in the near-IR region. One possibility to enable near-IR absorption of Ag and Au NPs is via the control of the plasmonic coupling through tuning the interparticle distance.<sup>18</sup> Using dielectric spacer materials, e.g. a SiO<sub>2</sub> layer,<sup>259</sup> enables such tuning. In FSP, an amorphous spacer SiO<sub>2</sub> layer can easily be obtained by (i) injection of SiO<sub>2</sub> precursor (i.e. hexamethyldisiloxan - HMDSO) vapor above an enclosed flame reactor<sup>19,260,261</sup> or by (ii) co-mixing a SiO<sub>2</sub> precursor into the liquid precursor solution.<sup>20,21</sup> The former allows for a hermetical sealing of the primary NPs, whereas the latter has the advantage of being easily employed in a standard FSP reactor set-up that does not require a reactor enclosure. Moreover, it readily permits the direct deposition of the SiO<sub>2</sub>-coated NP aggregates onto substrates.

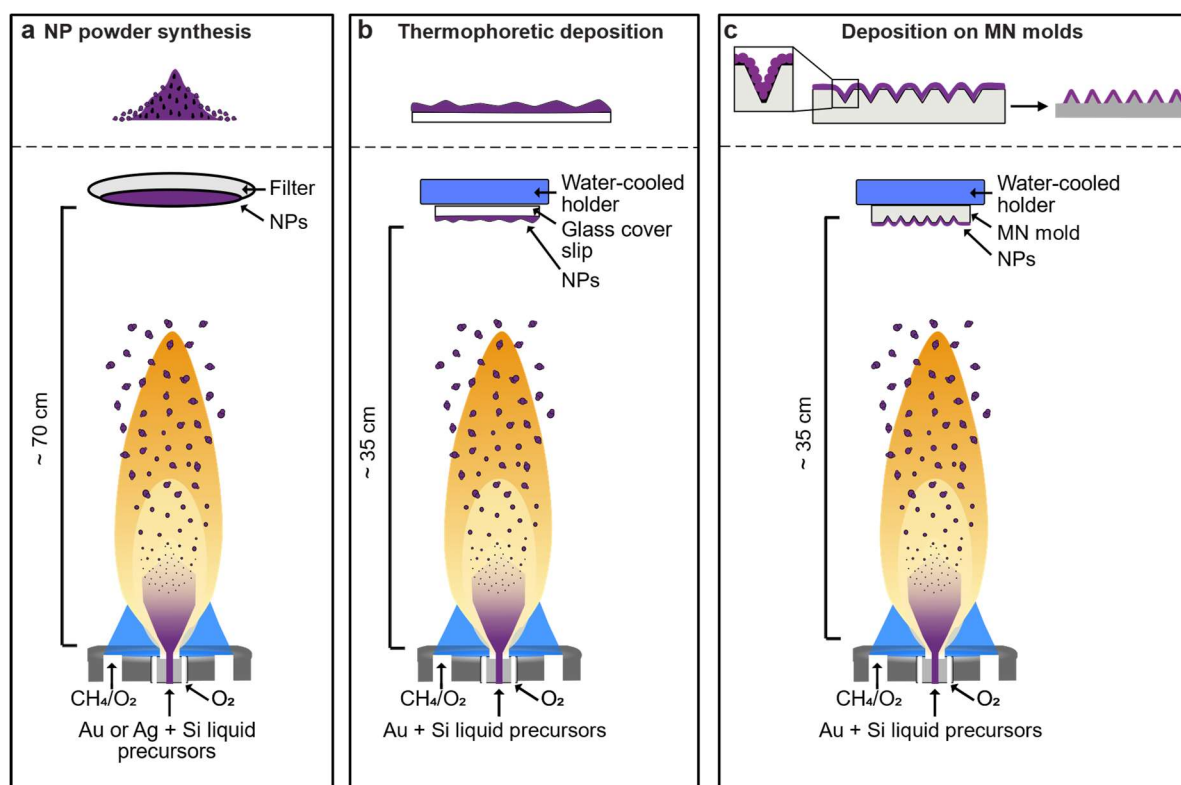


Figure 7: Schematic depiction of the fabrication methods of various NP products using the FSP reactor (not to scale). a) Synthesis of NPs made from Au or Ag + SiO<sub>2</sub> precursor as employed in **Paper II-IV** of this thesis. b,c) Fabrication of NP-films on glass coverslips or MN molds made with Au + SiO<sub>2</sub> NPs as in **Paper II**.

### ***Film formation in FSP***

The retrieval of NPs from the aerosol is often achieved via different routes (Figure 7). On the one hand, the NPs are collected as powders via the filtration of the aerosol with the aid of vacuum suction and synthetic or glass fiber filters. Alternatively, electrostatic precipitators can be employed for the down-stream separation of NPs from the gas.<sup>262</sup> On the other hand, the FSP technique allows for the direct *in situ* deposition of NPs onto substrates. The direct deposition of NP aggregates from the hot aerosol is achieved by securing a substrate onto a water-cooled holder which is orientated orthogonal to the impinging hot aerosol above the burner.<sup>257</sup> The deposition rate of NPs in such a temperature gradient, as obtained between the hot aerosol and the cooled substrate, is mainly controlled by thermophoresis. The morphology of the NP films can easily be tuned: Tricoli *et al.* found that for concentrated organometallic precursor solutions (0.05 – 0.5 mol L<sup>-1</sup>) important process parameters influencing the deposition rate are (i) the precursor vapor concentration and (ii) the temperature difference with increasing either resulting higher deposition rates.<sup>22</sup> Furthermore, for temperature difference above 120 K a thermal equilibrium is obtained which allows for a constant film growth rate. Increasing the deposition time at specific molarities linearly increases the film thickness (confirmed for deposition times up to 6 min).<sup>22</sup> In addition, micropatterns of NPs films can be created by employing a stainless steel mask covering the substrate.<sup>263</sup>

### ***FSP-made NPs for infectious diseases***

The flexibility of FSP for the synthesis of a wide variety of inorganic NPs lead to the rapid expansion of the commercialization and research of functional nanomaterials for application in the clinics. Most notably, the companies Hemotune AG and Anova Medical Inc. utilize flame-made NPs for therapy. Hemotune AG harnesses the capabilities of magnetic NPs for the blood purification in dialysis for the therapy of infections, intoxications, or autoimmune diseases.<sup>264</sup> Anavo Medical Inc. develops a medical nanoglue loaded with flame-made metal oxide NPs for application in surgical or skin wounds.<sup>265–267</sup> Furthermore, flame-made Ag NPs have been studied for their antibacterial properties due to ion release or as PTT treatments, successfully reducing bacterial growth of species such as *E. coli*,<sup>268</sup> *P. aeruginosa*,<sup>20</sup> and *S. aureus*.<sup>269</sup> Therefore, FSP-made NPs are promising for clinical therapies and may be further translated to the treatment of SSTIs. To do so, one needs to develop appropriate skin delivery platforms for the delivery of the therapy provided by flame-made NPs. An intra- and transdermal skin delivery platform for NPs and drugs that has recently gained traction are MNs.

## **2.3 MN arrays**

The overall goal of the work in this thesis was to develop a novel treatment strategy for the simultaneous delivery of high local antibiotic concentrations and PTT from nanomedicine. The employed delivery devices were MN arrays. MNs were first developed for transdermal drug delivery by Henry *et al.* (research group around Prof. Prausnitz)<sup>270</sup> in 1998 and since

---

then have been extensively studied and successfully brought to market.<sup>271</sup> MNs are miniature needles with heights in the micron-scale that pierce the skin to deliver their cargo. Often, hundreds of MNs are located on single skin plasters which are referred to as MN patches or arrays. These MN arrays are promising and novel medical devices which could potentially revolutionize the field of intradermal drug delivery as highlighted by the World Economic Forum through their nomination of MNs as one of the “Top 10 Emerging Technologies in 2020”.<sup>272</sup>

### *Advantages of MNs*

Due to their micron-scaled sizes, MN arrays cause less pain compared to classic hypodermic needles<sup>27</sup> which is promising for increasing patient comfort and compliance (Figure 8). The application of MN arrays is straightforward, does not require trained personnel, and does not leave sharp waste<sup>273</sup> making it an attractive medical device for the outpatient setting.

Furthermore, MN arrays are able to breach the skin’s protective barrier, the *stratum corneum*, to deliver molecules into the epidermis and dermis or sample biomolecules from the interstitial fluid.<sup>274</sup> The MN arrays designs and the corresponding drug delivery applications are manifold extending their clinical application from administering small molecules to large micron-sized particles.

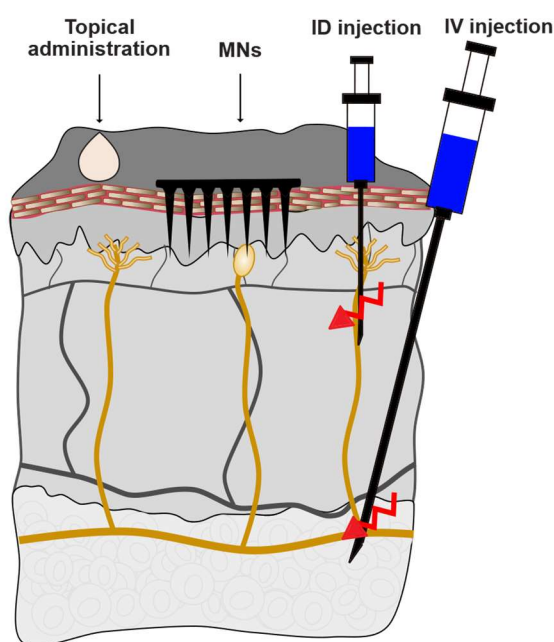


Figure 8: Schematic illustration of MN application for drug delivery compared to alternative administration routes, such as topical application of creams, ointments, or transdermal patches, ID or IV injection. MN administration combines the benefits of topical administration through reduced pain (pain indicated with red arrows) and ease of application while benefitting from increased drug delivery because of the effective penetration through the *stratum corneum*.

### ***MNs enable delivery of substances previously inhibited from topical administration***

As explained in more detail above (chapter 2.1.4) the protective function of the skin inhibits the delivery of hydrophilic, high molecular weight (> 500 Da) drugs via the topical route. Furthermore, the *stratum corneum* and the epidermal-dermal basement membrane are barriers in the skin permeation of topically applied NPs.<sup>275</sup> MN arrays have been extensively studied for the delivery of hydrophilic, large molecules and NPs<sup>276</sup> since the piercing of the *stratum corneum* and basement membrane breaches the protective function effectively allowing substances to be delivered transdermally which typically were unamenable to this administration route.<sup>277</sup> For this reason, MN arrays specifically disrupt the field of vaccination as a pain-less, easy applicable delivery platform owing to the potential of MNs to deliver large antigens via the topical route to directly interact with the abundant dermal immune cells.<sup>28,278</sup> Another example of novel avenues for transdermal delivery of large biomolecules is the administration of insulin with MN arrays,<sup>279</sup> which, besides application in the skin, was recently also reported as an oral insulin delivery platform.<sup>280,281</sup> Furthermore, using MN arrays micro- and NPs can be delivered into the skin as presented by Permana *et al.* who delivered Ag NPs incorporated in bacteria-responsive microparticles via MNs showing higher antibacterial effects against *S. aureus* and *P. aeruginosa* biofilms compared to a cream formulation.<sup>282</sup>

### ***The design of MNs influences the drug delivery***

Overall, the design of MN arrays can be summarized in four main categories: (i) solid, (ii) hollow, (iii) coated, (iii) dissolving, and (iv) hydrogel-forming MNs.<sup>283</sup> Solid metal and silicon MNs are used to perforate the skin to stimulate tissue regeneration and create channels for improved skin penetration of topical formulation; such metal MNs are already widely employed in the cosmetic industry.<sup>284</sup> Hollow MNs are solid needles with an inner channel that allow for intradermal injections of solutions as successfully marketed by companies like nanoBioSciences LLC.<sup>285</sup> Furthermore, solid MNs can be coated with a drug formulation and upon piercing the skin the coating is deposited into the skin. The company Vaxxas Inc.<sup>286</sup> recently (November 2022) initiated a phase 1 clinical trial for evaluating their coated MN patches for the vaccination against COVID-19. Alternatively, the MNs can be completely made of dissolving polymer or of the crystalline drug allowing higher drug quantities to be delivered intradermally compared to coated MNs. Companies such as Micron Biomedical Inc.<sup>287</sup> and LTS Lohmann AG<sup>288</sup> are exploiting such soluble MN arrays. Lastly, if the dissolving polymer is hydrogel-forming, the MNs arrays can be combined with a topical drug depot allowing for a sustained diffusion of drugs from the depot into the skin.<sup>289</sup> The work in this thesis employed polymeric MNs which will be introduced in the following chapter.

#### **2.3.1 Polymeric MNs for drug delivery**

Polymeric MNs are specifically attractive in the field of drug delivery because of their straightforward fabrication protocol, easy administration, biocompatibility, cost-effectiveness, and control over delivery kinetics.<sup>31</sup> Polymeric MN arrays are most commonly

made following a mold-and-casting method where flexible molds made of polydimethylsiloxane (PDMS) are produced as a negative copy of a metal MN array fabricated with micromachining or lithography. The polymer of choice can be loaded with dyes, drugs, or particles, concentrated in the MN mold, and detached as the final MN array after drying. The mold-and-casting method is easily employed in standard laboratories especially since the commercialization of the MN molds from companies such as Micropoint Technology Ltd. Besides the mold-and-casting method, several alternative methods, such as droplet-born air blowing,<sup>290</sup> allow for the fabrication of polymeric MNs, each methodology with their own advantages and shortcomings.<sup>31</sup> However, in the scope of this thesis specific focus will be placed on polymeric MNs fabricated from a MN mold. Utilizing mold-and-casting, MN arrays made from dissolvable polymers have been widely researched which upon insertion into the skin disintegrate and deliver their drug cargo.<sup>31</sup> Furthermore, responsive polymers, e.g. polycaprolactone (PCL), allow control over the drug delivery via external stimuli such as heat.<sup>291,292</sup> By contrast, only few studies reported the use of non-dissolvable polymers in the fabrication of MNs arrays, e.g. Choi *et al.* used polymethylmethacrylate (PMMA) for the production of electrically active MNs.<sup>293</sup>

#### ***Overcoming the limitations of drug loading in polymeric MNs***

One major obstacle in the successful drug delivery via polymeric MNs is the amount of drug that can be incorporated into the MNs. The amount of incorporated drug is limited by (i) the small size of the MNs, and (ii) the drug solubility in the polymer solution. Increasing the size or number of the MNs allows for incorporation of more drug per skin area; however, increasing the MN size and thickness increases pain of insertion<sup>294</sup> whereas increasing the amount of MNs per patch results in reduced MN insertion due to the “bed-of-nails” effect.<sup>295</sup> Alternatively, the overall MN patch can be enlarged to deliver more drug, although this approach necessitates the use of a flexible backing layer to allow MN insertion over curved skin.<sup>296</sup> Furthermore, the drug loading can be improved by using a tablet as a reservoir secured onto hydrogel-forming MNs to sustain intradermal drug diffusion over time.<sup>297</sup> To overcome the shortcoming of low drug solubility in polymers, MNs can be fabricated from pure drug by melt casting or concentration of the crystalline drug into MN cavities which may expand MN-based delivery to drugs requiring high doses to be systemically effective.<sup>298,299</sup>

#### ***Strategies to increase the deliverable drug dose in polymeric MN arrays***

Another shortcoming of polymeric MN arrays is the small relative fraction of drug effectively delivered into the skin due to the distribution of the drug from the MNs into the backing layer. Moreover, due to the viscoelasticity of the skin, MNs are typically only inserted to 10 – 80% of their length.<sup>300</sup> To achieve higher delivery efficiency and lower pharmaceutical waste, the drug should ideally be concentrated in the MN tips and approaches introduced in the literature to achieve this are summarized in Figure 9. Two-layered polymeric MNs fabricated in a two-step mold-and-casting method may result in MN tips with high drug concentration,<sup>301</sup>

---



although such highly drug-loaded MN tips depend on the specific drug and polymer selections. Alternatively, increasing the viscosity of the polymers by increasing the weight concentration of the aqueous polymer solution<sup>302</sup> or utilization a fast-evaporating solvent in the backing layer<sup>303</sup> effectively reduces the unwanted drug diffusion. Furthermore, introducing a bubble between the MN and backing layer allows for highly concentrated MN tips increasing the drug delivery efficiency.<sup>302,304</sup> However, high polymer concentrations and the introduction of a bubble decreases the mechanical strength of the MNs against compression which needs to be accounted for to ensure successful skin penetration.<sup>302</sup> Finally, allowing complete drying of the drug-loaded MNs with subsequent attachment to backing metal shafts<sup>305</sup> or insertion of MNs without backing layer with the aid of micropillars<sup>306</sup> both inhibits drug diffusion from the MNs; however, complex fabrication and precise needle alignment may be shortcomings of such inventions.

In the scope of this thesis (**Paper I**), the obstacle of drug diffusion from the MNs into the support layer was addressed by using the water-insoluble polymer PMMA as opposed to the water-soluble polymer polyvinylpyrrolidone (PVP) in the MN backing following a simple two-step casting method. Simultaneously to our work, Li *et al.* showed that using water-insoluble polymers as the material to form the MN backing layer effectively increases the drug localization in the MN tips resulting in higher drug delivery efficiency in skin as opposed to using water-soluble MN backings which held true for drugs of varying molecular weight.<sup>307</sup> They hypothesize that such decreased drug diffusion within the MN patch is caused by a phase separation between the MNs and backing due to the immiscibility of the polymers and solvents forming a physical diffusion barrier of hydrophobic backing polymer at the interface to the MN.

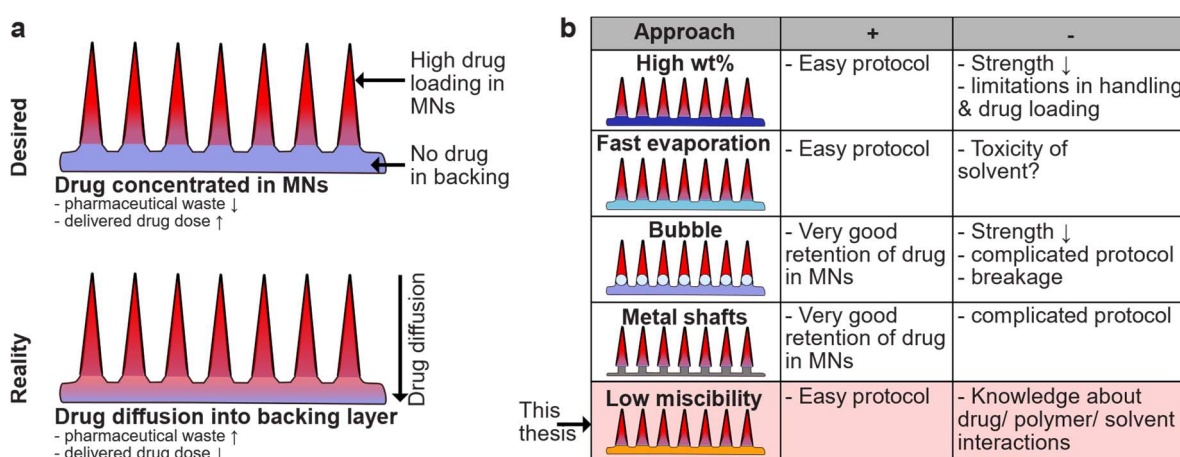


Figure 9: Illustration of the problem of drug diffusion within polymeric MN arrays and approaches used in literature to overcome the problem. a) Schematic depicting the unwanted drug diffusion within polymeric MN arrays resulting in wasted drug in the backing layer. b) Overview of selected approaches to prevent unwanted drug diffusion and allow for high drug loading in the MNs as introduced in the literature.

### 2.3.2 Antibacterial MNs

Initially, MN arrays were explored in the field of vaccination, but the scientific community quickly expanded the MN technology to other therapeutic areas including infectious diseases. MN-assisted treatment can be applied to various infectious diseases such as viral,<sup>308</sup> fungal,<sup>309</sup> and parasitic infections.<sup>310</sup> Furthermore, MN arrays have extensively been explored for potential treatment of bacterial infections.<sup>29</sup> As such, antibacterial MNs have been developed (i) with coatings or inherent antibacterial functionality for self-sterilizing effects, (ii) for systemic antibiotic delivery against infections, and (iii) for local antibiotic delivery for potential treatment of SSTIs.

#### *Inherently antibacterial properties and coatings for self-sterilizing MNs*

Although Donnelly *et al.* showed in 2009 that the infection risk after MN application is lower compared to the use of hypodermic needles,<sup>311,312</sup> several studies developed MN arrays containing antibacterial coatings or as inherently antibacterial to allow a self-sterilizing of the MN arrays and thus reduce any MN-associated infection risk. To the best of the author's knowledge, in 2009 Gittard *et al.* were the first to report the development of antibacterial MN patches by deposition of a silver coating on ceramic MNs showing antibacterial effect against *S. aureus*.<sup>313</sup> Building on this, Gittard *et al.* later reported alternative coatings from silver and zinc oxide also on acrylate-based MNs which inhibited the growth of common skin-associated bacteria.<sup>314</sup> Likewise, zinc oxide was applied in form of nanobushes on the surface of MNs by Chew *et al.* reducing the growth of *S. aureus*.<sup>315</sup> These studies enable antibacterial properties on non-dissolvable MNs; however, MNs intended for drug delivery are often made from dissolvable polymers. Several studies show that the rational selection of dissolvable polymers for the fabrication of MNs can be exploited to provide antibacterial functionality. For example, MNs made from the polymer Gantrez<sup>®</sup> AN 169 restricted bacterial growth of bacteria such as *E. faecalis*, *E. coli*, and *S. aureus*.<sup>316</sup> Likewise, natural antibacterial materials such as chitosan<sup>317</sup> or manuka honey<sup>318</sup> were successfully employed for fabrication of antibacterial MNs. Besides inherently antibacterial properties, MNs have been extensively developed as a drug delivery platform for antibacterial compounds.

#### *Systemic antibiotic delivery via MNs*

Dissolvable MNs can be used to administer drugs transdermally due to the permeation of the drug through the skin into the blood circulation. Such transdermal delivery of antibiotics may have the advantage of reducing first pass metabolism and resistance development in the gut microbiome which are associated with oral antibiotic administration. To the best of the author's knowledge, the first study to deliver antibiotics via MNs was the study by Gittard *et al.* in 2010 who delivered gentamicin via dissolvable MNs.<sup>319</sup> The study was later expanded by the research group around Prof. Donnelly, showing similar gentamicin plasma concentrations in rats after MN administration compared to intramuscular injection<sup>320</sup> and successful treatment of lung infections in mice caused by *Klebsiella pneumoniae*.<sup>321</sup> Besides overcoming the disadvantages of oral antibiotic delivery, MNs also enable the delivery of

antibiotics which typically can only be given IV. One such antibiotic is the glycopeptide VAN which was explored to be delivered with MNs locally into the skin in the work of this thesis (**Paper I**) and at the same time by Ramadan *et al.* showing systemic delivery of clinically relevant VAN concentrations in mice.<sup>322</sup> Interestingly, Ramadan *et al.* also reported the local VAN concentration in the skin, showing an approximate 500-fold higher intradermal VAN concentration after MN delivery compared to IV administration. Therefore, MN-assisted local delivery of VAN can potentially be applied for the treatment of skin infections, which we elucidated in **Paper I** of this thesis work.

#### ***Local delivery of antibiotics via MNs***

Various antibiotics have been delivered and tested in *in vitro* models potentially relevant to SSTIs, e.g. polymyxin against planktonic *E. coli*,<sup>323</sup> cephalixin for the inhibition of *E. coli* and *S. aureus* lawns,<sup>324</sup> and tetracycline against *S. aureus*.<sup>325</sup> Furthermore, doxycycline encapsulated in nanosuspension was successfully delivered into *ex vivo* porcine skin for treatment of biofilm skin infections.<sup>326</sup> However, other studies also explored MN-assisted antibiotic delivery in clinically more relevant *in vivo* models: clindamycin was delivered in ROS-responsive MNs for growth inhibition of *P. acnes*<sup>327</sup> or ofloxacin<sup>328</sup> for the inhibition of *E. coli* and *S. aureus* with both approaches contributing to improved skin wound healing. Highly relevant to the work presented in this thesis are the results recently published by Su *et al.* who explored the delivery of VAN by dissolvable MNs together with AgNO<sub>3</sub> and Ga(NO<sub>3</sub>)<sub>3</sub> into human *ex vivo* biofilm skin models of *S. aureus* and *P. aeruginosa*.<sup>329</sup> They showed that the antibacterial effect increased when using MNs opposed to needle-free mats presumably associated with the improved penetration into the biofilm and skin. Furthermore, the combination of three antibacterial modalities improved the biofilm reduction in a synergistic fashion allowing VAN to show antibacterial effect against polymicrobial biofilms. This highlights the potential of synergistic interactions to improve the antibiotic efficiency specifically in the context of treatment of often polymicrobial SSTIs.

#### **2.3.3 Photothermal MNs**

The incorporation of photothermal agents into MNs has mostly been applied for the delivery of anticancer drugs and treatments. Often, dissolvable polymeric MNs are fabricated incorporating both a photothermal agent and a therapeutic. Upon MN insertion into the skin, the photothermal agent and drug are delivered intradermally. Irradiation of typically near-IR light at the local skin site results in heat dissipation from the photothermally active agent, which may increase the treatment outcome by direct ablation of harmful cells or through synergistic effects with the delivered drug. Besides therapy improvement, photothermal agents in MNs can be exploited as a control mechanism for MN dissolution when combined with heat-responsive polymers.<sup>292,330–332</sup>

### ***Photothermal MNs for synergistic anti-tumor treatments***

MNs are an attractive administration route for the treatment of superficial tumors and skin cancers since they can aid in overcoming drawbacks associated with successful clinical translation of anti-cancer PTT.<sup>333</sup> One obstacle is the delivery of high amounts of photothermal agent locally into the tumor, which can be easily achieved by the delivery of the agent via MNs into superficial tumors. Furthermore, another drawback is to provide a mild temperature of up to approximately 50 °C that ablates malignant cells without causing high damage to the surrounding, healthy tissue. One way to reduce PTT therapy to mild temperature regions is to combine dual therapeutic modalities. MNs can easily be developed for dual delivery of photothermal agents and drugs by combined incorporation in the polymeric matrix. Photothermal agents incorporated into MNs that showed successful treatment of superficial tumors includes melanin,<sup>334</sup> and indocyanine green,<sup>335–340</sup> and various inorganic nanomaterials, such as lanthanum hexaboride (LaB<sub>6</sub>) NPs,<sup>291,341,342</sup> Au NR,<sup>343,344</sup> Au nanocages,<sup>345</sup> and Au-core silica shells.<sup>346</sup> All of the above studies evaluated the PTT in synergy with pharmaceutical anti-cancer treatments, allowing for tumor growth reductions at temperatures mostly around 50 °C.

### ***Photothermal MNs for treatment of SSTIs***

MNs show similar opportunities in PTT against SSTIs as they do for skin tumor therapy, i.e. MNs allow the dual delivery of photothermal agents and antibiotics thus enabling synergistic antibacterial treatments at mild temperature increases locally at the infected site. Although substantial efforts have been devoted to the development of PTT-MNs for skin tumor treatment, the application of PTT-MNs for antibacterial therapy is relatively scarce. Two studies explored the antibacterial effect of PTT from MNs as an additional sterilization functionality besides the intended anti-tumor application reporting inhibition of *S. aureus* above 90% at 50 °C *in vitro*<sup>347</sup> and *in vivo*.<sup>348</sup> Similar temperature increases to 50 °C were used to synergistically eradicate *S. aureus in vitro* combining PTT with nanozyme function (i.e. ROS production) thus contributing to improved wound healing.<sup>349</sup> Likewise, the synergism between PTT at 45 °C for 6 min and AMP resulted in similar *S. aureus* growth inhibition requiring only approximately 60% of the drug dosage.<sup>350</sup> Furthermore, the authors reported that the healing of diabetic foot ulcers in an *in vivo* rat model was higher for PTT and AMP delivery via MNs compared to a topical formulation, highlighting the advantage of using MNs for intradermal delivery. Similarly encouraging results were reported for MN-assisted PTT in synergy with the delivery of  $\alpha$ -amylase for the degradation of biofilm and the antibiotic levofloxacin.<sup>351</sup> The triple action resulted in 80% bacterial killing of pre-formed, polymicrobial biofilm of *S. aureus* and *P. aeruginosa* in an *in vivo* model. Synergistic effects of PTT and the antibiotic VAN delivered via MNs was explored in **Paper IV** of this work for inhibition of MRSA.

***Avoiding nanotoxicological concerns of photothermal MNs***

All the above studies developing photothermal MNs employed dissolvable polymers in the fabrication of the MN patches thus delivering nanomaterials into the skin tissue. This can be a potential bottleneck in the clinical translation of such MNs due to the uncertainty of the long-term bioaccumulation in the body and ecosystem and the associated toxicological effects of the nanomaterials.<sup>352,353</sup> Although some studies mentioned above, report negligible toxic side-effects from the employed photothermal agents,<sup>330,332,340</sup> it is difficult to hypothesize about potential long-term effects and the fate of nanomaterials in the ecosystem. Therefore, removal of NPs after treatment from the body could be advantageous in order to avoid such nanotoxicological concerns altogether. In fact, a recent publication from 2020 developed an Au NR-coated, non-dissolvable MN array to remove the nanomaterial from the skin after PTT.<sup>32</sup> However, the study had multiple limitations such as (i) the thick Au coating decreased the MN skin insertion capabilities, (ii) MN arrays resulted in intradermal temperature increases of only approximately 5 °C at high laser intensities of 2 W cm<sup>-2</sup>, (iii) the authors did not quantitatively study any reduced NPs deposition in the skin. To address those limitations, in **Paper II** and **Paper III** of this thesis various methods are introduced to fabricate non-dissolvable MNs with metal NPs for PTT.



### 3 RESEARCH AIMS

The overall aim of this thesis was to develop a MN technology that combines local antibiotic drug release with near-IR PTT for the potential treatment of bacterial skin infections (Figure 10). We set out to explore a novel treatment option for SSTIs in which we chose to deliver the antibiotic VAN, commonly administered only IV for the treatment of MRSA-associated SSTIs, locally to the skin using MNs. Furthermore, we introduced various fabrication methods for PTT MNs with the ultimate aim to combine VAN-MNs with PTT in a single hybrid MN array.

More specifically the aims were:

- I. To employ a MN array for the local delivery of high concentrations of the antibiotic VAN and to show its effectiveness in an *ex vivo* porcine skin infection model with MRSA (**Paper I**).
- II. To develop various fabrication methods for non-dissolvable, photothermal MN arrays using flame-made, plasmonic Au nanoaggregates to demonstrate the potential of reduced NP deposition in skin (**Paper II**).
- III. To produce photothermal MN arrays with a low-cost stereolithography 3D printer using flame-made, plasmonic Ag nanoaggregates and explore the antibacterial effect against SSTI-associated bacteria (**Paper III**).
- IV. To combine the local delivery of the antibiotic VAN with PTT in a hybrid MN array to synergistically eradicate MRSA (**Paper IV**).

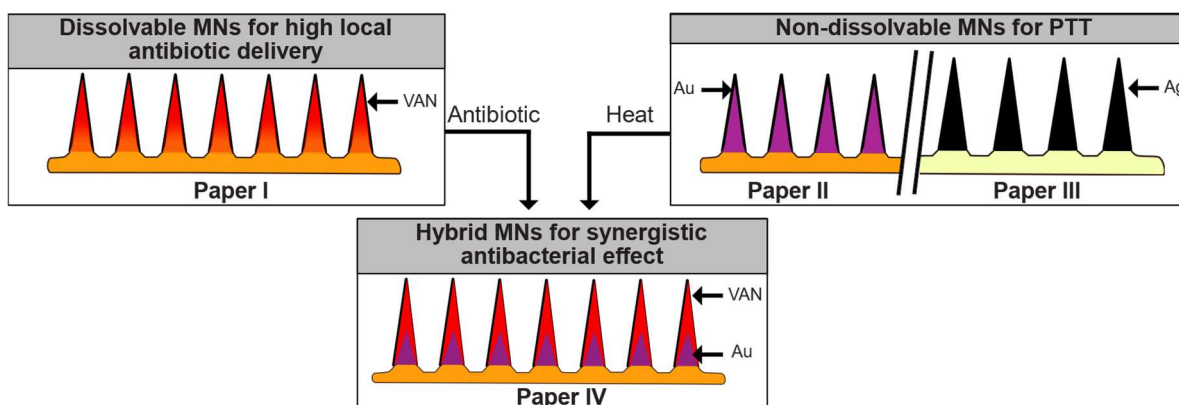


Figure 10: Graphical abstract of the research aims of the work in this doctoral thesis to develop a hybrid antibacterial MN array employing high local antibiotic delivery combined with local PTT for improved antibacterial treatment of bacterial SSTIs.





## 4 METHODOLOGICAL CONSIDERATIONS

This chapter provides an overview of the methodologies used across the work in this thesis and considerations of the chosen methodology are discussed. Where applicable, the method description is combined for multiple publications and the detailed description can be found in the Experimental Sections of the respective publication.

### 4.1 Regarding MN fabrication and characterization

MNs are the core theme running through all of the here presented publications. Therefore, it is important to elucidate the fabrication of such MNs and their characterization first. In three publications (**Paper I, II, and IV**) the MN arrays were fabricated following a common mold-and-casting method. On the other hand, in **Paper III** stereolithography (SLA) 3D printing was selected to produce the MN arrays.

#### *The mold-and-casting method*

The mold-and-casting method is likely the most commonly employed methodology to produce polymeric MN arrays in the literature.<sup>354</sup> In this method a solid master MN template is produced often by nanolithography and a negative copy mold of the master template is fabricated using typically the flexible polymer PDMS. Subsequently, a polymer-drug mixture can be casted into the mold, concentrated with e.g. centrifugation or vacuum suction, dried, and detached from the mold. The resulting polymeric MNs resembles the original solid master template. In this thesis, the majority of MN arrays were fabricated via mold-and-casting method because the molds can be obtained commercially at desired dimensions and MN arrays can easily be produced with standard laboratory equipment. Furthermore, the mold-and-casting method can be employed for a wide variety of different choices of polymers, which was important in the scope of this thesis since both water-soluble and water-insoluble polymers were used to fabricate the MN arrays. To fabricate the dissolvable MNs containing drug and dye the water-soluble polymers polyvinyl alcohol (PVA) and PVP were selected due to their known sufficient mechanical strength in MN applications, ease of handling, safety consideration according to FDA-approvals, and quick dissolution after skin insertion.<sup>355</sup> For non-dissolvable MNs the water-insoluble polymer PMMA was chosen based on a previous publication successfully employing PMMA in the mold-and-casting method of MN arrays.<sup>293</sup>

***SLA printing***

3D-printing techniques can generally be divided into three groups: (i) material extrusion, (ii) vat photopolymerization, or (iii) powder bed fusion.<sup>356</sup> In the material extrusion and powder bed fusion printing, heat is utilized to melt a thermoplastic polymeric filament with a heating extrusion head or to sinter the particle powders through a heating beam, respectively. Compared to vat photopolymerization, these two methods result in non-smooth surfaces and might suffer from low resolution and printing accuracy.<sup>356</sup> Therefore, the majority of 3D printed MNs thus far are fabricated using vat photopolymerization techniques. SLA printing utilizes a light source, such as a laser beam, to selective cure UV-sensitive resin which attaches to a building platform that moves upwards in a layer-by-layer fashion. In micro-SLA printing an UV light source such as a liquid crystal display (LCD) is covered selectively with a mask to cure the resin of each layer onto the building platform. In LCD SLA printing, the printing resolution is defined by the pixel size and intensity whereas laser-based SLA often allows for higher resolution defined by the accuracy of laser movement and spot size. However, LCD SLA allows for faster prints compared to laser-based SLA since the complete layer is cured at the same time and benefits from low printer costs. In **Paper III**, an LCD SLA printer was employed for the fabrication of photothermal MN by mixing NPs into the UV-curable resin enabling fast and low-cost printing of photothermal MN arrays.

***Mechanical strength testing***

The MNs in all of the publications of this thesis were analyzed for their mechanical strength. In **Paper I** the MNs were tested for their failure against transverse force application whereas in **Paper II-IV** MNs were analyzed for their height reduction after compression at axial load.<sup>357</sup> Analysis of the stress-strain curve of MNs under compression is a commonly utilized methodology to explore the axial load the MNs can withstand without failure aiming to model the insertion of the MNs into skin. Furthermore, the group around Donnelly *et al.* reported the typical force potentially applied to a MN array when inserted into skin by a human thumb to be around 32 N.<sup>358</sup> Therefore, the height reduction of various MN arrays after exposure to axial compression at 32 N for 30 sec allows for interpretation of differences in mechanical strength of the MNs modelling real-world settings. Finally, the parafilm insertion method was introduced by the same group to elucidate the insertion depth of MNs in an *in vitro* model after finding only minor deviations of insertion depths of MNs in stacked parafilm layers compared to *ex vivo* porcine skin.<sup>358</sup> Both the height reduction after compression as well as the parafilm insertion test were employed in publications of this thesis.

***Drug quantification via high-pressure liquid chromatography (HPLC)***

HPLC is an analytical methodology used to separate components of a sample and measure them for example via their absorption with a UV/Vis detector. In HPLC, a column filled with adsorbent material is used to separate the components based on specific interactions such as hydrophobic or ionic interactions between the material and the component. The interaction and thus the component separation is dependent on the temperature and the solvent, referred to as the mobile phase, employed. The flow of the mobile phase through the column is operated with a high pressure which allows for the separation of small samples. By running

---

a standard material of known concentration, HPLC can be used to quantify specific components of a mixture since the detector signal is a function of the component concentration. In **Paper I** and **IV** a reversed-phase HPLC was employed to detect the concentration of VAN loaded in MN arrays or from samples obtained of the transdermal diffusion model. A previously published method for detection of VAN was used, employing an aqueous, high-phosphate mobile phase and a non-polar C18 column.<sup>359</sup> The buffer ammonium dihydrogen phosphate had been reported suitable due to the low signal interference of the VAN absorption in the UV-region (here 220 nm).<sup>359</sup> The use of HPLC allows for increased accuracy, precision, and sensitivity compared to immune-enzymatic assays which normally have quantification limits of a 1 – 5  $\mu\text{g mL}^{-1}$ .<sup>359</sup> Alternatively, liquid chromatography for separation coupled with mass spectroscopy for detection (LC-MS) can be used for the quantification of VAN with detection limits as low as 1  $\text{ng mL}^{-1}$ . However, their implementation and operation is considered a high-cost investment and not feasible for many laboratories.

#### ***Transdermal diffusion model***

Horizontal diffusion cell, such as the Franz diffusion cell, is the most common technique to evaluate dermal absorption *in vitro* and was used to evaluate VAN delivery from MNs in **Paper I**.<sup>360</sup> In this technique, a membrane or skin sample is mounted between a donor chamber and a receptor chamber. The donor chamber in horizontal settings is exposed to air thus if skin samples are used typically the epidermis is facing towards the donor chamber allowing for the application of the test substance. The receptor chamber is filled with a fluid suitable to solubilize the test substance. The receptor fluid has a physiological pH and is often temperature-controlled to 32 – 37 °C. If skin is used, freshly excised human skin is the ideal model to replace *in vivo* human model. However, often porcine skin is taken as a replacement due to reduced ethical concerns (see below). Furthermore, the skin may be frozen and thawed and it is important to keep the freeze-thawing cycles to as low as possible to not interfere with the permeability of the skin samples. After application of a test substance to the donor chamber, samples from the receptor chamber are withdrawn and analyzed over a suitable time frame.<sup>360</sup> Thus, the penetration and permeation capacity across the skin of the tested substance can be obtained. The skin preparation can vary from using split-thickness or full-thickness skin samples. When using full-thickness skin the amount of drug retained in the skin may be dependent on the skin thickness, thus flux calculations may not be reliable in this setting.<sup>361</sup>

#### ***Melting-point depression model***

To predict the drug-polymer solubility the thermoanalytical technique differential scanning calorimetry (DSC) can be used. In this method, the melting point of a sample can be determined by evaluating the heat flow from the sample in comparison to a reference material over a heating ramp. Upon phase transition the heat flow to the sample will increase or decrease relative to the reference to maintain both at the same temperature. For example, if the sample undergoes an endothermic transition from solid to liquid the sample require more heat. If a crystalline drug is mixed with a polymer of high solubility more impurities in the

crystal structure of the drug will lead to a depression of the melting point. Contrary, if the drug-solubility is low the melting point depression is reduced. The data obtained for DSC can further be modelled using the Flory-Huggins model to evaluate the drug-polymer solubility at room temperature.<sup>362,363</sup> The analysis for drug-polymer solubilities in **Paper I** were performed by co-author Nele-J. Hempel.

## 4.2 Regarding NPs synthesis and characterization

### *NP synthesis with FSP*

The NPs used in the work of this thesis were synthesized with the FSP technique. In this synthesis method a liquid precursor solution is atomized using a capillary and oxygen gas flow. Flamelets are employed to combust the organic part of the liquid precursor, resulting in a precursor gas. The molecules in the gas phase undergo nucleation forming small NPs that subsequently coalesce and sinter to larger nanoaggregates containing multiple primary NPs. With increasing distance to the burner and thus decreasing aerosol temperature the nanoaggregates further agglomerate. The fractal-like nanoaggregates and -agglomerates can be collected as a powder with the aid of vacuum suction and filtration or directly deposited onto substrates. The primary NPs can be controlled by various process parameters mainly influencing the high-temperature residence time, such as the precursor flow, the gas flow, or the enclosure of the reactor. Primary NPs sizes can be obtained with a few nanometers in diameter; however, the fractal-like aggregates and agglomerates can be various hundred micrometer in size. Although the primary NPs arrange in aggregates and agglomerates the exposed surface area is high allowing for the application of such flame-made NPs powders in biomedical settings. Overall, FSP is a scalable and reproducible synthesis technique for fractal-like nanoaggregates.

### *NP characterization*

In **Paper II** and **III** the size and morphology of the NPs and their films were analyzed using X-ray diffraction, SEM, transmission electron microscopy (TEM), and energy-dispersive X-ray spectroscopy (EDX)/ electron energy loss spectroscopy (EELS). In X-ray diffraction a material can be analyzed for the crystal structure and atomic spacing. A finely ground and homogenized powder of the material is exposed to monochromatic X-rays which subsequently is diffracted by the crystal atoms. In crystalline materials the atoms are arranged in lattices and depending on the lattice spacing and the incidence angle of the X-ray wavelength the diffracted X-rays can interfere constructively. The diffracted X-rays are recorded over a range of angles and when constructive interference occurs a peak in intensity is registered. The height and width of these peaks are characteristic for different materials. By fitting the experimental data to a calculated profile from a known material library, information about the material identification is obtained. Furthermore, analyzing the peak shape allows for calculation of the crystalline size at different angles of the material. In SEM, a focused electron beam is scanned over a sample resulting in the interaction of the electron with the atoms of the material. Such interaction can result in emission of secondary electrons which are typically low in energy thus only able to escape from the superficial layers of the

---

material providing information about the sample topography. The electrons can also interact with the atoms of the specimen by elastic scattering resulting in back-scattered electrons. These electrons are typically of high energy thus possibly emerging from deeper layers in the sample. Compared to secondary electrons, back-scattered electrons give less resolution about the specimen surface; however, since heavier atoms scatter more, back-scattered electrons give information of the sample composition. TEM also employs the exposure of sample material to an electron beam, but unlike SEM it forms images by detecting the transmission of the electrons through the sample. Therefore, samples need to be very thin typically less than 100 nm. In **Paper II** and **Paper III**, the size distribution of primary NPs in flame-made nanoaggregates were analyzed based on TEM images. A type of TEM is scanning TEM in which a focused electron beam is scanned over the sample of a fine spot. When the incident electron beam excites an electron of the inner shell of the atom, the ejected electron leaves an electron hole that can be occupied from an outer shell electron. Upon changing of the electron from the high-energy outer shell to the low-energy inner shell the energy difference is released via X-ray. The emitted X-ray is dependent on the energy difference of the two shells which in turn are characteristic to the emitting atom. By measuring the emitted X-ray via EDX, information about the sample composition can be obtained. However, the process of ejecting an inner shell electron is relatively scarce. Furthermore, information of the sample composition can be obtained by measuring the amount of lost energy due to inelastic scattering of the incident electrons via EELS. In **Paper II** co-author Thomas Thersleff performed combined EDX/EELS analysis on STEM images in order to provide spatial information about the composition of the nanoaggregates.<sup>364</sup>

#### ***Elemental quantification with inductively coupled plasma mass spectrometry (ICP-MS)***

The quantification of the Au content in MN and skin tissue samples in **Paper II** was performed by the collaborator L. Vilela with help in method development by A. Julander, K. Midander, and S. McCarrick. In ICP-MS a sample is nebulized, atomized, and finally ionized using an ICP. The sample is nebulized with argon gas upon entering a spray chamber and large droplets of the aerosol mist are removed. The fine droplets are transferred into a torch that sustains an ICP. The ICP is obtained by flowing argon gas into the torch which end is placed inside an induction coil. The radio frequency induction coil generates a fluctuating magnetic field and upon introducing an electric discharge the alternating electric field results in the oscillation of electrons which collide with and ionize the argon and sample atoms. The positively charged, ionized atoms subsequently enter the MS where they are separated based on their mass-to-charge ratio. By measuring a material standard of known concentration an unknown sample can be quantified since the signal intensity is proportional to the sample concentration.

### **4.3 Regarding bacterial work**

The bacteria used in this work were quantified using two different methods. For adjustments of liquid bacterial cultures, the optical density at 600 nm (OD<sub>600</sub>) was measured and diluted to represent a predefined bacterial concentration. Additionally, in **Paper IV** the OD<sub>600</sub> over

time was recorded to calculate the relative growth inhibition after 24 h. Based on this growth inhibition, a synergy score was estimated with the aid of the software Combenefit utilizing the Loewe additivity. For quantification of live bacteria after experimental interventions, serial dilutions of the liquid bacteria were spread on agar plates. Due to the spatial confinement on the agar the bacteria duplicate and grow in confined colonies, called colony forming units (CFU), which represent metabolically active bacteria. In **Paper I** and **IV** the bacteria employed was the strain SF8300 USA300-0114, a clinical wild-type isolate of community-associated MRSA. USA300 is associated with the epidemic outbreaks of MRSA infection specifically in North America. Furthermore, SF8300 USA300 has higher growth rates on different carbon sources, which may partially contribute to the virulence of MRSA in the skin tissue environment compared to methicillin-sensitive *S. aureus* making it specifically suitable for testing in *ex vivo* infection models as employed in **Paper I**.<sup>365</sup> In **Paper III** the clinical isolates of *S. aureus* (ATC 25923) and *P. aeruginosa* (PA01) were employed as representatives gram-positive and -negative strains, respectively, commonly associated with SSTIs.

#### **4.4 Ex vivo skin models**

To evaluate the application of MN arrays it is specifically relevant to test their successful insertion and activity in realistic environments. Therefore, analyzing the insertion of MNs into excised skin and the delivery of their drug cargo to and across the tissue is crucial in predicting their clinical potential. Generally, freshly excised human skin is the best *ex vivo* model that can be employed in this context. However, due to ethical considerations (more further below) and restriction in availability, alternative *ex vivo* porcine skin samples have been employed in **Paper I-III**. Full-thickness porcine skin from still-born piglets was collected within 24 h after death and the thickness of the skin was measured. Skin samples were frozen at -20 °C and utilized within one year after excision. Before use, the skin was thawed at room temperature and the hair was shortened using a scissor to reduce the risk of damaging the *stratum corneum*. Generally, porcine skin is the most suitable mammal model for human skin due to the similarities in physiology, cellular composition, and drug permeability.<sup>366</sup> However, the freeze-thawing process significantly interferes with the integrity and thus with the mechanical stability of the tissue.<sup>366</sup> Therefore, additional analysis in freshly excised human skin was performed to evaluate the MN insertion in **Paper I** of this thesis. Another advantage in utilizing fresh skin samples is the potential to quantitatively analyze the cellular composition via immunohistochemistry, which may be limited in previously frozen tissues due to the incurred cell damage and death.

#### **4.5 Ethical considerations**

Scientific research on human samples as was performed in the scope of **Paper I** of this thesis requires ethical permits to reduce the risk of harm to the patient, safeguard the protection of privacy and to ensure research conduct with respect to human dignity. The collection of human skin in **Paper I** was performed only after approval of the ethical permit by the Ethics Examination Committee according to the principles of the Declaration of Helsinki and

---

written consent from the patient. To safeguard the privacy of the patient the material was handled confidentially and coded at all times. Furthermore, the human skin used in the work of this thesis was surgical excess after plastic surgery conducted at the Department of Reconstructive Plastic Surgery, Karolinska University Hospital, Stockholm, Sweden. Therefore, the patients were not recruited specifically for this work.

Besides human skin, in **Paper I-III** experiments were performed on excised porcine skin from stillborn piglets. The animals were bred for agriculture purpose and the piglets died of a natural cause. Stillborn piglets were collected after death and no animal was bred or harmed with the intention to be used in scientific research. It was previously confirmed with the Swedish Board of Agriculture (Jordbruksverket) that for the use of tissue material from stillborn piglets no ethical permits are required as they are considered agricultural waste.





## 5 RESULTS & DISCUSSION

### **Paper I: Vancomycin-Loaded Microneedle Arrays against Methicillin-Resistant *Staphylococcus Aureus* Skin Infections**

The overall aim of **Paper I** was to explore a novel local antibiotic delivery platform, namely MN arrays, in the treatment of MRSA-associated SSTIs (Figure 11). The investigated antibiotic was chosen to be the glycopeptide VAN which due to its large molecular weight and hydrophilicity can almost exclusively be administered IV. However, systemic administration of VAN suffers from shortcomings such as site effects and low local drug concentration. Therefore, we set out to evaluate the local delivery of VAN to the skin using MN arrays.

The MN arrays were fabricated following a traditional mold-and-casting method utilizing the water-soluble polymer PVA to form the VAN-loaded MNs. As the backing layer the two polymers PVP (water-soluble) and PMMA (water-insoluble) were explored to investigate the effect of the polymer choice in the backing layer on the drug diffusion within the MN array. As described previously, polymeric MN arrays produced via mold-and-casting method might suffer from low drug delivery efficiency and high pharmaceutical waste due to the diffusion of the drug from the MNs into the whole array which restricts the delivery of the full drug dose. We explored whether such drug diffusion within the MN array can be reduced by using the water-insoluble PMMA instead of the water-soluble PVP. Loading the MNs with a dye visually confirmed the reduced dye diffusion when using PMMA. Furthermore, DSC analysis revealed that VAN has a lower solubility in PMMA compared to PVP which may contribute to a reduced diffusion of VAN to the backing layer when PMMA is used.

The two-layered VAN-loaded MN arrays were subsequently tested for their mechanical strength, insertion capability, and drug delivery. Insertion into a model membrane, parafilm, and mechanical testing against transverse force showed no clear effect of VAN loading up to 150  $\mu\text{g}$  per MN array on the insertion depth or strength of the array. However, digital images of the parafilm layers after removal of the MN array revealed high breakage of the MNs from the array for VAN loading at around 100  $\mu\text{g}$ . Therefore, VAN-MN arrays with 100  $\mu\text{g}$  were tested for their insertion into thawed porcine skin and freshly excised human skin. The MNs successfully pierced the skin with insertion depths of 16 – 33% of their height, which is comparable to the literature. Furthermore, employment of freshly excised human skin allowed for histochemical analysis showing that the MNs successfully pierced the basement

---

membrane which may be beneficial to ensure VAN delivery into the viable part of the skin. Finally, the intra- and transdermal delivery of VAN was analyzed using the Franz diffusion assay and we observed local delivery in line with previous reports which evaluated VAN delivery from dissolvable MN arrays in an *in vivo* mouse model. Furthermore, the results of the transdermal VAN delivery after 10 min or 24 h of MN array application resulted in choosing 10 min as the application time for subsequent *ex vivo* infection experiments.

Finally, the activity of VAN was studied after release from the MN array in an *in vitro* agar disk diffusion assay and an *ex vivo* MRSA porcine skin infection model. The growth inhibition of MRSA in the agar disk diffusion test is similar between the VAN released from the MN array and the positive control (aqueous VAN solution on filter paper) indicating that the incorporation of VAN in the MN array developed here does not seem to negatively impact the antibiotic activity. Finally, the antibacterial effect of VAN was evaluated in an *ex vivo* MRSA infection model in which significant growth inhibition was achieved after twice application of VAN-MN for ten minutes. The bacterial inhibition was higher for decreasing initial bacterial infection load or decreasing establishment time for the infection which may be associated with biofilm formation. To summarize, **Paper I** demonstrated the successful development of MNs arrays for the local delivery of the antibiotic VAN for potential treatment of MRSA-associated SSTIs.

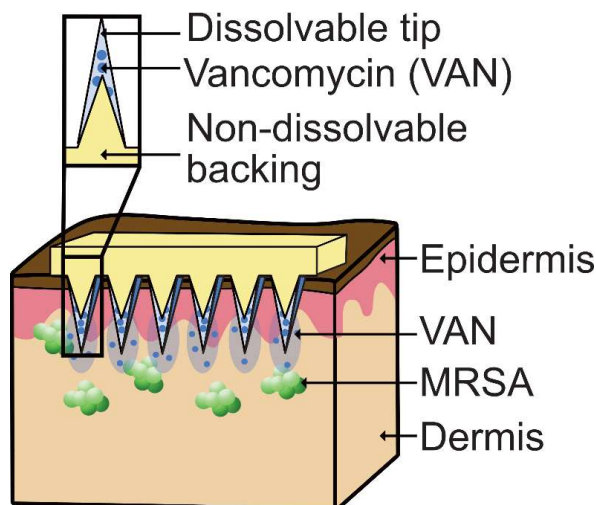


Figure 11: Illustration of the VAN-loaded MN arrays developed in Paper I and its potential application in MRSA-associated skin infections. MN arrays were developed comprised of water-soluble VAN-loaded MNs and a water-insoluble backing layer. Upon insertion into the skin tissue, the water-soluble MNs dissolve, releasing high concentrations of VAN intradermally. In case of SSTIs, the intradermal VAN can locally interact and inhibit the bacterial growth for example of the common SSTI-associated bacteria MRSA.

## Paper II: Highly Efficient Near-IR Photothermal Microneedles with Flame-Made Plasmonic Nanoaggregates for Reduced Intradermal Nanoparticle Deposition

In **Paper II**, four different mold-and-casting methods for the fabrication of photothermal MNs employing flame-made, plasmonic Au nanoaggregates were developed (Figure 12). The interparticle distance between the primary Au NPs and their plasmonic coupling was controlled by the addition of SiO<sub>2</sub> which acts as a spacer material. The non-dissolvable, photothermal MN arrays were produced with different mold-and-casting methods employing (i) direct *in situ* deposition of the nanoaggregates in the flame, or (ii) collected NP powders. The fabrication methods were compared in terms of the MN morphology, the photothermal effect in air and in skin, and the temperature increase as a function of Au content. Finally, the reduction of intradermal NP deposition from photothermal MN arrays by rational choice of the polymer and fabrication method was evaluated in *ex vivo* porcine skin.

The Au/ SiO<sub>2</sub> nanoaggregates with varying SiO<sub>2</sub> content (0 – 50 wt%) were deposited on glass coverslips and analyzed for their extinction in the near-IR region. Decreasing the SiO<sub>2</sub> content increases the near-IR extinction in line with previous findings<sup>20</sup> confirming a red-shifted plasmonic coupling in flame-made Ag/SiO<sub>2</sub> aggregates. Furthermore, correlating the increased extinction with the photothermal response at near-IR laser irradiation showed ideal temperature increases at SiO<sub>2</sub> contents of 0.5 – 6 wt% and 4 wt% was selected for subsequent experiments.

The NPs were located and distributed within the photothermal MNs depending on the employed fabrication method as interpreted from microscopic analyses. The *in situ* direct deposition (deposition method) results in MNs with a thin Au coating, whereas the collection of the NPs as powders and redispersion in solvent results in thicker coatings for dispersion in liquid (coating method) or in NP nanocomposite MNs for dispersion in polymer (incorporation method). Furthermore, a fourth method was developed in which an outer, thin polymeric layer was casted before adding the NPs dispersed in liquid (sandwich method). MN arrays made from all methods successfully increased the temperature upon near-IR irradiation, with the sandwich method outperforming the other three methods in terms of reproducibility and heat increase. However, upon analyzing the heat efficiency by plotting the temperature increase as a function of Au content in the arrays, the deposition method results in the highest heating efficiency. This improved photothermal efficiency for MN arrays fabricated by the deposition method may be associated with the utilization of centrifugation in the other three methods resulting in highly agglomerated, thick NP layers. This is further supported by higher photothermal efficiency for all methods at lower NP content highlighting the importance of evenly distributed NPs within photothermal MN arrays to reduce material waste.

Finally, the photothermal MNs were evaluated for their performance in *ex vivo* porcine skin. For the MN arrays at selected conditions, the MNs fabricated with either of the four methods successfully pierced the skin. Upon near-IR radiation for 10 min the MN arrays heated the

skin to 13–18 °C with the coating and sandwich method resulting in the highest temperature increase. Such temperature increases lie in the therapeutical relevant range, showing the potential of the developed MN array to be employed for improved therapy. Finally, the deposition of NPs from the MN into the skin was compared for non-dissolvable MNs developed here compared to equivalent MN arrays fabricated with a dissolvable polymer as commonly employed in the literature. We found a 127-fold reduction of NPs deposition when employing non-dissolvable polymers. Furthermore, the deposition method resulted in the lowest NP deposition of all four methods. Upon evaluating the NPs deposition relative to the Au mass in the MNs, the sandwich method resulted in the lowest NP fraction released from the MN array. This is specifically interesting since it indicates that the outer polymeric shell fabricated in the sandwich method may act as a protective layer reducing the NP-tissue interface. Compared to the deposition method, the protocol of the sandwich method is more feasibly employed in a standard laboratory and serves as a potential novel methodology to reduce NP deposition after usage of photothermal MNs. Overall, the work in **Paper II** introduced four fabrication methods for photothermal MNs utilizing flame-made Au nanoaggregates.

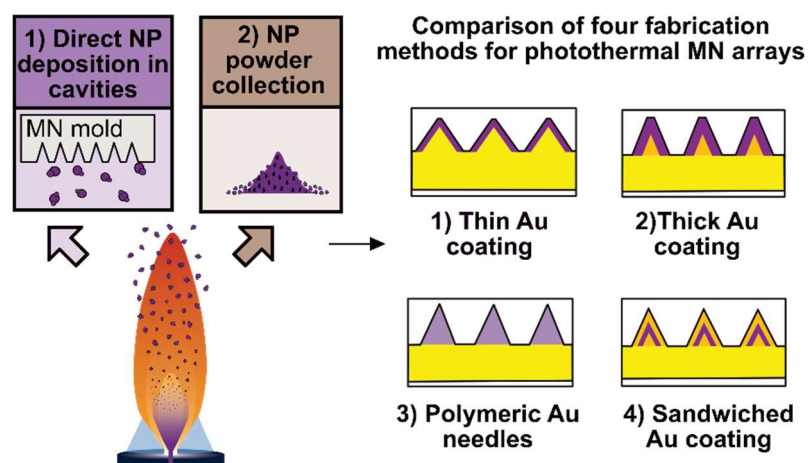


Figure 12: Schematic illustration of the study concept in Paper II. FSP was used to fabricate Au/SiO<sub>2</sub> nanoaggregates that were employed in the mold-and-casting fabrication of photothermal MNs via (i) direct deposition of the nanoaggregates on the MN molds, or (ii) collection of the NP powder. The four different fabrication methods resulted in control over the MN morphology and the location of the NPs which in turn influenced their photothermal performance and the deposition of NPs intradermally.

### **Paper III: Customizable Fabrication of Photothermal Microneedles with Plasmonic Nanoaggregates Using Low-cost Stereolithography 3D-printing**

**Paper III** describes the use of low-cost SLA 3D-printing employing nanocomposites with flame-made Ag/SiO<sub>2</sub> nanoaggregates for the fabrication of photothermal MNs (Figure 13). In the literature, photothermal MNs are typically fabricated following a multi-step mold-and-casting method, which commonly requires overnight procedures. In **Paper III**, the use of 3D-printing allowed for the fabrication of photothermal MNs in only approximately 2 – 3 hours. These photothermal MNs showed sufficient mechanical strength to pierce the skin and heat skin to therapeutically relevant temperatures upon near-IR irradiation. Finally, we showed that the photothermal MNs can be employed to eradicate two SSTI-associated bacterial strains *S. aureus* and *P. aeruginosa*.

The flame-made, plasmonic Ag/SiO<sub>2</sub> nanoaggregates used in **Paper III** have previously been evaluated for their ideal plasmonic coupling and photothermal performance by our group.<sup>20</sup> After confirming that 2 wt% SiO<sub>2</sub> results in a high extinction in the near-IR spectrum, in line with the previous evaluations, the dispersion of such nanoaggregates in UV-curable resin was explored. Nanocomposites were prepared by (i) vortexing, (ii) sonicating, or (iii) homogenizing the nanoaggregates in the 3D-printing resin. Cured droplets of nanocomposites were imaged with SEM and the average agglomerate size was measured revealing that the use of sonication and homogenization improves the dispersion of the aggregates resulting in reduced agglomerate sizes. Furthermore, the improved dispersion results in an increased photothermal response of the nanocomposites.

In order to evaluate the potential of such nanocomposites for the printing of a medical device, photothermal MNs were produced with nanoaggregates only present in the MNs. The printer settings anti-aliasing, grey level, and image blurring were optimized. Photothermal MNs with optimized printer settings were successfully printed at varying dimensions, height-to-width (H/W) ratios, and heights (1.5 – 2 mm). In line with previous results in the literature,<sup>367</sup> the output height of the MNs was significantly smaller than the input height with a difference of approximately 50 – 75%. However, the reduction followed a linear trend for all three H/W ratios. The mechanical stability of the photothermal MNs was analyzed showing reduction in strength against compression for higher H/W ratios and NPs concentrations. Higher H/W ratios lead to thinner needles thus explaining a higher height reduction under compression. Furthermore, increasing NPs concentrations in the nanocomposite might interfere with the complete and even curing of the resin which may reduce the mechanical strength.

The 3D-printed photothermal MN arrays heated up successfully under near-IR irradiation at 808 nm showing higher temperature increases for decreasing H/W ratio, increasing NP concentration, and increasing laser intensities. Furthermore, disinfection of the MNs with ethanol did not negatively impact their heating response for up to five heating cycles. The photothermal MNs were subsequently tested in *ex vivo* porcine skin and bright field microscopy of tissue cross-section show successful penetration into the skin. The intradermal

temperature increase of full-thickness skin of approximately 1.2 cm thickness was evaluated under near-IR irradiation at 808 nm showing high temperature increases up to  $\Delta T_{\max}$  of 40 °C within 10 min of irradiation at only 0.5 W cm<sup>-2</sup> laser intensity. The heating profile confirmed a decrease of  $\Delta T_{\max}$  for increasing distance to the MN array.

Finally, the antibacterial effect against planktonic bacteria of the photothermal MNs arrays was studied under near-IR radiation for increasing time. After 10 min irradiation the growth of both bacterial species *S. aureus* and *P. aeruginosa* was reduced by 4-log corresponding to a killing of 99.99% of the bacteria. Importantly, *P. aeruginosa* was more susceptible to the heat damage with maximum antibacterial effect reached within 5 min of treatment, which may be associated with the thin bacterial cell wall of gram-negative bacteria. However, the temperature of the planktonic culture reached 65 °C after 10 min treatment which may be disadvantageous for application in the human body. It is advised to explore combinational treatment with such 3D-printed, photothermal MN arrays in the future to reduce the final temperature increase. To conclude, in **Paper III** the use of flame-made nanocomposites with 3D-printing is introduced for the fast and low-cost fabrication of customizable photothermal MN arrays.

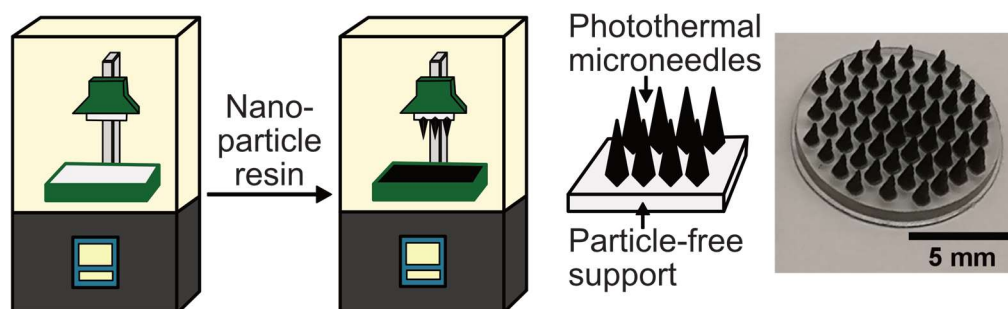


Figure 13: Graphical abstract of the content of Paper III in which SLA 3D-printing was employed to fabricate photothermal MN arrays. MN arrays with NP-free support layer were printed in a customizable, cost-effective, and fast manner. The printed, photothermal MN arrays successfully pierced and heated skin locally. Furthermore, high antibacterial effect against the SSTI-associated bacteria *S. aureus* and *P. aeruginosa* was demonstrated after 10 or 5 min near-IR irradiation, respectively.

---

#### **Paper IV: Hybrid Microneedle Arrays for Antibiotic and near-IR Photothermal Synergistic Antimicrobial Effect Against Methicillin-Resistant *Staphylococcus aureus***

The overall aim of this thesis was to combine local antibiotic delivery with PTT in a single, hybrid MN array which is described in **Paper IV** and Figure 14. Two-layered MNs were developed comprising of a VAN-loaded, dissolvable outer layer and an Au-SiO<sub>2</sub> nanoaggregate-loaded, non-dissolvable core. The influence of the choice of polymer used in the fabrication of the outer, drug-loaded layer on the MN morphology, the photothermal effect, and the drug delivery was evaluated. Finally, the growth inhibition against MRSA was studied and synergistic effects evaluated.

Two water-soluble polymers, PVA and PVP, were studied for their use as the matrix material of the outer, drug-loaded layer in the hybrid MNs. Using PVP resulted in the formation of a drug-loaded MN tip, whereas PVA formed an outer shell around the MN which was confirmed with bright-field, fluorescence, and SEM microscopy. Using PVP in the fabrication of the hybrid MNs results in lower drug-loading and photothermal response compared to MNs fabricated with PVA. The lower drug-loading may be caused by a decreased drug diffusion into the non-dissolvable photothermal core when employing PVA compared to PVP since VAN has a higher solubility in PVA as was shown in **Paper I**. Furthermore, the higher photothermal response in hybrid MNs fabricated with PVA might be explained with the formation of a complete needle when using PVA, opposed to a stub as is formed when PVP is employed.

Finally, the synergism of the antibacterial effect between VAN and PTT from the hybrid MN arrays was explored. The investigation revealed additive to synergistic interactions between VAN and PTT on the growth inhibition of MRSA. Furthermore, increasing the treatment duration in the therapeutic temperature window of >45 °C from 10 to 15 min *in vitro* did not significantly increase the growth inhibition of MRSA. However, upon utilizing MN arrays for the treatment of MRSA, 15 min MN application under near-IR irradiation resulted in around 10 min temperature therapy of >45 °C and such discrepancy between MN and effective treatment application is important to be corrected for. Upon treating MRSA for 15 min with hybrid MNs under near-IR radiation, a time-dependent growth inhibition as observed with increasing treatment effect after 24 h for high VAN concentrations of 10 µg mL<sup>-1</sup>. Furthermore, the heat increase enhanced the antibacterial effect. To conclude, **Paper IV** describes the development of hybrid MN arrays for potential application against MRSA.

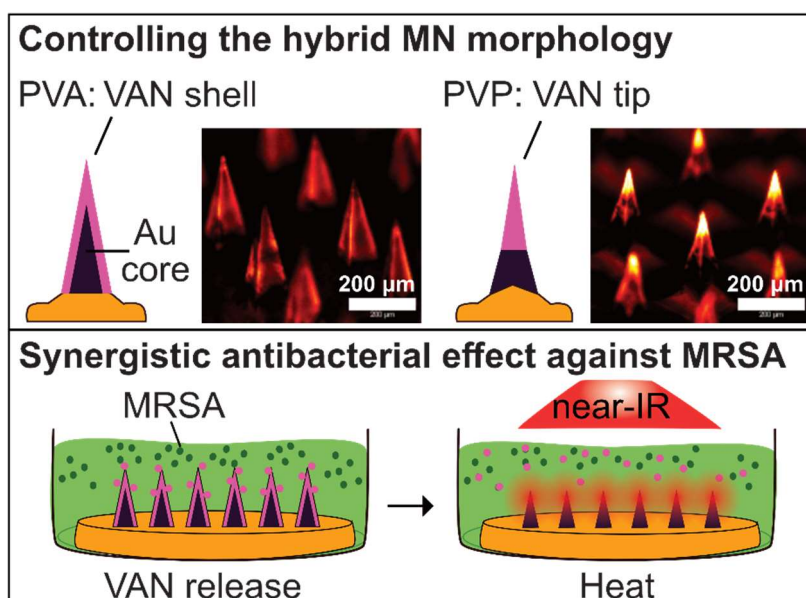


Figure 14: Graphical summary of the development of hybrid MN arrays described in Paper IV. Two different water-soluble polymers, PVA and PVP, were employed for the fabrication of an outer, drug-loaded layer and the water-insoluble polymer PMMA loaded with flame-made Au/SiO<sub>2</sub> nanoaggregates was used for the fabrication of a photothermal core. The antibacterial effect of hybrid MN arrays under near-IR irradiation against MRSA was evaluated *in vitro*.



## 6 CONCLUSIONS

Throughout the work of this thesis various MN arrays have been developed and evaluated for potential novel treatment of bacterial SSTIs. The two major treatment modalities explored were (i) high intradermal antibiotic delivery and (ii) PTT via flame-made metal nanoaggregates in MNs. Ultimately, the two modalities were combined into a single hybrid MN array allowing for simultaneous release of VAN and PTT under near-IR irradiation successfully inhibiting the growth of MRSA.

Delivery of high local VAN concentration was achieved by developing MN arrays with a water-insoluble backing layer and VAN-loaded MNs. Such VAN-MN arrays successfully breached the biological skin barriers the *stratum corneum* and the basement membrane in freshly excised human skin. Furthermore, after twice application of VAN-MN arrays for 10 min the growth of MRSA in an *ex vivo* porcine skin model was significantly reduced indicating the potential of MN arrays as novel drug delivery platforms for antibiotic delivery in the treatment of SSTIs.

Furthermore, various fabrication methods for photothermal MNs were developed using flame-made Au/ SiO<sub>2</sub> or Ag/ SiO<sub>2</sub> nanoaggregates. Following four different mold-and-casting methods, flame-made Au/ SiO<sub>2</sub> were used to produce photothermal MN arrays with difference in MN morphology, NPs distribution in the MNs, PTT efficiency and removal of NPs after skin application. Importantly, we introduced a novel fabrication step of adding an outer polymeric layer to photothermal MN arrays which allows for the reduction of the NP-tissue interface and thus the relative intradermal NPs deposition. In addition, Ag/ SiO<sub>2</sub> nanoaggregates were incorporated in nanocomposites with UV-curable resin for the customizable, cost-efficient, and quick fabrication of photothermal MNs using SLA 3D-printing. Such 3D-printed MNs showed high photothermal efficiency under near-IR irradiation and successfully killed *S. aureus* and *P. aeruginosa*. However, high final temperatures might limit the application of photothermal MN alone, thus combinational antibacterial might be a suitable approach to reduce the required temperature.

Such combinational antibacterial therapy between high local VAN delivery and PTT was achieved through the development of hybrid MN arrays. The rational choice of the polymer used for the outer, dissolvable, drug-loaded layer of such hybrid MN arrays allows for the optimization of drug loading and photothermal performance. Finally, synergistic interaction of VAN and PTT resulted in successful growth inhibition of MRSA *in vitro*.



## 7 FUTURE PERSPECTIVE

The overall way forward for the work in this thesis, would be to evaluate the hybrid MN arrays in clinically more relevant *ex vivo* and *in vivo* models in order to better define potential treatment regimens and the real-world therapeutic potential. Thus far, the conceptual development of MN arrays was described; however, it remains to be elucidated if and how such hybrid MN arrays can be translated to the clinics. Especially in the context of the high variety of clinical presentations of SSTIs as outlined in the literature review of this thesis, prospective work would urgently need to define the specific dermatological application of such antibacterial hybrid MN arrays and to evaluate their effectiveness in suitable models. It might be beneficial to also consider testing the hybrid MN arrays in polymicrobial infections as they are often encountered in the clinics. Furthermore, studies evaluating any side effects from high local VAN release, PTT or polymer deposition into the skin would be crucial for successful clinical translation of such MNs. Finally, an additional important question could also be to evaluate the immune reaction of the skin to the MN application which could be explored using immunohistochemistry analysis on freshly excised human skin samples.

Besides the overall potential clinical translation of antibacterial hybrid MNs, during the work of each of the sub-projects in this thesis additional avenues of investigation have presented themselves. In **Paper I**, in collaboration with the co-authors, the DSC methodology was utilized to study the solubility of the drug VAN in three different polymers in an attempt to explore possibilities to reduce unwanted drug diffusion within MN arrays. However, undoubtful the approach is rather simplified and a more systematic analysis of the influencing factors in the drug diffusion of antibiotics within MN arrays would potentially advance the field of polymeric MNs. Scientific questions left unanswered could be: what role plays the drug-polymer, the drug-solvent, and polymer-solvent solubility in the drug diffusion during MN array fabrication? What is the degree of impact on drug diffusion of the drug size compared to solubility and miscibility of the different polymer matrices? It would also be important to evaluate whether the effects of drug-polymer solubility as explored in **Paper I** hold true for other antibiotic-polymer selections.

The fabrication methods of photothermal MN arrays described in **Paper II** can also be evaluated further. In terms of photothermal efficiency, the MN arrays fabricated with the deposition method showed the highest promise for industrial translation. However, there are still some obstacles that would need to be elucidated in order for the deposition method to

---

show commercial potential. First of all, the MN molds that were able to be coated simultaneously was very limited and reduction in reproducibility was observed for increasing the number of molds deposited at the same time, potentially caused by the dilution of the NP-aerosol on the edges of the flame due to air entrainment. It could be of interest to place MN molds instead of a filter higher above the burner than the substrate holder in **Paper II**. However, in such scenario the deposition rate likely will not be governed by thermophoresis due to a smaller temperature gradient thus it remains to be elucidated whether photothermal MNs can be fabricated in industrial scale utilizing the deposition method. The other three methods could prospectively be improved upon by trialing to obtain a more even distribution of the NPs within the mold and replacing the strong centrifugation employed in the work here with alternative coating strategies.

The MN arrays fabricated in **Paper III** show great potential for clinical translation because of their customizability, low-cost and fast fabrication method. However, the temperature needed to obtain an antibacterial effect is too high to be employed in the clinics as a monotherapy for SSTIs. Future studies could develop hybrid MNs based on 3D-printed photothermal MNs. Preliminary studies performed based on previous literature evaluated to produce an outer soluble polymeric layer onto the 3D-printed photothermal MNs by (i) pressing the photothermal MNs into a MN mold filled with drug-loaded polymers, or (ii) by drop coating. Such combinational therapies might allow for a reduction of heat dose through additive and synergistic effects making this invention potentially more attractive for application in the human body.

Finally, the work presented in **Paper IV** could be improved by exploring the properties of the polymers on the formation of an outer tip or shell in more detail. The exact processes governing the formation of the different shapes of MNs remain to be elucidated and a key question left unanswered is: what is the role of surface attraction of the polymer to the PDMS mold and the molecular weight of the polymer on the tip formation? Furthermore, an evaluation of the intradermal heating of the hybrid MN arrays needs to be performed.

## 8 ACKNOWLEDGEMENTS

Throughout my doctoral studies in Stockholm, I have met many great people both in the professional and private surrounding who have supported me along the way and whom I am incredibly thankful for.

I would like to start thanking my supervisors **Georgios A. Sotiriou**, **Keira Melican**, and **Liv Eidsmo** for their supervision, intellectual input, and scientific support during the scope of my doctoral thesis. Thank you for providing me with the scientific environment to perform the studies of my research work, and for being available to exchange ideas and discuss my findings. I appreciated the opportunity to have supervised students, to independently develop methodologies, to be able to conduct my research, and to work with many talented researchers at Karolinska Institute.

I would also like to thank **Birgitta Henriques-Normark** and **Staffan Normark** for their impressive wealth of knowledge which they were always very kind and happy to share with me thus helping me to develop my research projects. I am very thankful to have worked in the BHN group and for the support I have received from you.

There are many people at KI and in the BHN group that I like to thank for being part of the past four years of my professional life:

I am particularly thankful for having worked with **Padryk Merkl**. Thank you for knowing (almost! 😊) everything, for always reaching a helping hand, for answering all my silly questions, and for discussing my research with me literally at any point. I will miss working next to you and I am sure I will never again have an officemate that so patiently ignores me when I am annoying them – thank you for making my PhD more interesting and fun!

Thanks also to **Anshika Maheshwari** for being such an intelligent, confident, and ass-kicking woman. Having you in the office and lab made everything more fun and enjoyable. You have the most contagious laughter I have ever heard, and your wit is admirable.

**Felix Geissel** with whom I have started my PhD almost at the same time. I enjoyed the nights out and beers we had and it's inspiring how much passion you are putting into your sports.

**Vasiliki Tsikourkitoudi** I was so thankful when you started in the lab for finally not being the only one interested in keeping the lab clean. You are also very funny, and you have a great stamina in overcoming scientific problems. Also, don't believe Padryk, I am pretty sure he was the one stealing your pen!

**Eleni Bletsa** who has always been a great support to me. I really enjoyed our lunches and the collaborative work we did. I wish you all the best with your husband in Greece.

**Haipeng Li** The last post-doc that joined the lab during my time here. You are one of the kindest, most humble, and at the same time talented and hard-working people I know. But above all, you are always happy to listen and give advice, while also being very fun to hang out with.

**Justina Venckute Larsson** who has been in the lab since before I started. I will miss your nice bakery so much! Thank you for being such a sweet, smart, and kind soul that is always happy to help and organize fun things.

**Yael del Carmen Suárez López** and **Stefanie Dietl** both of you have only stayed shortly in the lab, but you still made the office and lab a fun place with your always positive and happy attitudes and your smarts. I am certain you both will do greatly in your PhDs.

I would also like to thank all the students I have had the opportunity to supervise. Thanks to **Aashini Patel**, **Ann Maria Pandipilly Samson**, **Lidija Marija Smertinaite**, and **Isabel Sondén**. You all did absolutely great work and it was a fantastic learning opportunity exploring your projects together. Specifically, I have to thank Isabel, who stayed 1.5 years in the lab with me for the fantastic work you performed actually contributing most of a whole publication to my thesis!

**Hannes Eichner** and **Jannik Martens** for always cracking jokes, for baking nice cakes at home, and for just being super intelligent researchers and humorous people.

**Jens Karlsson** and **Hayrie Aptula** for being fun people to hang out with. I really enjoyed the beers we had, the board games we played, and God do you know how to throw a party. I wish you both all the best in your career and future together.

Thanks to **John Boss** who is one of the kindest people I know. I could not imagine you ever getting angry at anything, you are so funny, kind, and keen on discussing all sorts of random things.

I have also developed an interest in doing regular sports which would not have been the case if it wasn't for **Kim Vestö**, **Franscesco Righetti**, **Genevieve Garriss**, and **Christian Spoerry** who are great role models for incorporating sporty activities in everyday life.

---

I would also like to thank **Edmund Loh** for the interesting discussions we had in the office and at lunch.

Furthermore, there are and have been many other members in the BHN group that I really enjoyed talking to and joking around with, such as **Anuj Pathak, Karina Hentrich, Vicky Sender, Stephen Pieterman, Sarp Bamyaci, Meztlli Gaytan, Rebecca Dookie, Anandi Narayana Moorthy, Pedro Henriques, Ana-Rita Narciso, and Sigrún Thórsdóttir**. I also appreciate the opportunity to have worked with and been provided with scientific feedback by **Mikael Rhen, Marie-Stéphanie Aschtgen, Karin Blomqvist, Priyanka Nannapaneni, Sandra Muschiol, Elisabeth Reithuber, Vitor Oliviera, Mario Codemo, Federico Iovino, Karthik Subramanian, and Katrin Pütsep**. You all have made the BHN group such a welcoming, funny, and interesting workplace – thank you for that! Finally, I would like to thank **Maria Carlson** for always helping with bureaucratic problems and providing such a great support.

Besides the BHN group there have been other people at KI that have helped me during the past four years. First of all, I would like to thank **Gesan Alurampalan** and **Åsa Belin** for being a great support for me, for always giving advice and having an open ear.

I would also like to thank everybody at the MTC Student Association and specifically **Benedek Bozoky** who I enjoyed many interesting discussions at lunch and outside of KI with.

I also really appreciated the little “Life after PhD” group that we formed in the final stretch of our PhDs. Thanks to **Stelia Ntika, Jan Reising, Jessica Gracias Lekander, Lourdes Sainero Alcolado** and **Dina Dabaghie** for the many beers and fun stories we shared.

Besides the people at KI, there have been many external people that greatly influenced my life in the past 4.5 years in Stockholm and without whom my time here would have been very different.

I specifically enjoyed meeting everybody in the department of equity research at SEB in the last year of my PhD. Among all of them, I highly appreciated to be working with such a great boss as **Christopher W. Uhde** from whom I have learned an incredible amount of things. Thanks for getting out of your own way to support me and for being a fantastic person.

Besides work, I have made many friends that I keep very close to my heart and without whom I would have not made it through the PhD. Thanks to the Kammis-fam **Olivia Linderoth, Fabian Hohn** and **Siri Stjernfeldt** for being such generously kind, happy, intelligent, and super funny people. I could not imagine better friends than you! Besides being amazing

friends, you also showed me the Swedish culture and together with **Ola & Cinna Linderoth** you will always be what I remember when I think of Sweden.

I also appreciate my friendship with **Aurelie Miglar** and the many interesting talks and conversations we had. Your support helped me to get to this point in my life.

Darüber hinaus, möchte ich **meinen Eltern, meiner Familie und meinen Freunden in Deutschland** danken, die immer zur Hilfe bereit stehen und mich unterstützen während ich um die Welt wandere. Es ist immer so schön nach Hause zu kommen, um mich zu Entspannen und mich dick zu futtern. Besonders dankbar bin ich für meine Geschwister, die mich immer zum Lachen bringen und für die ich dann hoffentlich ab bald Dr. Jilli-Brilli-Kaka-Lilli bin. Auch **Sophia Tessaro** bin ich dankbar für die jahrelange Freundschaft, für die Hilfe im Schreiben meiner Arbeiten, und dafür, dass sie eine supernette und unterstützende Freundin ist.

Aparte de mi familia de sangre, también agradezco mucho mi familia chapina (**Fernando, Mercedes, Manu, Christina, Pablo, y Tomás**). Gracias por haberme dado una casa increíble donde me puede asolear y relajar, por apoyarme y darme consejos en mi vida, y por compartir conmigo sus viajes alrededor del mundo.

Last but not least, I like to thank my fiancé **Fernando Aguilar Lopez** without whom I would certainly never have started the PhD in the first place, let alone finished it. Thank you for believing in me no matter what, for making me laugh, and for simply being wonderful.







---

## 9 REFERENCES

1. Tun, K., Shurko, J. F., Ryan, L. & Lee, G. C. Age-based health and economic burden of skin and soft tissue infections in the United States, 2000 and 2012. *PLoS One* **13**, e0206893 (2018).
  2. Byrd, A. L., Belkaid, Y. & Segre, J. A. The human skin microbiome. *Nat. Rev. Microbiol.* **16**, 143–155 (2018).
  3. Zhu, F. *et al.* Household Transmission of Community-Associated Methicillin-Resistant Staphylococcus Aureus. *Front. Public Heal.* **9**, (2021).
  4. Stevens, D. L. *et al.* Practice guidelines for the diagnosis and management of skin and soft tissue infections: 2014 update by the infectious diseases society of America. *Clin. Infect. Dis.* **59**, e10–e52 (2014).
  5. Theuretzbacher, U. Antibiotic innovation for future public health needs. *Clin. Microbiol. Infect.* **23**, 713–717 (2017).
  6. Bayata, S. & Türel Ermertcan, A. Thermotherapy in dermatology. *Cutan. Ocul. Toxicol.* **31**, 235–240 (2012).
  7. Mallory, M., Gogineni, E., Jones, G. C., Greer, L. & Simone, C. B. Therapeutic hyperthermia: The old, the new, and the upcoming. *Crit. Rev. Oncol. Hematol.* **97**, 56–64 (2016).
  8. Kirtane, A. R. *et al.* Nanotechnology approaches for global infectious diseases. *Nat. Nanotechnol.* **16**, 369–384 (2021).
  9. Slavin, Y. N., Asnis, J., Häfeli, U. O. & Bach, H. Metal nanoparticles: Understanding the mechanisms behind antibacterial activity. *J. Nanobiotechnology* **15**, 1–20 (2017).
  10. Tsikourkitoudi, V., Henriques-Normark, B. & Sotiriou, G. A. Inorganic nanoparticle engineering against bacterial infections. *Curr. Opin. Chem. Eng.* **38**, 100872 (2022).
  11. Chen, Y. *et al.* Nanomaterials-based photothermal therapy and its potentials in antibacterial treatment. *J. Control. Release* **328**, 251–262 (2020).
  12. Wang, Y., Meng, H. M. & Li, Z. Near-infrared inorganic nanomaterial-based nanosystems for photothermal therapy. *Nanoscale* **13**, 8751–8772 (2021).
  13. Kim, M., Lee, J. & Nam, J. Plasmonic Photothermal Nanoparticles for Biomedical Applications. *Adv. Sci.* **6**, 1900471 (2019).
  14. Hong, G., Antaris, A. L. & Dai, H. Near-infrared fluorophores for biomedical imaging. *Nat. Biomed. Eng.* **1**, 0010 (2017).
  15. Wegner, K. & Pratsinis, S. E. Scale-up of nanoparticle synthesis in diffusion flame reactors. *Chem. Eng. Sci.* **58**, 4581–4589 (2003).
  16. Teoh, W. Y., Amal, R. & Mädler, L. Flame spray pyrolysis: An enabling technology for nanoparticles design and fabrication. *Nanoscale* **2**, 1324–1347 (2010).
  17. Sotiriou, G. A. Biomedical applications of multifunctional plasmonic nanoparticles. *Wiley Interdiscip. Rev. Nanomedicine Nanobiotechnology* **5**, 19–30 (2013).
  18. Kelesidis, G. A., Gao, D., Starsich, F. H. L. & Pratsinis, S. E. Light Extinction by Agglomerates of Gold Nanoparticles: A Plasmon Ruler for Sub-10 nm Interparticle Distances. *Anal. Chem.* **94**, 5310–5316 (2022).
  19. Sotiriou, G. A. *et al.* Non-toxic dry-coated nanosilver for plasmonic biosensors. *Adv.*
-

- Funct. Mater.* **20**, 4250–4257 (2010).
20. Merkl, P. *et al.* Plasmonic Coupling in Silver Nanoparticle Aggregates and Their Polymer Composite Films for Near - Infrared Photothermal Biofilm Eradication. *ACS Appl. Nano Mater.* **4**, 5330–5339 (2021).
  21. Li, H., Merkl, P., Sommertune, J., Thersleff, T. & Sotiriou, G. A. SERS Hotspot Engineering by Aerosol Self-Assembly of Plasmonic Ag Nanoaggregates with Tunable Interparticle Distance. *Adv. Sci.* 2201133 (2022). doi:10.1002/advs.202201133
  22. Tricoli, A. & Elmøe, T. D. Flame spray pyrolysis synthesis and aerosol deposition of nanoparticle films. *AIChE J.* **58**, 3578–3588 (2012).
  23. Huo, J. *et al.* Emerging photothermal-derived multimodal synergistic therapy in combating bacterial infections. *Chem. Soc. Rev.* **50**, 8762–8789 (2021).
  24. Xu, M., Li, L. & Hu, Q. The recent progress in photothermal-triggered bacterial eradication. *Biomater. Sci.* **9**, 1995–2008 (2021).
  25. Prausnitz, M. R. Microneedles for transdermal drug delivery. *Adv. Drug Deliv. Rev.* **56**, 581–587 (2004).
  26. Kim, Y.-C. C., Park, J.-H. H. & Prausnitz, M. R. Microneedles for drug and vaccine delivery. *Adv. Drug Deliv. Rev.* **64**, 1547–1568 (2012).
  27. Gill, H. S., Denson, D. D., Burris, B. A. & Prausnitz, M. R. Effect of microneedle design on pain in human volunteers. *Clin. J. Pain* **24**, 585–594 (2008).
  28. Sullivan, S. P. *et al.* Dissolving polymer microneedle patches for influenza vaccination. *Nat. Med.* **16**, 915–920 (2010).
  29. Jamaledin, R. *et al.* Advances in Antimicrobial Microneedle Patches for Combating Infections. *Adv. Mater.* **32**, 2002129 (2020).
  30. Zhi, D., Yang, T., O’Hagan, J., Zhang, S. & Donnelly, R. F. Photothermal therapy. *J. Control. Release* **325**, 52–71 (2020).
  31. Singh, P. *et al.* Polymeric microneedles for controlled transdermal drug delivery. *J. Control. Release* **315**, 97–113 (2019).
  32. Cárcamo-Martínez, Á. *et al.* Plasmonic photothermal microneedle arrays and single needles for minimally-invasive deep in-skin hyperthermia. *J. Mater. Chem. B* **8**, 5425–5433 (2020).
  33. Mosteller, R. D. Simplified calculation of body-surface area. *N. Engl. J. Med.* **317**, 1098 (1987).
  34. Leider, M. On the Weight of the Skin. *J. Invest. Dermatol.* **12**, 187–191 (1949).
  35. Yousef, H. & Sharma, S. Anatomy, Skin (Integument), Epidermis. in *StatPearls* (2018).
  36. Whitton, J. T. & Everall, J. D. The thickness of the epidermis. *Br. J. Dermatol.* **89**, 467–76 (1973).
  37. Sandby-Møller, J., Poulsen, T. & Wulf, H. C. Epidermal Thickness at Different Body Sites: Relationship to Age, Gender, Pigmentation, Blood Content, Skin Type and Smoking Habits. *Acta Derm. Venereol.* **83**, 410–413 (2003).
  38. Oltulu, P., Ince, B., Kökbudak, N., Findik, S. & Kiliç, F. Measurement of epidermis, dermis, and total skin thicknesses from six different body regions with a new ethical histometric technique. *Turkish J. Plast. Surg.* **26**, 56–61 (2018).
  39. Murphrey, M. B. & Zito, P. M. *Histology, Stratum Corneum. StatPearls* (StatPearls Publishing, 2018).
  40. Matsui, T. & Amagai, M. Dissecting the formation, structure and barrier function of the stratum corneum. *Int. Immunol.* **27**, 269–280 (2015).
  41. Elias, P. M. Structure and function of the stratum corneum permeability barrier. *Drug Dev. Res.* **13**, 97–105 (1988).
  42. Nemes, Z. & Steinert, P. M. Bricks and mortar of the epidermal barrier. *Exp. Mol. Med.* **31**, 5–19 (1999).

43. Elias, P. M. Stratum corneum defensive functions: An integrated view. *J. Invest. Dermatol.* **125**, 183–200 (2005).
44. Kubo, A. *et al.* The stratum corneum comprises three layers with distinct metal-ion barrier properties. *Sci. Rep.* **3**, 1–11 (2013).
45. Clausen, M. L., Slotved, H. C., Kroghfelt, K. A. & Agner, T. Measurements of AMPs in stratum corneum of atopic dermatitis and healthy skin-tape stripping technique. *Sci. Rep.* **8**, 1–8 (2018).
46. Elias, P. M. & Choi, E. H. Interactions among stratum corneum defensive functions. *Exp. Dermatol.* **14**, 719–726 (2005).
47. Elias, P. M. The how, why and clinical importance of stratum corneum acidification. *Exp. Dermatol.* **26**, 999–1003 (2017).
48. Bosko, C. A. Skin Barrier Insights: From Bricks and Mortar to Molecules and Microbes. *J. Drugs Dermatol.* **18**, s63-67 (2019).
49. Song, S. J. *et al.* Cohabiting family members share microbiota with one another and with their dogs. *Elife* **2013**, (2013).
50. Musgrave, R. D. A Comparison of Mammal Skin Tissues. (1962).
51. Gutowska-Owsiak, D., Podobas, E. I., Eggeling, C., Ogg, G. S. & Bernardino de la Serna, J. Addressing Differentiation in Live Human Keratinocytes by Assessment of Membrane Packing Order. *Front. Cell Dev. Biol.* **8**, 1078 (2020).
52. Feingold, K. R. Lamellar bodies: The key to cutaneous barrier function. *J. Invest. Dermatol.* **132**, 1951–1953 (2012).
53. Sandilands, A., Sutherland, C., Irvine, A. D. & McLean, W. H. I. Filaggrin in the frontline: Role in skin barrier function and disease. *J. Cell Sci.* **122**, 1285–1294 (2009).
54. Freeman, S. C. & Sonthalia, S. *Histology, Keratohyalin Granules. StatPearls* (StatPearls Publishing, 2019).
55. Gutowska-Owsiak, D. *et al.* Orchestrated control of filaggrin-actin scaffolds underpins cornification. *Cell Death Dis.* **9**, (2018).
56. Potten, C. S. Epidermal transit times. *Br. J. Dermatol.* **93**, 649–658 (1975).
57. Koren, E. *et al.* Thyl marks a distinct population of slow-cycling stem cells in the mouse epidermis. *Nat. Commun.* **13**, 4628 (2022).
58. Blanpain, C. & Fuchs, E. Epidermal Stem Cells of the Skin. *Annu. Rev. Cell Dev. Biol.* **22**, 339–373 (2006).
59. Fuchs, E. & Nowak, J. A. Building Epithelial Tissues from Skin Stem Cells. *Cold Spring Harb. Symp. Quant. Biol.* **73**, 333–350 (2008).
60. Kaplan, D. H. In vivo function of Langerhans cells and dermal dendritic cells. *Trends Immunol.* **31**, 446–451 (2010).
61. Fukunaga, A., Khaskhely, N. M., Sreevidya, C. S., Byrne, S. N. & Ullrich, S. E. Dermal Dendritic Cells, and Not Langerhans Cells, Play an Essential Role in Inducing an Immune Response. *J. Immunol.* **180**, 3057–3064 (2008).
62. Clayton, K., Vallejo, A. F., Davies, J., Sirvent, S. & Polak, M. E. Langerhans cells-programmed by the epidermis. *Front. Immunol.* **8**, 1676 (2017).
63. Nishibu, A. *et al.* Behavioral responses of epidermal Langerhans cells in situ to local pathological stimuli. *J. Invest. Dermatol.* **126**, 787–796 (2006).
64. West, H. C. & Bennett, C. L. Redefining the Role of Langerhans Cells As Immune Regulators within the Skin. *Front. Immunol.* **8**, 1941 (2018).
65. Van Der Aar, A. M. G. *et al.* Langerhans cells favor skin flora tolerance through limited presentation of bacterial antigens and induction of regulatory T cells. *J. Invest. Dermatol.* **133**, 1240–1249 (2013).
66. Rajesh, A., Wise, L. & Hibma, M. The role of Langerhans cells in pathologies of the skin. *Immunol. Cell Biol.* **97**, 700–713 (2019).
67. Abdo, J. M., Sopko, N. A. & Milner, S. M. The applied anatomy of human skin: A model for regeneration. *Wound Med.* **28**, 100179 (2020).

68. de Pereda, J. M., Ortega, E., Alonso-García, N., Gómez-Hernández, M. & Sonnenberg, A. Advances and perspectives of the architecture of hemidesmosomes: Lessons from structural biology. *Cell Adh. Migr.* **3**, 361–364 (2009).
69. Schneider, T. E. *et al.* Measuring stem cell frequency in epidermis: A quantitative in vivo functional assay for long-term repopulating cells. *Proc. Natl. Acad. Sci. U. S. A.* **100**, 11412–11417 (2003).
70. Potten, C. A comparison of cell replacement in bone marrow, testis and three regions of surface epithelium. *Biochim. Biophys. Acta - Rev. Cancer* **560**, 281–299 (1979).
71. Alonso, L. & Fuchs, E. Stem cells of the skin epithelium. *Proc. Natl. Acad. Sci. U. S. A.* **100**, 11830–11835 (2003).
72. Ghadially, R. 25 Years of Epidermal Stem Cell Research. *J. Invest. Dermatol.* **132**, 797–810 (2012).
73. Blanpain, C. & Fuchs, E. Epidermal homeostasis: A balancing act of stem cells in the skin. *Nat. Rev. Mol. Cell Biol.* **10**, 207–217 (2009).
74. Gonzalez-Celeiro, M., Zhang, B. & Hsu, Y.-C. Fate by Chance, not by Choice: Epidermal Stem Cells Go Live. *Cell Stem Cell* **19**, 8–10 (2016).
75. Sotiropoulou, P. A. & Blanpain, C. Development and homeostasis of the skin epidermis. *Cold Spring Harb. Perspect. Biol.* **4**, 1–9 (2012).
76. Aragona, M. *et al.* Defining stem cell dynamics and migration during wound healing in mouse skin epidermis. *Nat. Commun.* **8**, 1–14 (2017).
77. Díaz-García, D., Filipová, A., Garza-Veloz, I. & Martinez-Fierro, M. L. A beginner's introduction to skin stem cells and wound healing. *Int. J. Mol. Sci.* **22**, 11030 (2021).
78. Breitkreutz, D., Mirancea, N. & Nischt, R. Basement membranes in skin: Unique matrix structures with diverse functions? *Histochem. Cell Biol.* **132**, 1–10 (2009).
79. Breitkreutz, D., Koxholt, I., Thiemann, K. & Nischt, R. Skin Basement Membrane: The Foundation of Epidermal Integrity—BM Functions and Diverse Roles of Bridging Molecules Nidogen and Perlecan. *Biomed Res. Int.* **2013**, 1–16 (2013).
80. Gorzelanny, C., Mess, C., Schneider, S. W., Huck, V. & Brandner, J. M. Skin barriers in dermal drug delivery: Which barriers have to be overcome and how can we measure them? *Pharmaceutics* **12**, 1–31 (2020).
81. Brown, T. M. & Krishnamurthy, K. *Histology, Dermis. StatPearls* (StatPearls Publishing, 2019).
82. Clark, R. A. *et al.* The Vast Majority of CLA<sup>+</sup> T Cells Are Resident in Normal Skin. *J. Immunol.* **176**, 4431–4439 (2006).
83. Nestle, F. O., Di Meglio, P., Qin, J. Z. & Nickoloff, B. J. Skin immune sentinels in health and disease. *Nat. Rev. Immunol.* **9**, 679–691 (2009).
84. Mills, K. H. G. IL-17 and IL-17-producing cells in protection versus pathology. *Nat. Rev. Immunol.* 1–17 (2022). doi:10.1038/s41577-022-00746-9
85. Milner, J. D. *et al.* Impaired TH17 cell differentiation in subjects with autosomal dominant hyper-IgE syndrome. *Nature* **452**, 773–776 (2008).
86. Hibbs, R. G., Burch, G. E. & Phillips, J. H. The fine structure of the small blood vessels of normal human dermis and subcutis. *Am. Heart J.* **56**, 662–670 (1958).
87. Lopez-Ojeda, W. & Oakley, A. M. *Anatomy, Skin (Integument). StatPearls* (StatPearls Publishing, 2018).
88. Nakatsuji, T. *et al.* The microbiome extends to subepidermal compartments of normal skin. *Nat. Commun.* **4**, 1431 (2013).
89. Boxberger, M., Cenizo, V., Cassir, N. & La Scola, B. Challenges in exploring and manipulating the human skin microbiome. *Microbiome* **9**, 125 (2021).
90. Murphy, B. *et al.* Alteration of barrier properties, stratum corneum ceramides and microbiome composition in response to lotion application on cosmetic dry skin. *Sci. Rep.* **12**, 1–11 (2022).
91. Fluhr, J. W. *et al.* Acidic skin care promotes cutaneous microbiome recovery and skin

- physiology in an acute stratum corneum stress model. *Skin Pharmacol. Physiol.* **35**, 266–277 (2022).
92. Grice, E. A. & Segre, J. A. The skin microbiome. *Nat. Rev. Microbiol.* **9**, 244–253 (2011).
  93. Grice, E. A. *et al.* Topographical and Temporal Diversity of the Human Skin Microbiome. *Science* **324**, 1190 (2009).
  94. Oh, J., Byrd, A. L., Park, M., Kong, H. H. & Segre, J. A. Temporal Stability of the Human Skin Microbiome. *Cell* **165**, 854–866 (2016).
  95. Coates, M., Lee, M. J., Norton, D. & MacLeod, A. S. The Skin and Intestinal Microbiota and Their Specific Innate Immune Systems. *Front. Immunol.* **10**, 2950 (2019).
  96. Wertheim, H. F. L. *et al.* The role of nasal carriage in *Staphylococcus aureus* infections. *Lancet Infect. Dis.* **5**, 751–762 (2005).
  97. Totté, J. E. E. *et al.* Prevalence and odds of *S. taphylococcus aureus* carriage in atopic dermatitis: a systematic review and meta-analysis. *Br. J. Dermatol.* **175**, 687–695 (2016).
  98. Nakatsuji, T. *et al.* Antimicrobials from human skin commensal bacteria protect against *Staphylococcus aureus* and are deficient in atopic dermatitis. *Sci. Transl. Med.* **9**, (2017).
  99. Ramsey, M. M., Freire, M. O., Gabriliska, R. A., Rumbaugh, K. P. & Lemon, K. P. *Staphylococcus aureus* Shifts toward commensalism in response to corynebacterium species. *Front. Microbiol.* **7**, 1230 (2016).
  100. Erin Chen, Y., Fischbach, M. A. & Belkaid, Y. Skin microbiota-host interactions. *Nature* **553**, 427–436 (2018).
  101. Cruz, A. R., van Strijp, J. A. G., Bagnoli, F. & Manetti, A. G. O. Virulence Gene Expression of *Staphylococcus aureus* in Human Skin. *Front. Microbiol.* **12**, 1–10 (2021).
  102. Thurlow, L. R. *et al.* Functional modularity of the arginine catabolic mobile element contributes to the success of USA300 methicillin-resistant *staphylococcus aureus*. *Cell Host Microbe* **13**, 100–107 (2013).
  103. Miller, M. B. & Bassler, B. L. Quorum Sensing in Bacteria. *Annu. Rev. Microbiol.* **55**, 165–199 (2001).
  104. Mairpady Shambat, S. *et al.* A point mutation in AgrC determines cytotoxic or colonizing properties associated with phenotypic variants of ST22 MRSA strains. *Sci. Rep.* **6**, 1–13 (2016).
  105. Hersh, A. L. National Trends in Ambulatory Visits and Antibiotic Prescribing for Skin and Soft-Tissue Infections. *Arch. Intern. Med.* **168**, 1585 (2008).
  106. Miller, L. G. *et al.* Incidence of skin and soft tissue infections in ambulatory and inpatient settings, 2005–2010. *BMC Infect. Dis.* **15**, 362 (2015).
  107. Morgan, E., Hohmann, S., Ridgway, J. P., Daum, R. S. & David, M. Z. Decreasing Incidence of Skin and Soft-tissue Infections in 86 US Emergency Departments, 2009–2014. *Clin. Infect. Dis.* **68**, 453–459 (2019).
  108. Brauner, A. *Medicinsk mikrobiologi & immunologi*. (Studentlitteratur, 2015).
  109. Moffarah, A. S., Al Mohajer, M., Hurwitz, B. L. & Armstrong, D. G. Skin and soft tissue infections. *Microbiol. Spectr.* **4**, DMIH2-0014–2015 (2016).
  110. Dryden, M. S. Complicated skin and soft tissue infection. *J. Antimicrob. Chemother.* **65**, iii35–iii44 (2010).
  111. Sunderkötter, C. & Becker, K. Frequent bacterial skin and soft tissue infections: diagnostic signs and treatment. *JDDG J. der Dtsch. Dermatologischen Gesellschaft* **13**, 501–526 (2015).
  112. Cole, C. & Gazewood, J. Diagnosis and treatment of impetigo. *Am. Fam. Physician* **75**, (2007).

113. Amagai, M., Matsuyoshi, N., Wang, Z. H., Andl, C. & Stanley, J. R. Toxin in bullous impetigo and staphylococcal scalded-skin syndrome targets desmoglein 1. *Nat. Med.* **6**, 1275–1277 (2000).
114. Donovan, B., Rohrsheim, R., Bassett, I. & Mulhall, B. P. Bullous impetigo in homosexual men - A risk marker for HIV-1 infection? *Genitourin. Med.* **68**, 159–161 (1992).
115. Stevens, D. L. & Bryant, A. E. *Impetigo, Erysipelas and Cellulitis. Streptococcus pyogenes : Basic Biology to Clinical Manifestations* (University of Oklahoma Health Sciences Center, 2016).
116. Raff, A. B. & Kroshinsky, D. Cellulitis: A review. *JAMA* **316**, 325 (2016).
117. Anaya, D. A. & Dellinger, E. P. Necrotizing soft-tissue infection: Diagnosis and management. *Clin. Infect. Dis.* **44**, 705–710 (2007).
118. Hakkarainen, T. W., Kopari, N. M., Pham, T. N. & Evans, H. L. Necrotizing soft tissue infections: Review and current concepts in treatment, systems of care, and outcomes. *Curr. Probl. Surg.* **51**, 344–362 (2014).
119. Wong, C. H. *et al.* Necrotizing fasciitis: Clinical presentation, microbiology, and determinants of mortality. *J. Bone Jt. Surg.* **85**, 1454–1460 (2003).
120. Mishra, S. P., Singh, S. & Gupta, S. K. Necrotizing Soft Tissue Infections: Surgeon’s Prospective. *Int. J. Inflamm.* **2013**, 1–7 (2013).
121. Luelmo-Aguilar, J. & Santandreu, M. S. Folliculitis: Recognition and management. *Am. J. Clin. Dermatol.* **5**, 301–310 (2004).
122. Stulberg, D. L., Penrod, M. A. & Blatny, R. A. Common Bacterial Skin Infections. *Am. Acad. Fam. Physicians* **66**, 119–143 (2002).
123. Pinkus, H. Furuncle. *J. Cutan. Pathol.* **6**, 517–518 (1979).
124. Jain, A. K. C. ‘Carbuncle Is an Uncle of Furuncle’-A Case Report East African Scholars Journal of Medicine and Surgery Abbreviated Key Title: EAS J Med Surg. *East African Sch. J. Med. Surg.* **1**, 175–176 (2019).
125. Singer, A. J. & Talan, D. A. Management of Skin Abscesses in the Era of Methicillin-Resistant Staphylococcus aureus. *N. Engl. J. Med.* **370**, 1039–1047 (2014).
126. Bagnall, N. M., Vig, S. & Trivedi, P. Surgical-site infection. *Surgery* **27**, 426–430 (2009).
127. Leaper, D. J. Surgical-site infection. *Br. J. Surg.* **97**, 1601–1602 (2010).
128. Brook, I. Management of human and animal bite wound infection: An overview. *Curr. Infect. Dis. Reports 2009 115* **11**, 389–395 (2009).
129. Abrahamian, F. M. & Goldstein, E. J. C. Microbiology of animal bite wound infections. *Clin. Microbiol. Rev.* **24**, 231–246 (2011).
130. Smith, K. *et al.* One step closer to understanding the role of bacteria in diabetic foot ulcers: Characterising the microbiome of ulcers. *BMC Microbiol.* **16**, 1–12 (2016).
131. Dowd, S. E. *et al.* Polymicrobial nature of chronic diabetic foot ulcer biofilm infections determined using bacterial tag encoded FLX amplicon pyrosequencing (bTEFAP). *PLoS One* **3**, e3326 (2008).
132. Bowler, P. G. & Davies, B. J. The microbiology of infected and noninfected leg ulcers. *Int. J. Dermatol.* **38**, 573–578 (1999).
133. Carmona-Cruz, S., Orozco-Covarrubias, L. & Sáez-de-Ocariz, M. The Human Skin Microbiome in Selected Cutaneous Diseases. *Front. Cell. Infect. Microbiol.* **12**, 145 (2022).
134. Suaya, J. A. *et al.* Incidence and cost of hospitalizations associated with Staphylococcus aureus skin and soft tissue infections in the United States from 2001 through 2009. *BMC Infect. Dis.* **14**, 1–8 (2014).
135. Turner, N. A. *et al.* Methicillin-resistant Staphylococcus aureus: an overview of basic and clinical research. *Nat. Rev. Microbiol.* **17**, 203–218 (2019).
136. Talan, D. A. *et al.* Comparison of Staphylococcus aureus From Skin and Soft-Tissue



- Infections in US Emergency Department Patients, 2004 and 2008. *Clin. Infect. Dis.* **53**, 144–149 (2011).
137. Frazee, B. W. *et al.* High prevalence of methicillin-resistant *Staphylococcus aureus* in emergency department skin and soft tissue infections. *Ann. Emerg. Med.* **45**, 311–320 (2005).
  138. Moet, G. J., Jones, R. N., Biedenbach, D. J., Stilwell, M. G. & Fritsche, T. R. Contemporary causes of skin and soft tissue infections in North America, Latin America, and Europe: Report from the SENTRY Antimicrobial Surveillance Program (1998-2004). *Diagn. Microbiol. Infect. Dis.* **57**, 7–13 (2007).
  139. Ray, G. T., Suaya, J. A. & Baxter, R. Incidence, microbiology, and patient characteristics of skin and soft-tissue infections in a U.S. population: A retrospective population-based study. *BMC Infect. Dis.* **13**, 1–11 (2013).
  140. Tiwari, A. K. & Lal, R. Study to evaluate the role of severity stratification of skin and soft tissue infections (SSTIs) in formulating treatment strategies and predicting poor prognostic factors. *Int. J. Surg.* **12**, 125–133 (2014).
  141. Garau, J., Blasi, F., Medina, J., McBride, K. & Ostermann, H. Early response to antibiotic treatment in European patients hospitalized with complicated skin and soft tissue infections: Analysis of the REACH study. *BMC Infect. Dis.* **15**, 1–9 (2015).
  142. Esposito, S. *et al.* Epidemiology and Microbiology of Skin and Soft Tissue Infections: Preliminary Results of a National Registry. *J. Chemother.* **31**, 9–14 (2019).
  143. Esposito, S., Noviello, S. & Leone, S. Epidemiology and microbiology of skin and soft tissue infections. *Curr. Opin. Infect. Dis.* **29**, 109–115 (2016).
  144. Moran, G. J. *et al.* Methicillin-Resistant *S. aureus* Infections among Patients in the Emergency Department. *N. Engl. J. Med.* **355**, 666–74 (2006).
  145. Spornovasilis, N., Psychogiou, M. & Poulakou, G. Skin manifestations of *Pseudomonas aeruginosa* infections. *Curr. Opin. Infect. Dis.* **34**, 72–79 (2021).
  146. Esposito, S., Ascione, T. & Pagliano, P. Management of bacterial skin and skin structure infections with polymicrobial etiology. *Expert Rev. Anti. Infect. Ther.* **17**, 17–25 (2019).
  147. Mitragotri, S. Devices for overcoming biological barriers: The use of physical forces to disrupt the barriers. *Adv. Drug Deliv. Rev.* **65**, 100–103 (2013).
  148. Bos, J. D. & Meinardi, M. M. H. M. The 500 Dalton rule for the skin penetration of chemical compounds and drugs. *Exp. Dermatol.* **9**, 165–169 (2000).
  149. Finnin, B. C. & Morgan, T. M. Transdermal penetration enhancers: Applications, limitations, and potential. *J. Pharm. Sci.* **88**, 955–958 (1999).
  150. Chen, Y., Quan, P., Liu, X., Wang, M. & Fang, L. Novel chemical permeation enhancers for transdermal drug delivery. *Asian J. Pharm. Sci.* **9**, 51–64 (2014).
  151. Yu, Y.-Q., Yang, X., Wu, X.-F. & Fan, Y.-B. Enhancing Permeation of Drug Molecules Across the Skin via Delivery in Nanocarriers: Novel Strategies for Effective Transdermal Applications. *Front. Bioeng. Biotechnol.* **9**, 200 (2021).
  152. Bonamonte, D. *et al.* Topical antibiotics in the dermatological clinical practice: Indications, efficacy, and adverse effects. *Dermatol. Ther.* **33**, e13824 (2020).
  153. Williamson, D. A., Carter, G. P. & Howden, B. P. Current and Emerging Topical Antibacterials and Antiseptics: Agents, Action, and Resistance Patterns. *Clin. Microbiol. Rev.* **30**, 827–860 (2017).
  154. Elston, D. M. Topical antibiotics in dermatology: emerging patterns of resistance. *Dermatol. Clin.* **27**, 25–31 (2009).
  155. Gajdacs, M. Intravenous or oral antibiotic therapy: Sophie’s choice? *Gen. Intern. Med. Clin. Innov.* **4**, (2019).
  156. McCarthy, K. & Avent, M. Oral or intravenous antibiotics? *Aust. Prescr.* **43**, 45–48 (2020).
  157. Andrzejewski, A. M. & Viehman, J. A. 191. oral versus Intravenous Antibiotic

- Treatment in Skin and Soft Tissue Infections as a Consequence of Intravenous Drug Use: A Retrospective Study to Demonstrate Noninferiority. in *Open Forum Infectious Diseases* **7**, S224–S224 (Oxford University Press, 2020).
158. Aboltins, C. A. *et al.* Oral versus parenteral antimicrobials for the treatment of cellulitis: A randomized non-inferiority trial. *J. Antimicrob. Chemother.* **70**, 581–586 (2015).
  159. Li, H. K., Agweyu, A., English, M. & Bejon, P. An Unsupported Preference for Intravenous Antibiotics. *PLoS Med.* **12**, e1001825 (2015).
  160. Lemaitre, F. *et al.* Propofol, midazolam, vancomycin and cyclosporine therapeutic drug monitoring in extracorporeal membrane oxygenation circuits primed with whole human blood. *Crit. Care* **19**, 1–6 (2015).
  161. Wilhelm, M. P. & Estes, L. Vancomycin. in *Symposium on Antimicrobial Agents - Mayo Clinic proceedings.* **74**, 928–935 (1999).
  162. Bal, A. M. *et al.* Future trends in the treatment of methicillin-resistant *Staphylococcus aureus* (MRSA) infection: An in-depth review of newer antibiotics active against an enduring pathogen. *J. Glob. Antimicrob. Resist.* **10**, 295–303 (2017).
  163. Savoldi, A., Azzini, A. M., Baur, D. & Tacconelli, E. Is there still a role for vancomycin in skin and soft-tissue infections? *Curr. Opin. Infect. Dis.* **31**, 120–130 (2018).
  164. Skhirtladze, K. *et al.* Impaired target site penetration of vancomycin in diabetic patients following cardiac surgery. *Antimicrob. Agents Chemother.* **50**, 1372–1375 (2006).
  165. Mohammed, M. I. *et al.* Transdermal delivery of vancomycin hydrochloride using combination of nano-ethosomes and iontophoresis: in vitro and in vivo study. *Drug Deliv.* **23**, 1558–1564 (2016).
  166. Mohammed, M. I., Makky, A. M. A. & Abdellatif, M. M. Formulation and characterization of ethosomes bearing vancomycin hydrochloride for transdermal delivery. *Int. J. Pharm. Pharm. Sci.* **6**, 190–194 (2014).
  167. Salih, M. *et al.* Supramolecular self-assembled drug delivery system (SADDs) of vancomycin and tocopherol succinate as an antibacterial agent: in vitro, in silico and in vivo evaluations. *Pharm. Dev. Technol.* **25**, 1090–1108 (2020).
  168. Hassan, D. *et al.* Delivery of novel vancomycin nanoplexes for combating methicillin resistant *Staphylococcus aureus* (MRSA) infections. *Int. J. Pharm.* **558**, 143–156 (2019).
  169. Simpkin, V. L., Renwick, M. J., Kelly, R. & Mossialos, E. Incentivising innovation in antibiotic drug discovery and development: progress, challenges and next steps. *J. Antibiot.* **70**, 1087–1096 (2017).
  170. DeFeudis, N. More than 150 industry groups urge Congress to act on antimicrobial resistance. *Endpoints News* (2022). Available at: <https://endpts.com/more-than-150-industry-groups-urge-congress-to-act-on-antimicrobial-resistance/>. (Accessed: 26th November 2022)
  171. Tacconelli, E., Carrara, E., Savoldi, A., Kattula, D. & Burkert, F. *Global Priority List of Antibiotic-Resistant Bacteria to Guide Research, Discovery, and Development of new Antibiotics.* (2017).
  172. Berliner, M. N. & Maurer, A. I. Effect of Different Methods of Thermotherapy on Skin Microcirculation. *Am. J. Phys. Med. Rehabil.* **83**, 292–297 (2004).
  173. Gao, X. & Chen, H. Hyperthermia on skin immune system and its application in the treatment of human papillomavirus-infected skin diseases. *Front. Med.* **8**, 1–5 (2014).
  174. Franco Baronzio, G. *et al.* Effects of Local and Whole Body Hyperthermia on Immunity. in *Hyperthermia in Cancer Treatment: A Primer* 247–275 (Springer, Boston, MA, 2006). doi:10.1007/978-0-387-33441-7\_20
  175. Dewhurst, M. W., Vujaskovic, Z., Jones, E. & Thrall, D. Re-setting the biologic

- rationale for thermal therapy. *Int. J. Hyperth.* **21**, 779–790 (2005).
176. Mantso, T. *et al.* Hyperthermia induces therapeutic effectiveness and potentiates adjuvant therapy with non-targeted and targeted drugs in an in vitro model of human malignant melanoma. *Sci. Rep.* **8**, 1–16 (2018).
  177. Soballe, P. W., Nimbkar, N. V., Hayward, I., Nielsen, T. B. & Drucker, W. R. Electric cautery lowers the contamination threshold for infection of laparotomies. *Am. J. Surg.* **175**, 263–266 (1998).
  178. Ibelli, T., Templeton, S. & Levi-Polyachenko, N. Progress on utilizing hyperthermia for mitigating bacterial infections. *Int. J. Hyperth.* **34**, 144–156 (2018).
  179. Onyango, L. A., Dunstan, R. H., Gottfries, J., von Eiff, C. & Roberts, T. K. Effect of low temperature on growth and ultra-structure of staphylococcus spp. *PLoS One* **7**, (2012).
  180. Kosaka, T. *et al.* Capacity for survival in global warming: Adaptation of mesophiles to the temperature upper limit. *PLoS One* **14**, e0215614 (2019).
  181. Mackowiak, P. A. Direct effects of hyperthermia on pathogenic microorganisms: Teleologic implications with regard to fever. *Rev. Infect. Dis.* **3**, 508–520 (1981).
  182. Pollo, S. M. J., Zhaxybayeva, O. & Nesbø, C. L. Insights into thermoadaptation and the evolution of mesophily from the bacterial phylum thermotogae. *Can. J. Microbiol.* **61**, 655–670 (2015).
  183. Badgwell Doherty, C., Doherty, S. D. & Rosen, T. Thermotherapy in dermatologic infections. *J. Am. Acad. Dermatol.* **62**, 909–927 (2010).
  184. Tsuchido, T., Katsui, N., Takeuchi, A., Takano, M. & Shibasaki, I. Destruction of the outer membrane permeability barrier of Escherichia coli by heat treatment. *Appl. Environ. Microbiol.* **50**, 298–303 (1985).
  185. Russell, A. D. Lethal Effects of Heat on Bacterial Physiology and Structure. *Sci. Prog.* **86**, 115–137 (2003).
  186. Eshraghi, N., Wainberg, R. H., Walden, T. L., Tsuchido, T. & Yatvin, M. B. Effects of heat and amino acid supplementation on the uptake of arginine and its incorporation into proteins in escherichia coli. *Int. J. Hyperth.* **10**, 79–88 (1994).
  187. Yuan, W. *et al.* Cell wall thickening is associated with adaptive resistance to amikacin in methicillin-resistant Staphylococcus aureus clinical isolates. *J. Antimicrob. Chemother.* **68**, 1089–1096 (2013).
  188. Cui, L. *et al.* Cell wall thickening is a common feature of vancomycin resistance in Staphylococcus aureus. *J. Clin. Microbiol.* **41**, 5–14 (2003).
  189. Mao, C. *et al.* Reversing Multidrug-Resistant Escherichia coli by Compromising Its BAM Biogenesis and Enzymatic Catalysis through Microwave Hyperthermia Therapy. *Adv. Funct. Mater.* **32**, 2202887 (2022).
  190. Pavlovsky, L., Sturtevant, R. A., Younger, J. G. & Solomon, M. J. Effects of temperature on the morphological, polymeric, and mechanical properties of Staphylococcus epidermidis bacterial biofilms. *Langmuir* **31**, 2036–2042 (2015).
  191. Alumutairi, L., Yu, B., Filka, M., Nayfach, J. & Kim, M. H. Mild magnetic nanoparticle hyperthermia enhances the susceptibility of Staphylococcus aureus biofilm to antibiotics. *Int. J. Hyperth.* **37**, 66–75 (2020).
  192. Kaur, K. *et al.* Combating Drug-Resistant Bacteria Using Photothermally Active Nanomaterials: A Perspective Review. *Frontiers in Microbiology* **12**, 3405 (2021).
  193. Bollen, C., Dewachter, L. & Michiels, J. Protein Aggregation as a Bacterial Strategy to Survive Antibiotic Treatment. *Front. Mol. Biosci.* **8**, 1–9 (2021).
  194. Qiu, Y. *et al.* Photothermal therapy may be a double-edged sword by inducing the formation of bacterial antibiotic tolerance. *Biomater. Sci.* **10**, 1995–2005 (2021).
  195. Soares, S., Sousa, J., Pais, A. & Vitorino, C. Nanomedicine: Principles, Properties, and Regulatory Issues. *Front. Chem.* **6**, 360 (2018).
  196. Domingues, C. *et al.* Where Is Nano Today and Where Is It Headed? A Review of

- Nanomedicine and the Dilemma of Nanotoxicology. *ACS Nano* **16**, 9994–10041 (2022).
197. Ikuta, K. S. *et al.* Global mortality associated with 33 bacterial pathogens in 2019: a systematic analysis for the Global Burden of Disease Study 2019. *Lancet* **400**, 2221–2248 (2022).
198. Gao, P., Nie, X., Zou, M., Shi, Y. & Cheng, G. Recent advances in materials for extended-release antibiotic delivery system. *J. Antibiot.* **64**, 625–634 (2011).
199. Zhang, L., Pornpattananangkul, D., Hu, C.-M. & Huang, C.-M. Development of Nanoparticles for Antimicrobial Drug Delivery. *Curr. Med. Chem.* **17**, 585–594 (2010).
200. Drug Approval Package: Ambisome (Amphotericin B) NDA# 050740. Available at: [https://www.accessdata.fda.gov/drugsatfda\\_docs/nda/97/050740\\_ambisome\\_toc.cfm](https://www.accessdata.fda.gov/drugsatfda_docs/nda/97/050740_ambisome_toc.cfm). (Accessed: 1st November 2022)
201. Griffith, D. E. *et al.* Amikacin liposome inhalation suspension for treatment-refractory lung disease caused by Mycobacterium avium complex (CONVERT) a prospective, open-label, randomized study. *Am. J. Respir. Crit. Care Med.* **198**, 1559–1569 (2018).
202. FDA. *Approval Package for: Arikayce, 590 mg (amikacin liposome inhalation suspension). NDA# 4327567.* (2019).
203. Bilton, D. *et al.* Amikacin liposome inhalation suspension for chronic Pseudomonas aeruginosa infection in cystic fibrosis. *J. Cyst. Fibros.* **19**, 284–291 (2020).
204. Gao, W., Chen, Y., Zhang, Y., Zhang, Q. & Zhang, L. Nanoparticle-based local antimicrobial drug delivery. *Advanced Drug Delivery Reviews* **127**, 46–57 (2018).
205. Alipour, M., Halwani, M., Omri, A. & Suntres, Z. E. Antimicrobial effectiveness of liposomal polymyxin B against resistant Gram-negative bacterial strains. *Int. J. Pharm.* **355**, 293–298 (2008).
206. Omri, A., Suntres, Z. E. & Shek, P. N. Enhanced activity of liposomal polymyxin B against Pseudomonas aeruginosa in a rat model of lung infection. *Biochem. Pharmacol.* **64**, 1407–1413 (2002).
207. Li, L. L. *et al.* Core-shell supramolecular gelatin nanoparticles for adaptive and ‘on-demand’ antibiotic delivery. *ACS Nano* **8**, 4975–4983 (2014).
208. Shaaban, M. I., Shaker, M. A. & Mady, F. M. Imipenem/cilastatin encapsulated polymeric nanoparticles for destroying carbapenem-resistant bacterial isolates. *J. Nanobiotechnology* **15**, 1–12 (2017).
209. Möhler, J. S., Sim, W., Blaskovich, M. A. T., Cooper, M. A. & Ziora, Z. M. Silver bullets: A new lustre on an old antimicrobial agent. *Biotechnol. Adv.* **36**, 1391–1411 (2018).
210. Sim, W., Barnard, R., Blaskovich, M. A. T. & Ziora, Z. Antimicrobial Silver in Medicinal and Consumer Applications: A Patent Review of the Past Decade (2007–2017). *Antibiotics* **7**, 93 (2018).
211. Makabenta, J. M. V. *et al.* Nanomaterial-based therapeutics for antibiotic-resistant bacterial infections. *Nat. Rev. Microbiol.* **19**, 23–36 (2021).
212. Yang, B., Chen, Y. & Shi, J. Reactive oxygen species (ROS)-based nanomedicine. *Chem. Rev.* **119**, 4881–4985 (2019).
213. Fujishima, A. & Honda, K. Electrochemical photolysis of water at a semiconductor electrode. *Nature* **238**, 37–38 (1972).
214. Li, Q., Liu, Y., Dai, X., Jiang, W. & Zhao, H. Nanozymes Regulate Redox Homeostasis in ROS-Related Inflammation. *Front. Chem.* **9**, 1–13 (2021).
215. Hussain, S., Aneggi, E. & Goi, D. Catalytic activity of metals in heterogeneous Fenton-like oxidation of wastewater contaminants: a review. *Environ. Chem. Lett.* **19**, 2405–2424 (2021).
216. Dryden, M. Reactive oxygen species: a novel antimicrobial. *Int. J. Antimicrob. Agents* **51**, 299–303 (2018).

- 
217. Li, H. *et al.* Reactive Oxygen Species in Pathogen Clearance: The Killing Mechanisms, the Adaption Response, and the Side Effects. *Front. Microbiol.* **11**, (2021).
  218. Cheng, G. & Li, B. Nanoparticle-based photodynamic therapy: new trends in wound healing applications. *Mater. Today Adv.* **6**, 100049 (2020).
  219. Kühn, K. P. *et al.* Disinfection of surfaces by photocatalytic oxidation with titanium dioxide and UVA light. *Chemosphere* **53**, 71–77 (2003).
  220. Schäfer, M. & Werner, S. Oxidative stress in normal and impaired wound repair. *Pharmacol. Res.* **58**, 165–171 (2008).
  221. Kaur, P., Aliru, M. L., Chadha, A. S., Asea, A. & Krishnan, S. Hyperthermia using nanoparticles – Promises and pitfalls. *Int. J. Hyperth.* **32**, 76–88 (2016).
  222. Suriyanto, Ng, E. Y. K. & Kumar, S. D. Physical mechanism and modeling of heat generation and transfer in magnetic fluid hyperthermia through Néelian and Brownian relaxation: a review. *Biomed. Eng. Online* **16**, 36 (2017).
  223. Mahmoudi, M., Sant, S., Wang, B., Laurent, S. & Sen, T. Superparamagnetic iron oxide nanoparticles (SPIONs): Development, surface modification and applications in chemotherapy. *Adv. Drug Deliv. Rev.* **63**, 24–46 (2011).
  224. Martins, P. M., Lima, A. C., Ribeiro, S., Lanceros-Mendez, S. & Martins, P. Magnetic Nanoparticles for Biomedical Applications: From the Soul of the Earth to the Deep History of Ourselves. *ACS Appl. Bio Mater.* **4**, 5839–5870 (2021).
  225. Thomas, L. A. *et al.* Carboxylic acid-stabilised iron oxide nanoparticles for use in magnetic hyperthermia. *J. Mater. Chem.* **19**, 6529–6535 (2009).
  226. Kim, M. H. *et al.* Magnetic nanoparticle targeted hyperthermia of cutaneous staphylococcus aureus infection. *Ann. Biomed. Eng.* **41**, 598–609 (2013).
  227. FDA. FDA Drug Safety Communication: FDA strengthens warnings and changes prescribing instructions to decrease the risk of serious allergic reactions with anemia drug Feraheme (ferumoxytol). (2015). Available at: <https://www.fda.gov/drugs/drug-safety-and-availability/fda-drug-safety-communication-fda-strengthens-warnings-and-changes-prescribing-instructions-decrease>. (Accessed: 7th November 2022)
  228. Khan, M. S., Bhaisare, M. L., Gopal, J. & Wu, H. F. Highly efficient gold nanorods assisted laser phototherapy for rapid treatment on mice wound infected by pathogenic bacteria. *J. Ind. Eng. Chem.* **36**, 49–58 (2016).
  229. Li, C. *et al.* Flexible Nanoholey Patches for Antibiotic-Free Treatments of Skin Infections. *ACS Appl. Mater. Interfaces* **9**, 36665–36674 (2017).
  230. Huang, X. W. *et al.* Water-Based Black Phosphorus Hybrid Nanosheets as a Moldable Platform for Wound Healing Applications. *ACS Appl. Mater. Interfaces* **10**, 35495–35502 (2018).
  231. Zhou, L. *et al.* Injectable Self-Healing Antibacterial Bioactive Polypeptide-Based Hybrid Nanosystems for Efficiently Treating Multidrug Resistant Infection, Skin-Tumor Therapy, and Enhancing Wound Healing. *Adv. Funct. Mater.* **29**, 1806883 (2019).
  232. Laser Institute of America. *ANSI Z136.1 Standards - American National Standard for Safe Use of Lasers.* (2007).
  233. Li, M. *et al.* Noninvasive rapid bacteria-killing and acceleration of wound healing through photothermal/photodynamic/copper ion synergistic action of a hybrid hydrogel. *Biomater. Sci.* **6**, 2110–2121 (2018).
  234. Xu, X. *et al.* Controlled-temperature photothermal and oxidative bacteria killing and acceleration of wound healing by polydopamine-assisted Au-hydroxyapatite nanorods. *Acta Biomater.* **77**, 352–364 (2018).
  235. Fan, X. *et al.* Metal-Organic-Framework-Derived 2D Carbon Nanosheets for Localized Multiple Bacterial Eradication and Augmented Anti-infective Therapy. *Nano Lett.* **19**, 5885–5896 (2019).
-

- 
236. Tao, B. *et al.* Copper-nanoparticle-embedded hydrogel for killing bacteria and promoting wound healing with photothermal therapy. *J. Mater. Chem. B* **7**, 2534–2548 (2019).
  237. Huang, S. *et al.* Functionalized GO Nanovehicles with Nitric Oxide Release and Photothermal Activity-Based Hydrogels for Bacteria-Infected Wound Healing. *ACS Appl. Mater. Interfaces* **12**, 28952–28964 (2020).
  238. Wentao, W. *et al.* Functionalization of polyvinyl alcohol composite film wrapped in a-ZnO@CuO@Au nanoparticles for antibacterial application and wound healing. *Appl. Mater. Today* **17**, 36–44 (2019).
  239. Xu, Q. *et al.* PDA/Cu Bioactive Hydrogel with ‘hot Ions Effect’ for Inhibition of Drug-Resistant Bacteria and Enhancement of Infectious Skin Wound Healing. *ACS Appl. Mater. Interfaces* **12**, 31255–31269 (2020).
  240. Li, J. *et al.* Zinc-doped Prussian blue enhances photothermal clearance of *Staphylococcus aureus* and promotes tissue repair in infected wounds. *Nat. Commun.* **10**, 4490 (2019).
  241. Altinbasak, I. *et al.* Reduced Graphene-Oxide-Embedded Polymeric Nanofiber Mats: An “On-Demand” Photothermally Triggered Antibiotic Release Platform. *ACS Appl. Mater. Interfaces* **10**, 41098–41106 (2018).
  242. He, D. *et al.* Combined photothermal and antibiotic therapy for bacterial infection via acidity-sensitive nanocarriers with enhanced antimicrobial performance. *Appl. Mater. Today* **12**, 415–429 (2018).
  243. Gao, G., Jiang, Y. W., Jia, H. R. & Wu, F. G. Near-infrared light-controllable on-demand antibiotics release using thermo-sensitive hydrogel-based drug reservoir for combating bacterial infection. *Biomaterials* **188**, 83–95 (2019).
  244. Qing, G. *et al.* Thermo-responsive triple-function nanotransporter for efficient chemophotothermal therapy of multidrug-resistant bacterial infection. *Nat. Commun.* **10**, 1–12 (2019).
  245. He, J., Shi, M., Liang, Y. & Guo, B. Conductive adhesive self-healing nanocomposite hydrogel wound dressing for photothermal therapy of infected full-thickness skin wounds. *Chem. Eng. J.* **394**, 124888 (2020).
  246. Zhang, L. *et al.* Photon-Responsive Antibacterial Nanoplatfor for Synergistic Photothermal-/Pharmaco-Therapy of Skin Infection. *ACS Appl. Mater. Interfaces* **11**, 300–310 (2019).
  247. Xu, M. *et al.* Near-Infrared-Controlled Nanoplatfor Exploiting Photothermal Promotion of Peroxidase-like and OXD-like Activities for Potent Antibacterial and Anti-biofilm Therapies. *ACS Appl. Mater. Interfaces* **12**, 50260–50274 (2020).
  248. Xiao, Y. *et al.* Dual stimuli-responsive metal-organic framework-based nanosystem for synergistic photothermal/pharmacological antibacterial therapy. *Acta Biomater.* **122**, 291–305 (2021).
  249. Ali, M. R. K., Wu, Y. & El-Sayed, M. A. Gold-Nanoparticle-Assisted Plasmonic Photothermal Therapy Advances Toward Clinical Application. *J. Phys. Chem. C* **123**, 15375–15393 (2019).
  250. Rastinehad, A. R. *et al.* Gold nanoshell-localized photothermal ablation of prostate tumors in a clinical pilot device study. *Proc. Natl. Acad. Sci. U. S. A.* **116**, 18590–18596 (2019).
  251. Jain, P. K., Lee, K. S., El-Sayed, I. H. & El-Sayed, M. A. Calculated absorption and scattering properties of gold nanoparticles of different size, shape, and composition: Applications in biological imaging and biomedicine. *J. Phys. Chem. B* **110**, 7238–7248 (2006).
  252. Chen, J. *et al.* Collective Plasmon Coupling in Gold Nanoparticle Clusters for Highly Efficient Photothermal Therapy. *ACS Nano* **16**, 910–920 (2022).
  253. Jain, P. K. & El-Sayed, M. A. Plasmonic coupling in noble metal nanostructures.
-

- Chem. Phys. Lett.* **487**, 153–164 (2010).
254. Zhu, W. *et al.* Quantum mechanical effects in plasmonic structures with subnanometre gaps. *Nat. Commun.* **7**, (2016).
255. Roth, P. Particle synthesis in flames. *Proc. Combust. Inst.* **31 II**, 1773–1788 (2007).
256. Gutsch, A., Mühlenweg, H. & Krämer, M. Tailor-made nanoparticles via gas-phase synthesis. *Small* **1**, 30–46 (2005).
257. Strobel, R. & Pratsinis, S. E. Flame aerosol synthesis of smart nanostructured materials. *J. Mater. Chem.* **17**, 4743 (2007).
258. Meierhofer, F., Mädler, L. & Fritsching, U. Nanoparticle evolution in flame spray pyrolysis—Process design via experimental and computational analysis. *AIChE J.* **66**, e16885 (2020).
259. Shanthil, M., Thomas, R., Swathi, R. S. & George, T. K. Ag@SiO<sub>2</sub> core-shell nanostructures: Distance-dependent plasmon coupling and SERS investigation. *J. Phys. Chem. Lett.* **3**, 1459–1464 (2012).
260. Sotiriou, G. A. *et al.* Photothermal killing of cancer cells by the controlled plasmonic coupling of silica-coated Au/Fe<sub>2</sub>O<sub>3</sub> nanoaggregates. *Adv. Funct. Mater.* **24**, 2818–2827 (2014).
261. Moularas, C., Georgiou, Y., Adamska, K. & Deligiannakis, Y. Thermoplasmonic Heat Generation Efficiency by Nonmonodisperse Core–Shell Ag<sub>0</sub>@SiO<sub>2</sub> Nanoparticle Ensemble. *J. Phys. Chem. C* **123**, 22499–22510 (2019).
262. Wegner, K., Schimmoeller, B., Thiebaut, B., Fernandez, C. & Rao, T. N. Pilot plants for industrial nanoparticle production by flame spray pyrolysis. *KONA Powder Part. J.* **29**, 251–265 (2011).
263. Tricoli, A. *et al.* Micropatterning layers by flame aerosol deposition-annealing. *Adv. Mater.* **20**, 3005–3010 (2008).
264. hemotune | Technology. Available at: <https://www.hemotune.ch/technology>. (Accessed: 12th November 2022)
265. Nanotechnology | anavo | Switzerland. Available at: <https://www.anavo.ch/>. (Accessed: 12th November 2022)
266. Matter, M. T. *et al.* Multiscale Analysis of Metal Oxide Nanoparticles in Tissue: Insights into Biodistribution and Biotransformation. *Adv. Sci.* **7**, 2000912 (2020).
267. Matter, M. T. *et al.* Developing a tissue glue by engineering the adhesive and hemostatic properties of metal oxide nanoparticles. *Nanoscale* **9**, 8418–8426 (2017).
268. Sotiriou, G. A. *et al.* Nanosilver on nanostructured silica: Antibacterial activity and Ag surface area. *Chem. Eng. J.* **170**, 547–554 (2011).
269. Geissel, F. J. *et al.* Antibiofilm activity of nanosilver coatings against *Staphylococcus aureus*. *J. Colloid Interface Sci.* **608**, 3141–3150 (2022).
270. Henry, S., McAllister, D. V, Allen, M. G. & Prausnitz, M. R. Microfabricated microneedles: A novel approach to transdermal drug delivery. *J. Pharm. Sci.* **87**, 922–925 (1998).
271. Bhatnagar, S., Dave, K. & Venuganti, V. V. K. Microneedles in the clinic. *J. Control. Release* **260**, 164–182 (2017).
272. O’Day, E. *Top 10 Emerging Technologies 2019. World Economic Forum Annual Meeting 2019* (2019).
273. Indermun, S. *et al.* Current advances in the fabrication of microneedles for transdermal delivery. *J. Control. Release* **185**, 130–138 (2014).
274. Liu, G. S. *et al.* Microneedles for transdermal diagnostics: Recent advances and new horizons. *Biomaterials* **232**, 119740 (2020).
275. Rotomskis, R. Quantum Dot Migration Through Natural Barriers and Distribution in the Skin. in *Nanoscience in Dermatology* 307–321 (Academic Press, 2016). doi:10.1016/B978-0-12-802926-8.00024-0
276. Larrañeta, E., McCrudden, M. T. C., Courtenay, A. J. & Donnelly, R. F. Microneedles:

- A New Frontier in Nanomedicine Delivery. *Pharmaceutical Research* **33**, 1055–1073 (2016).
277. Prausnitz, M. R. & Langer, R. Transdermal drug delivery. *Nat. Biotechnol.* **26**, 1261–1268 (2008).
278. Sheng, T. *et al.* Microneedle-Mediated Vaccination: Innovation and Translation. *Adv. Drug Deliv. Rev.* **179**, 113919 (2021).
279. Zhang, Y. *et al.* Advances in transdermal insulin delivery. *Adv. Drug Deliv. Rev.* **139**, 51–70 (2019).
280. Abramson, A. *et al.* A luminal unfolding microneedle injector for oral delivery of macromolecules. *Nat. Med.* **25**, 1512–1518 (2019).
281. Abramson, A. *et al.* An ingestible self-orienting system for oral delivery of macromolecules. *Science (80-. )*. **363**, 611–615 (2019).
282. Permana, A. D. *et al.* Selective delivery of silver nanoparticles for improved treatment of biofilm skin infection using bacteria-responsive microparticles loaded into dissolving microneedles. *Mater. Sci. Eng. C* **120**, 111786 (2021).
283. Larrañeta, E., Lutton, R. E. M., Woolfson, A. D. & Donnelly, R. F. Microneedle arrays as transdermal and intradermal drug delivery systems: Materials science, manufacture and commercial development. *Materials Science and Engineering R: Reports* **104**, 1–32 (2016).
284. Dermalroller. Available at: <https://dermaroller.com/de/>. (Accessed: 14th November 2022)
285. AdminMed. Available at: <http://www.adminmed.com/>. (Accessed: 14th November 2022)
286. Vaxxas. Available at: <https://www.vaxxas.com/>. (Accessed: 14th November 2022)
287. Micron Biomedical. Available at: <https://micronbiomedical.com/>. (Accessed: 14th November 2022)
288. LTS Lohmann. Available at: <https://www.ltslohmann.com/de/>. (Accessed: 14th November 2022)
289. Donnelly, R. F. *et al.* Hydrogel-forming microneedle arrays for enhanced transdermal drug delivery. *Adv. Funct. Mater.* **22**, 4879–4890 (2012).
290. Kim, J. D., Kim, M., Yang, H., Lee, K. & Jung, H. Droplet-born air blowing: Novel dissolving microneedle fabrication. *J. Control. Release* **170**, 430–436 (2013).
291. Chen, M.-C., Wang, K.-W., Chen, D.-H., Ling, M.-H. & Liu, C.-Y. Remotely triggered release of small molecules from LaB<sub>6</sub>@SiO<sub>2</sub>-loaded polycaprolactone microneedles. *Acta Biomater.* **13**, 344–353 (2015).
292. Yu, W. *et al.* Near-infrared light triggered and separable microneedles for transdermal delivery of metformin in diabetic rats. *J. Mater. Chem. B* **5**, 9507 (2017).
293. Choi, S. O. *et al.* An electrically active microneedle array for electroporation. *Biomed. Microdevices* **12**, 263–273 (2010).
294. Jeong, H.-R., Lee, H.-S., Choi, I.-J. & Park, J.-H. Considerations in the use of microneedles: pain, convenience, anxiety and safety. *J. Drug Target.* **25**, 29–40 (2017).
295. Shu, W. *et al.* Insights into the mechanics of solid conical microneedle array insertion into skin using the finite element method. *Acta Biomater.* **135**, 403–413 (2021).
296. Ripolin, A. *et al.* Successful application of large microneedle patches by human volunteers. *Int. J. Pharm.* **521**, 92–101 (2017).
297. McAlister, E. *et al.* Directly Compressed Tablets: A Novel Drug-Containing Reservoir Combined with Hydrogel-Forming Microneedle Arrays for Transdermal Drug Delivery. *Adv. Healthc. Mater.* **10**, (2021).
298. Azizoglu, E., Ozer, O. & Prausnitz, M. R. Fabrication of pure-drug microneedles for delivery of montelukast sodium. *Drug Deliv. Transl. Res.* **12**, 444–458 (2022).
299. Caffarel-Salvador, E. *et al.* A microneedle platform for buccal macromolecule



- delivery. *Sci. Adv.* **7**, (2021).
300. Römgens, A. M., Bader, D. L., Bouwstra, J. A., Baaijens, F. P. T. & Oomens, C. W. J. Monitoring the penetration process of single microneedles with varying tip diameters. *J. Mech. Behav. Biomed. Mater.* **40**, 397–405 (2014).
  301. Ito, Y., Hirono, M., Fukushima, K., Sugioka, N. & Takada, K. Two-layered dissolving microneedles formulated with intermediate-acting insulin. *Int. J. Pharm.* **436**, 387–393 (2012).
  302. Wang, Q. L., Zhu, D. D., Liu, X. B., Chen, B. Z. & Guo, X. D. Microneedles with controlled bubble sizes and drug distributions for efficient transdermal drug delivery. *Sci. Rep.* **6**, 1–11 (2016).
  303. Wang, Q. *et al.* Investigation on fabrication process of dissolving microneedle arrays to improve effective needle drug distribution. *Eur. J. Pharm. Sci.* **66**, 148–156 (2015).
  304. Chu, L. Y., Choi, S.-O. & Prausnitz, M. R. Fabrication of Dissolving Polymer Microneedles for Controlled Drug Encapsulation and Delivery: Bubble and Pedestal Microneedle Designs. *J. Pharm. Sci.* **99**, 4228–4238 (2010).
  305. Chu, L. Y. & Prausnitz, M. R. Separable arrowhead microneedles. *J. Control. Release* **149**, 242–249 (2011).
  306. Lahiji, S. F., Dangol, M. & Jung, H. A patchless dissolving microneedle delivery system enabling rapid and efficient transdermal drug delivery. *Sci. Rep.* **5**, 7914 (2015).
  307. Li, S., Xia, D. & Prausnitz, M. R. Efficient Drug Delivery into Skin Using a Biphasic Dissolvable Microneedle Patch with Water-Insoluble Backing. *Adv. Funct. Mater.* **31**, 2103359 (2021).
  308. Paredes, A. J. *et al.* Systemic delivery of tenofovir alafenamide using dissolving and implantable microneedle patches. *Mater. Today Bio* **13**, 100217 (2022).
  309. Peng, K. *et al.* Dissolving microneedle patches loaded with amphotericin B microparticles for localised and sustained intradermal delivery: Potential for enhanced treatment of cutaneous fungal infections. *J. Control. Release* **339**, 361–380 (2021).
  310. Zare, M. R. *et al.* Dissolvable carboxymethyl cellulose/polyvinylpyrrolidone microneedle arrays for transdermal delivery of Amphotericin B to treat cutaneous leishmaniasis. *Int. J. Biol. Macromol.* **182**, 1310–1321 (2021).
  311. Donnelly, R. F. *et al.* Microneedle Arrays Allow Lower Microbial Penetration Than Hypodermic Needles In Vitro. *Pharm. Res.* **26**, 2513–2522 (2009).
  312. Donnelly, R. F. *et al.* Hydrogel-forming microneedle arrays exhibit antimicrobial properties: Potential for enhanced patient safety. *Int. J. Pharm.* **451**, 76–91 (2013).
  313. Gittard, S. D. *et al.* Pulsed laser deposition of antimicrobial silver coating on Ormocer microneedles. *Biofabrication* **1**, 41001 (2009).
  314. Gittard, S. D. *et al.* Deposition of antimicrobial coatings on microstereolithography-fabricated microneedles. *JOM* **63**, 59–68 (2011).
  315. Chew, S. W. T. *et al.* In Situ Generation of Zinc Oxide Nanobushes on Microneedles as Antibacterial Coating. *SLAS Technol.* **24**, 181–187 (2019).
  316. Boehm, R. D. *et al.* Indirect rapid prototyping of antibacterial acid anhydride copolymer microneedles. *Biofabrication* **4**, (2012).
  317. Chi, J. *et al.* Antibacterial and angiogenic chitosan microneedle array patch for promoting wound healing. *Bioact. Mater.* **5**, 253–259 (2020).
  318. Frydman, G. H. *et al.* Manuka honey microneedles for enhanced wound healing and the prevention and/or treatment of Methicillin-resistant *Staphylococcus aureus* (MRSA) surgical site infection. *Sci. Rep.* **10**, 1–11 (2020).
  319. Gittard, S. D. *et al.* Two Photon Polymerization-Micromolding of Polyethylene Glycol-Gentamicin Sulfate Microneedles. *Adv. Eng. Mater.* **12**, 77–82 (2010).
  320. González-Vázquez, P. *et al.* Transdermal delivery of gentamicin using dissolving microneedle arrays for potential treatment of neonatal sepsis. *J. Control. RELEASE*

- 265**, 30–40 (2017).
321. Rodgers, A. M. *et al.* Control of *Klebsiella pneumoniae* Infection in Mice by Using Dissolving Microarray Patches Containing Gentamicin. *Antimicrob. Agents Chemother.* **63**, e02612-18 (2019).
322. Ramadon, D. *et al.* Development, Evaluation, and Pharmacokinetic Assessment of Polymeric Microarray Patches for Transdermal Delivery of Vancomycin Hydrochloride. *Mol. Pharm.* **17**, 3353–3368 (2020).
323. Zhang, X., Chen, G., Yu, Y., Sun, L. & Zhao, Y. Bioinspired Adhesive and Antibacterial Microneedles for Versatile Transdermal Drug Delivery. *Research* **2020**, 1–9 (2020).
324. Gaware, S. A., Rokade, K. A., Bala, P. & Kale, S. N. Microneedles of chitosan-porous carbon nanocomposites: Stimuli (pH and electric field)-initiated drug delivery and toxicological studies. *J. Biomed. Mater. Res. A* **107**, 1582–1596 (2019).
325. Tsioris, K. *et al.* Fabrication of silk microneedles for controlled-release drug delivery. *Adv. Funct. Mater.* **22**, 330–335 (2012).
326. Permana, A. D., Mir, M., Utomo, E. & Donnelly, R. F. Bacterially sensitive nanoparticle-based dissolving microneedles of doxycycline for enhanced treatment of bacterial biofilm skin infection: A proof of concept study. *Int. J. Pharm. X* **2**, 100047 (2020).
327. Zhang, Y. *et al.* ROS-Responsive Microneedle Patch for Acne Vulgaris Treatment. *Adv. Ther.* **1**, 1800035 (2018).
328. Chen, Y. *et al.* Dissolving microneedles with a biphasic release of antibacterial agent and growth factor to promote wound healing. *Biomater. Sci.* **10**, 2409–2416 (2022).
329. Su, Y. *et al.* Simultaneous Delivery of Multiple Antimicrobial Agents by Biphasic Scaffolds for Effective Treatment of Wound Biofilms. *Adv. Healthc. Mater.* **10**, 2100135 (2021).
330. Liu, D. *et al.* Fabrication of Dissolving Microneedles with Thermal-Responsive Coating for NIR-Triggered Transdermal Delivery of Metformin on Diabetic Rats. *ACS Biomater. Sci. Eng.* **4**, 1687–1695 (2018).
331. Zhang, Y. *et al.* Separable Microneedles for Near-Infrared Light-Triggered Transdermal Delivery of Metformin in Diabetic Rats. *ACS Biomater. Sci. Eng.* **4**, 2879–2888 (2018).
332. Liu, T., Jiang, G., Song, G., Zhu, J. & Yang, Y. Fabrication of separable microneedles with phase change coating for NIR-triggered transdermal delivery of metformin on diabetic rats. *Biomed. Microdevices* **22**, 12 (2020).
333. Deng, X., Shao, Z. & Zhao, Y. Solutions to the Drawbacks of Photothermal and Photodynamic Cancer Therapy. *Adv. Sci.* **8**, 1–16 (2021).
334. Ye, Y. *et al.* A melanin-mediated cancer immunotherapy patch. *Sci. Immunol.* **2**, eaan5692 (2017).
335. Hao, Y. *et al.* Near-infrared responsive 5-fluorouracil and indocyanine green loaded MPEG-PCL nanoparticle integrated with dissolvable microneedle for skin cancer therapy. *Bioact. Mater.* **5**, 542–552 (2020).
336. Xu, Q., Li, X., Zhang, P. & Wang, Y. Rapidly dissolving microneedle patch for synergistic gene and photothermal therapy of subcutaneous tumor. *J. Mater. Chem. B* **8**, 4331–4339 (2020).
337. Chen, M. *et al.* Cold to Hot: Binary Cooperative Microneedle Array-Amplified Photoimmunotherapy for Eliciting Antitumor Immunity and the Abscopal Effect. *ACS Appl. Mater. Interfaces* **12**, 32259–32269 (2020).
338. Song, G. *et al.* Separable Microneedles for Synergistic Chemo-Photothermal Therapy against Superficial Skin Tumors. *ACS Biomater. Sci. Eng.* **6**, 4116–4125 (2020).
339. Pei, P. *et al.* Composite-dissolving microneedle patches for chemotherapy and photothermal therapy in superficial tumor treatment. *Biomater. Sci.* **6**, 1414–1423

- (2018).
340. Peng, T. *et al.* Dissolving Microneedles Loading TPGS Biphasic Functionalized PLGA Nanoparticles for Efficient Chemo-Photothermal Combined Therapy of Melanoma. *Adv. Ther.* **3**, 1900190 (2020).
  341. Chen, M.-C. C. *et al.* Near-Infrared Light-Responsive Composite Microneedles for On-Demand Transdermal Drug Delivery. *Biomacromolecules* **16**, 1598–1607 (2015).
  342. Chen, M. C., Lin, Z. W. & Ling, M. H. Near-infrared light-activatable microneedle system for treating superficial tumors by combination of chemotherapy and photothermal therapy. *ACS Nano* **10**, 93–101 (2016).
  343. Hao, Y. *et al.* Novel Approach of Using Near-Infrared Responsive PEGylated Gold Nanorod Coated Poly(l-lactide) Microneedles to Enhance the Antitumor Efficiency of Docetaxel-Loaded MPEG-PDLLA Micelles for Treating an A431 Tumor. *ACS Appl. Mater. Interfaces* **9**, 15317–15327 (2017).
  344. Hao, Y. *et al.* Near-Infrared Responsive PEGylated Gold Nanorod and Doxorubicin Loaded Dissolvable Hyaluronic Acid Microneedles for Human Epidermoid Cancer Therapy. *Adv. Ther.* **1**, 1800008 (2018).
  345. Dong, L. *et al.* Au Nanocage-Strengthened Dissolving Microneedles for Chemo-Photothermal Combined Therapy of Superficial Skin Tumors. *ACS Appl. Mater. Interfaces* **10**, 9247–9256 (2018).
  346. Moreira, A. F. *et al.* Poly (vinyl alcohol)/chitosan layer-by-layer microneedles for cancer chemo-photothermal therapy. *Int. J. Pharm.* **576**, 118907 (2020).
  347. Chen, Y. *et al.* Multifunctional Graphene-Oxide-Reinforced Dissolvable Polymeric Microneedles for Transdermal Drug Delivery. *ACS Appl. Mater. Interfaces* **12**, 352–360 (2020).
  348. Lei, Q. *et al.* Microneedle Patches Integrated with Biomineralized Melanin Nanoparticles for Simultaneous Skin Tumor Photothermal Therapy and Wound Healing. *Adv. Funct. Mater.* **32**, 2113269 (2022).
  349. Sun, Y. *et al.* NIR Laser-Triggered Microneedle-Based Liquid Band-Aid for Wound Care. *Adv. Funct. Mater.* **31**, 2100218 (2021).
  350. Lei, X. *et al.* Degradable microneedle patches loaded with antibacterial gelatin nanoparticles to treat staphylococcal infection-induced chronic wounds. *Int. J. Biol. Macromol.* **217**, 55–65 (2022).
  351. Yu, X., Zhao, J. & Fan, D. A dissolving microneedle patch for Antibiotic/Enzymolysis/Photothermal triple therapy against bacteria and their biofilms. *Chem. Eng. J.* **437**, 135475 (2022).
  352. Doughty, A. *et al.* Nanomaterial Applications in Photothermal Therapy for Cancer. *Materials (Basel)*. **12**, 779 (2019).
  353. Chen, F. & Cai, W. Nanomedicine for targeted photothermal cancer therapy: where are we now? *Nanomedicine* **10**, 1–3 (2015).
  354. Sartawi, Z., Blackshields, C. & Faisal, W. Dissolving microneedles: Applications and growing therapeutic potential. *J. Control. Release* **348**, 186–205 (2022).
  355. Wang, M., Hu, L. & Xu, C. Recent advances in the design of polymeric microneedles for transdermal drug delivery and biosensing. *Lab Chip* **17**, 1373–1387 (2017).
  356. Detamornrat, U., McAlister, E., Hutton, A. R. J., Larrañeta, E. & Donnelly, R. F. The Role of 3D Printing Technology in Microengineering of Microneedles. *Small* **18**, 2106392 (2022).
  357. Donnelly, R. F. *et al.* Design, optimization and characterisation of polymeric microneedle arrays prepared by a novel laser-based micromoulding technique. *Pharm. Res.* **28**, 41–57 (2011).
  358. Larrañeta, E. *et al.* A proposed model membrane and test method for microneedle insertion studies. *Int. J. Pharm.* **472**, 65–73 (2014).
  359. Jesús Valle, M. J. de, López, F. G. & Navarro, A. S. Development and validation of

- an HPLC method for vancomycin and its application to a pharmacokinetic study. *J. Pharm. Biomed. Anal.* **48**, 835–839 (2008).
360. Bartosova, L. & Bajgar, J. Transdermal Drug Delivery In Vitro Using Diffusion Cells. *Curr. Med. Chem.* **19**, 4671–4677 (2012).
361. OECD. Guidance Notes on Dermal Absorption. *OECD Environ. Heal. Saf. Publ.* **8**, 2019 (2011).
362. Knopp, M. M. *et al.* Comparative Study of Different Methods for the Prediction of Drug-Polymer Solubility. *Mol. Pharm.* **12**, 3408–3419 (2015).
363. Rask, M. B., Knopp, M. M., Olesen, N. E., Holm, R. & Rades, T. Comparison of two DSC-based methods to predict drug-polymer solubility. *Int. J. Pharm.* **540**, 98–105 (2018).
364. Thersleff, T., Budnyk, S., Drangai, L. & Slabon, A. Dissecting complex nanoparticle heterostructures via multimodal data fusion with aberration-corrected STEM spectroscopy. *Ultramicroscopy* **219**, 113116 (2020).
365. Thurlow, L. R., Joshi, G. S. & Richardson, A. R. Virulence strategies of the dominant USA300 lineage of community-associated methicillin-resistant *Staphylococcus aureus* (CA-MRSA). *FEMS Immunol. Med. Microbiol.* **65**, 5–22 (2012).
366. Ranamukhaarachchi, S. A. *et al.* A micromechanical comparison of human and porcine skin before and after preservation by freezing for medical device development. *Sci. Rep.* **6**, (2016).
367. Krieger, K. J. *et al.* Simple and customizable method for fabrication of high-aspect ratio microneedle molds using low-cost 3D printing. *Microsystems Nanoeng.* **5**, 1–14 (2019).